

PUMPED TRANSFORMER LASERS

Technical Summary Report #1, for the
Period 1 November 1964 to 1 May 1965

Contract Nonr-4718(00), ARPA Number 306

GPL Division, Aerospace Group, General Precision, Inc.

17 May 1965

COPY	2	OF	3
HARD COPY	\$.	5.00	
MICROFICHE	\$.	1.00	

JUN 17 1965

TISIA B

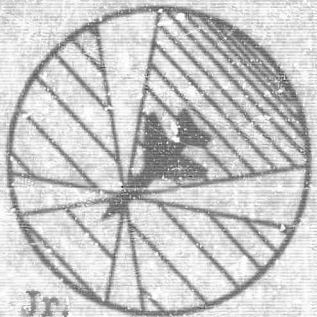
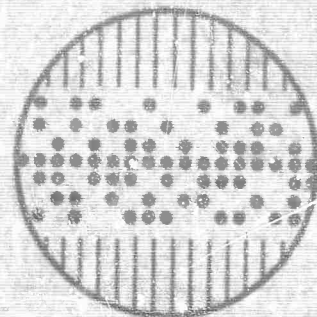
Report written by: Cecil B. Ellis
Work done by: Donald S. Bayley
Cecil B. Ellis
Ivan A. Greenwood, Jr.

This research is part of Project DEFENDER under the joint sponsorship of the Advanced Research Projects Agency, the Office of Naval Research, and the Department of Defense. Reproduction of this report in whole or in part is permitted for any purpose of the United States Government.

GFL DIVISION

**GENERAL
PRECISION
AEROSPACE**

GENERAL PRECISION INC.
PLEASANTVILLE, NEW YORK



ARCHIVE COPY

**BEST
AVAILABLE COPY**

PUMPED TRANSFORMER LASERS

'Technical' summary Report #1, for the
Period 1 November 1964 to 1 May 1965

Contract Nonr-4718(00), ARPA Number 306

GPL Division, Aerospace Group, General Precision, Inc.

17 May 1965

Report written by: Cecil B. Ellis
Work done by: Donald S. Bayley
Cecil B. Ellis
Ivan A. Greenwood, Jr.

This research is part of Project DEFENDER under the joint sponsorship of the Advanced Research Projects Agency, the Office of Naval Research, and the Department of Defense. Reproduction of this report in whole or in part is permitted for any purpose of the United States Government.

ABSTRACT

A new concept is presented and its analysis begun: the TRANSFORMER LASER. This arrangement is intended to convert the outputs from many lesser, and lower quality, auxiliary lasers into a single coherent plane-wavefront by absorption and re-emission in the normal transitions of a molecular gas medium.

Work during this contract period has dealt exclusively with analyses of suitable gaseous media to be pumped by a battery of Nd-glass lasers near 1.06μ . The most promising gas molecule found so far for this purpose is CN, which would be obtained from the preparatory exposure of normal $(\text{CN})_2$ gas to a pulse of UV light. The analysis to date indicates a probable potential for operation at very useful power densities, but only a few of the possible questions about such a system have yet been explored.

Alternative choices for the gas medium might be Cs_2 or metastable nitrogen molecules. Further analysis of these molecules as well as of CN is planned for the next period.

TABLE OF CONTENTS

	<u>Page No.</u>
1. <u>INTRODUCTION AND BACKGROUND</u>	1
1.1. Pre-contract studies; general	4
1.2. Pre-contract studies; media to be pumped by Nd glass lasers	7
2. <u>PRELIMINARY NOTES ON HCN, Cs₂ and N₂[*] as TRANSFORMER MEDIA WITH Nd-glass LASER PUMPING</u>	12
2.1 HCN Gas	12
2.2 Cesium Vapor	13
2.3 Metastable Nitrogen	21
3. <u>GENERAL DESCRIPTION OF CN LASER TRANSFORMER CONCEPT</u>	25
4. <u>ENERGY LEVELS OF THE CN MOLECULE</u>	29
4.1 Lowest Levels of the C and N Atoms	29
4.2 Electronic States of the CN Molecule	32
4.2.1 The CN Dissociation Limits and Theoretical States	32
4.2.2 The Observed Electronic States of CN	34
4.2.3 Fine Structure of the Three Lowest CN Electronic States	38
4.3 The CN Vibrational Levels and the Potential Curves	40
4.4 The CN Rotational Levels: Theory of Expected Patterns	43
4.4.1 The Unperturbed Rotational Levels of A ² Π	43
4.4.2 The Unperturbed Rotational Levels of X ² Σ ⁺ and B ² Σ ⁺	50
4.4.3 Perturbation Effects in Rotation Levels	53
5. <u>THE ALLOWED OPTICAL TRANSITIONS IN CN</u>	55
5.1 The Electronic Selection Rules	55
5.2 The Vibrational Transitions and the Nd Glass Laser Spectrum	58
5.3 The Rotational Branches of the (A-X) Bands	66
5.4 Intensity Relations for Rotation Lines	70

TABLE OF CONTENTS (cont.)

	<u>Page No.</u>
6. <u>STRUCTURE OF THE (6, 5) and (0, 0) BANDS</u>	72
6.1 The (6, 5) Band	72
6.2 The (0, 0) Band	80
7. <u>WAYS OF PREPARING CN·X</u>	82
7.1 Thermal Dissociation of (CN) ₂	82
7.2 Electric Discharges for Preparing CN	83
7.3 Value of the Heat of Dissociation of (CN) ₂	84
7.4 Photodissociation of (CN) ₂ ; Experiments	85
7.5 The Absorption Spectrum of (CN) ₂	89
7.6 Photodissociation of (CN) ₂ as a Two-stage Process	95
7.7 An Analogous Photo-collision Dissociation in Na ₂	100
7.8 Dissociation of (CN) ₂ by Chemical Reactions	106
7.9 Ways of Preparing CN from Other Starting Substances	106
8. <u>MECHANISMS FOR DISAPPEARANCE OF CN AND CN*</u>	109
8.1 Disappearance of CN through Polymerization of (CN) ₂	109
8.2 Three-Body Recombination of CN	112
8.3 Chemical Reaction of CN with Additives	117
8.4 Collision Quenching of CN*	118
9. <u>SUMMARY OF CN TRANSFORMER MEDIUM PARAMETERS</u>	121
10. <u>LASING POSSIBILITIES IN THE (6, 5) BAND AT 210° K.</u>	123
10.1 Boltzmann Distributions at 210° K in CN·X(v = 5)	123
10.2 Boltzmann Distributions at 210° K in CN·A(v = 6)	126
10.3 Excitation Required for Zero-Gain at Each (6, 5) Line Wavelength.	128
10.4 Pumping in R ₂₁ and Lasing in P ₁₂ .	136
11. CONCLUSION	146
12. BIBLIOGRAPHY	147

LIST OF FIGURES AND TABLES

<u>Figure</u>	<u>Page No.</u>
1. Schematic Diagram of Transformer Laser Arrangement	3
2. Lower Energy Levels of the Alkali Atoms	14
3. Electronic Levels of the Alkali Molecules	17
4. Lower Energy Levels of the Nitrogen Atom, Molecule, and Ions	22
5. C and N Low Levels, and CN Dissociation Limits	30
6. Electronic Energy Level Diagram for CN	37
7. Potential Curves for the CN Molecule	42
8. The Rotation Levels of CN· A ($v = 6$)	44
9. The Rotational Levels of CN·X($v = 5$)	51
10. Relative Values of I/ν^4 for CN· (A-X) Bands	59
11. Fluorescent Band Near 1.06μ of Nd Glasses, and Location of CN· (A-X) Bands	63
12. Labelling of the Rotational Branches of the CN· (A-X) Bands.	67
13. Relative Intensities of Rotation Lines of the (9, 3) Band.	71
14. Calculated (6, 5) Line Positions in the Range $9509-9543\text{ cm}^{-1}$	73
15. Calculated (6, 5) Lines Near the R_2 Head	75
16. The Complete (6, 5) Band as Deduced From Experimental Data	79
17. The (0, 0) Band, as Measured by Davis and Phillips	81
18. Electronic States and Dissociation Limits of $(\text{CN})_2$	93
19. Partial Energy Level Diagram for Na_2	101

LIST OF FIGURES AND TABLES (cont.)

<u>Figure</u>		<u>Page No.</u>
20.	Rotational Boltzmann Distribution for CN· X (v = 5) at 210° K.	125
21.	Rotational Boltzmann Distributions for CN· A (v = 6) at 210° K	127
22.	$\left[\begin{smallmatrix} Z \\ 0 \end{smallmatrix} \right]_{210}$ for the Lines of the (6, 5) Band	132
23.	The Steady-State Distributions for the R ₂₁ - P ₁₂ Pump- lase Cycle	139

Tables

1.	Possible Pumping Processes and Transformer Media	9
2.	Experimental Values of I/ν^4 for the Bands of the Red CN System	60
3.	Location of the Bands of the CN· (A-X) System	62

1. INTRODUCTION AND BACKGROUND

It is well-known that no system of optics placed between a pumping source and a laser active medium can put more energy within a given wavelength band into the medium than would result if the latter were surrounded with a solid wall whose entire area was emitting with the same intensity as the pumping surface. *

Therefore, no avenue of approach toward an ultra high power laser can result in very much more energy being pumped into the active lasing volume than can the method of raising the effective temperature of a luminous wall around the medium to extreme levels, while still keeping the spectral range of the radiation within the absorption capability of the medium.

Such an arrangement could be approximated by practically surrounding the volume with auxiliary lasers, whose beams enter the active medium and have wavelengths which are absorbable for pumping purposes by the atoms or molecules of the medium. The effective radiation temperature of the output surfaces of these auxiliary lasers can be many millions of degrees.

A lasing medium which is being laser-pumped in this way can be called a TRANSFORMER LASER. In effect, it takes the output beams from numerous auxiliary lasers, which need have no special phase

*Assuming that both pump and laser are immersed in ambient media of the same index of refraction.

relationship to each other and which do not even need to have precisely the same wavelength, and transforms this energy into a single coherent output beam. If the optical quality and geometrical arrangement of the transformer medium can be made sufficiently good, and the right combination of pump wavelength and active atom or molecule can be chosen, there arises the possibility of an output beam whose wavefront can be plane and diffraction-limited, and which will have a power close to the sum of the powers of the various pumping beams. Figure 1 illustrates a sample arrangement.

GPL Division originated the concept of a laser transformer system prior to July 1962, and for more than two years has pursued analytical work in development of the concept for output beams at wavelengths near 11.1μ , 4.71μ , 2.36μ , 1.06μ and 8100\AA , with company funds. Since 23 November 1964 further analysis of possible laser transformer systems has been proceeding under the present contract.

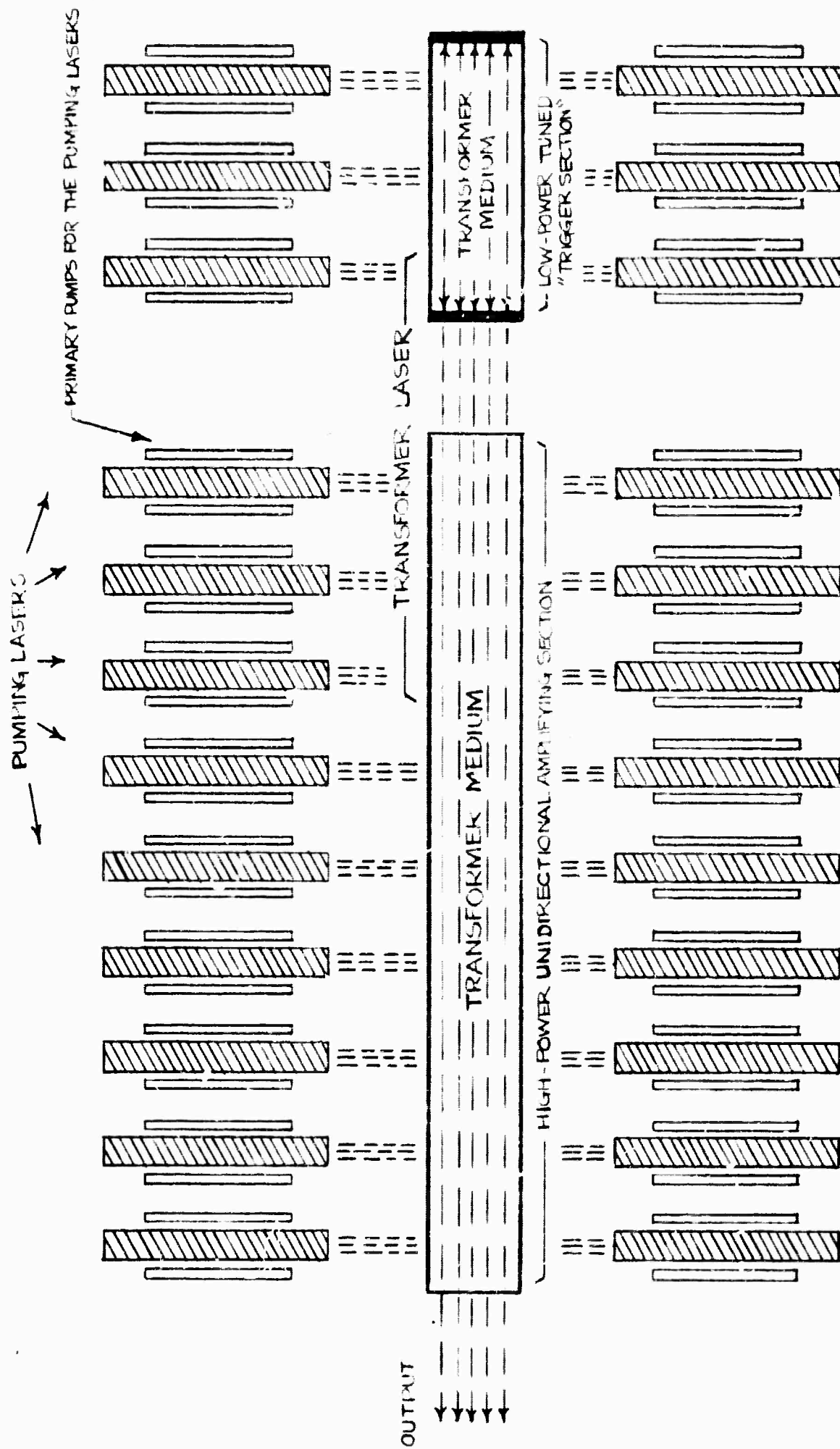


Figure 1

Schematic Diagram for one of many simple transformer laser arrangements.

1.1 Pre-Contract Studies, General

The first design studied in 1962 was the use of circulating carbon monoxide gas at 10 atm pressure and 100° K for the transformer medium, with a number of 2.36μ $\text{CaF}_2:\text{Dy}^{++}$ laser beams to provide the pumping energy for the CO. The gas would absorb the pump light in the broadened P(5) line of its (2-0) rotation-vibration band. Intermolecular collisions would quickly redistribute the absorbed energy over a great many rotation and vibration levels of the CO molecules. Analysis of these distributions showed that at high pumping powers strong inversion would occur for all the P-branch transitions of the (2-0) band beyond P(5); as well as for all the P-branch lines numbered higher than about P(3) of the (1-0), (2-1), (3-2), etc., bands which lie near 4.7μ . It was shown that suitable cavity design for the CO container could result in output beams near either 2.36μ or 4.71μ which (a) contained more than 90% of the total absorbed Dy-laser pumping energy, and (b) would not have their divergence quality appreciably impaired by variations in refractive index of the CO throughout a pulse of considerable length. The latter feature occurs because the various rotation-to-translation energy exchanges arising during CO-CO collisions practically balance out; while the type of collision which transforms vibrational energy into translation is relatively rare in CO gas at 100° K. For this reason, practically none of the absorbed pump energy can get into the form of sensible heat in the gas until long after a pulse is completed.

Next, various possible systems were analyzed for accepting the beams from a battery of ruby lasers as pumping energy. The best transformer medium appeared to be sodium vapor, approximately saturated at about 500° C and mixed with 20 atm of helium. The ruby laser light is to be Raman-shifted to a wavelength near 7940Å. This light will be absorbed by several broadened branch lines of each of a number of overlapping rotation-vibration bands, such as (13-1), (14-2), etc., of the ($A^1\Sigma_u^+ - X^1\Sigma_g^+$) electronic transition of the Na_2 molecules present in the vapor. Collisions between Na_2 and He will quickly diffuse the absorbed pumping energy and set up approximately Boltzmann level population distributions for the Na_2 , both in rotation and in vibration. Analysis showed that at high pumping powers inversion would occur for practically all lines of ($A^1\Sigma_u^+ - X^1\Sigma_g^+$) lying on the redward side of the pump wavelength. Since the spontaneous fluorescence emission from excited Na_2 molecules centers on the blue side of the pump wavelength, it was calculated that an energy balance could be arranged, so that again practically no net sensible heat is added to the transformer medium. The output beam could contain at least 90% of the total pumping energy absorbed within the gas.

Following this work, considerable study was given to the possibilities for a transformer laser whose output would lie near 11.1μ, but a suitable combination of pumping laser plus transformer medium had not been chosen before the goal of the analysis was shifted to the use of Nd-glass pumps at 1.06μ.

A moderately extensive literature search was made on the spectra and other properties of all gases which are known to, or could possibly be expected to, absorb with reasonable intensity near 1.06μ , or approximately 9430 cm^{-1} . This survey included not only atoms and molecules in their equilibrium ground states, as in the CO and Na_2 cases, but also atoms and molecules which might have been placed temporarily in excited states — i. e., "prepared" — by some external agency such as an electric discharge or some relatively low-powered auxiliary light source. A few details of this study are discussed in the next section.

1.2 Pre-Contract Studies; Media to be Pumped by Nd Glass Lasers

Table 1 presents an attempt at classifying all the possibilities for gas media into logical groups, according as to the use of atoms or molecules, allowed or forbidden transitions, electronic or rotation-vibration transitions, normal or "prepared" entities, etc., etc.

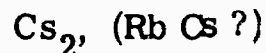
The right hand column gives the results for those cases studied.

The nomenclature of the molecular electronic states referred to is that used in standard spectroscopic level tables such as Herzberg (1950). *

It will be noted that many areas have not yet been studied under this contract.

However, from among the simpler kinds of systems, only the following examples of media appeared, in advance of serious study, to show much promise at all for the desired transformer application. Each has some potential disadvantages, as listed.

- A. Reasonably stable diatomic molecules, strongly absorbing, but with very small rotational constants and overlapping electronic levels:



* This standard work will be referenced in the remainder of this report simply as "Herzberg's book". Underscored names with dates in parenthesis are references, which are detailed in the Bibliography at the end of this report.

B. Reasonably stable molecules, but only very weakly absorbing near 9430 cm^{-1} :

HT, DF, and HF, (if their polymerization could be tolerated),

Rb₂, K₂, I₂, O₂, H₂, HCN, NH₃, C₂H₄ and numerous other polyatomic organics.

C. Both strong and weak absorbers, but either unstable or high temperature refractory entities, complex to produce and maintain:

TiO, SiO, CaO, NO*, BeO, BaH, NH₂(?), He₂*, C₂*,

CN, CP, Se₂, H₂*, N₂*, CO*.

D. Rather strong absorbers, fairly stable molecules; but polyatomic, with very complex vibrational interchange, very little data:

O₃, VCl₄, IrF₆, various rare earth fluorinated acetylacetonates.

After some general consideration, four candidates were chosen from this group. as seeming the most promising in advance of any concentrated study. These were: (a) ground-state Cs₂ molecules occurring naturally in cesium vapor, which would be at about 400°C, (b) room temperature HCN gas, (c) ground-state CN monomer molecules in temporarily partially dissociated cyanogen gas, and (d) metastable N₂ molecules in their $A^3\Sigma_u^+$ electronic state, in temporarily excited nitrogen gas. At this point work was begun under the present contract.

Table 1. Possible Pumping Processes and Absorbing Gases, for Transformer Media to be Pumped by Nd Glass Lasers Near 9430 cm^{-1} .

<u>Processes</u>	<u>Possibly Useful Transitions and Media</u>
Pump up from ground state of stable atoms; allowed transition	No transition available near 9430 cm^{-1} except possibly in high temperature refractory materials.
Same, but forbidden transition	None near 9430 cm^{-1} except high temperature materials.
Pump within electronic ground state of stable molecules; rotation-vibration transitions; diatomic molecules	None having center of any <u>strong</u> band within 900 cm^{-1} of 9430 cm^{-1} .
Same, but polyatomic molecules	Numerous cases of fairly <u>weak</u> bands, mostly organic molecules.
Pump up from electronic ground state of stable molecules; electronic-rotation-vibration transitions; diatomic molecules; allowed transitions	<p>The following five molecules will absorb the Nd glass laser light, but all have problems:</p> <p>Cs_2 - very complex spectrum; several electronic levels are superimposed</p> <p>RbCs - the vapor will necessarily include some Cs_2.</p> <p>Rb_2 - bands are extremely weak.</p> <p>K_2 - bands are extremely weak.</p> <p>I_2 - bands will be of negligible intensity except at temperatures such that dissociating collisions would cause too much quenching.</p>

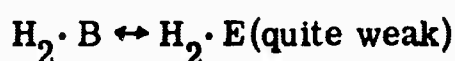
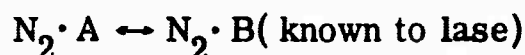
Table 1. (cont.) Possible Pumping Processes and Absorbing Gases,
for Transformer Media to be Pumped by Nd Glass Lasers
Near 9430 cm^{-1}

Same, but forbidden transition	Only O_2 , which is prohibitively weak.
Same, but polyatomic molecules, both allowed and forbidden transitions	O_3 , VCl_4 , IrF_6 , and other complexes.
Pump up from the electronic ground state of a stable molecule into the dissociation continuum, and lase one of the excited products	Not yet studied under this contract.
Pump up from a prepared excited state of a stable atom	Not yet studied.
Pump within the ground electronic state of a stable molecule in a rotation-vibration transition; pumping upward from a prepared higher vibrational level not normally well populated	Not yet studied.
Pump up from a prepared higher vibrational level in the ground electronic state of a stable molecule; an electronic-vibration-rotation transition to an upper state	Not yet studied.
Same, but pumping into the dissociation continuum and lasing one of the excited products	Not yet studied
Pump in a rotation-vibration transition within a prepared metastable excited electronic state of a stable molecule	Not yet studied.

Table 1. (cont. Possible Pumping Processes and Absorbing Gases,
For Transformer Media to be Pumped by Nd Glass Lasers,
Near 9430 cm⁻¹

Pump up from a prepared excited electronic state of a stable molecule; electronic-rotation-vibration transition

Excited states in N₂, CO, and H₂ look possible and might be prepared in an electric discharge. Also NH₃ may perhaps absorb weakly.



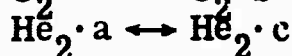
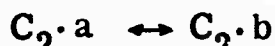
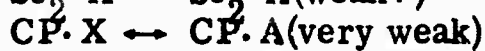
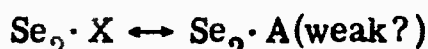
Pump prepared reactive (not chemically stable) neutral atoms from their ground state or from prepared excited states

Not yet studied.

Pump prepared ionized atoms from ground state or from prepared excited state

Not yet studied.

Pump prepared reactive molecules; within or up from the electronic ground state; or within or up from a prepared excited state; rotation-vibration or electronic-rotation-vibration transition.



Also, several high temperature oxides and hydrides, and a short-lived high level in NO.

Pump prepared ionized molecules; within or up from ground state or prepared excited state; positive or negative charged molecules; diatomic or polyatomic molecules; allowed or forbidden transitions; electronic or vibrational transitions; pumping into a stable fluorescing state or into a metastable state or into the dissociation continuum — in the latter case, lasing an excited atom product — an excited molecular fragment product.

Not yet studied.

2. Preliminary Notes on HCN, Cs_2 and N_2^* as Transformer Media With Nd-Glass Laser Pumping

2.1 HCN Gas

The rotation-vibration band constituting the third harmonic of the ν_3 fundamental vibration of the hydrocyanic acid molecule HCN would overlap the emission region of Nd glass lasers near 1.06μ . The same would be true for the hydrazoic acid molecule HN_3 , as well as for several other more complex molecules.

However, all of these $3\nu_3$ bands are extremely weak for transformer laser use. Although direct measurements are not available, from all the evidence found in the literature it seems likely that the natural lifetime of the upper level of the $3\nu_3$ band in HCN must be about 10^4 sec. Badger and Binder (1931) had to use a 280 cm tube at atmospheric pressure of HCN in order to get enough path length to observe the $4\nu_3$ and $(3\nu_3 + \nu_1)$ bands near 6000\AA .

In view of this, no further study has been made of the use of third harmonic rotation-vibration bands for the desired medium.

2.2 Cesium Vapor*

The vapors of the alkali metals are largely monatomic, but at elevated temperatures there is a component of diatomic molecules amounting to several percent. As mentioned in Section 1, the Na₂ molecule seemed serviceable as the medium for a laser transformer to be pumped by a battery of ruby lasers. However, the spectrum of the Cs₂ molecule is considerably more complicated than that of Na₂, because the molecule is heavier and so does not display such rigid electronic selection rules. Also, this spectrum has never been thoroughly mapped and only fragments of it have been analyzed. In order to estimate the probable behavior of Cs₂ as a transformer medium we shall have to extrapolate from what is known of the spectra of the other alkali molecules.

The energy levels of the diatomic alkali molecules may be understood most easily through their derivation from the parent monatomic alkali levels. The most important of these are sketched in Figure 2. Each of the neutral alkali atoms has a single s electron outside of closed shells, which produces $^2S_{\frac{1}{2}}$ ground states. The first excited levels for each atom arise when the single electron is moved into a p orbit, yielding 2P levels.

Now, when two identical alkali atoms in their ground states unite to form a diatomic alkali molecule, the resulting molecular states are

$$(2S_{\frac{1}{2}} + 2S_{\frac{1}{2}}) \rightarrow {}^1\Sigma_g^+ \text{ and } {}^3\Sigma_u^+.$$

* All of the standard molecular spectroscopic theory summarized for background in this and other succeeding sections of this report may be found discussed in more detail, in, for example, Herzberg's book.

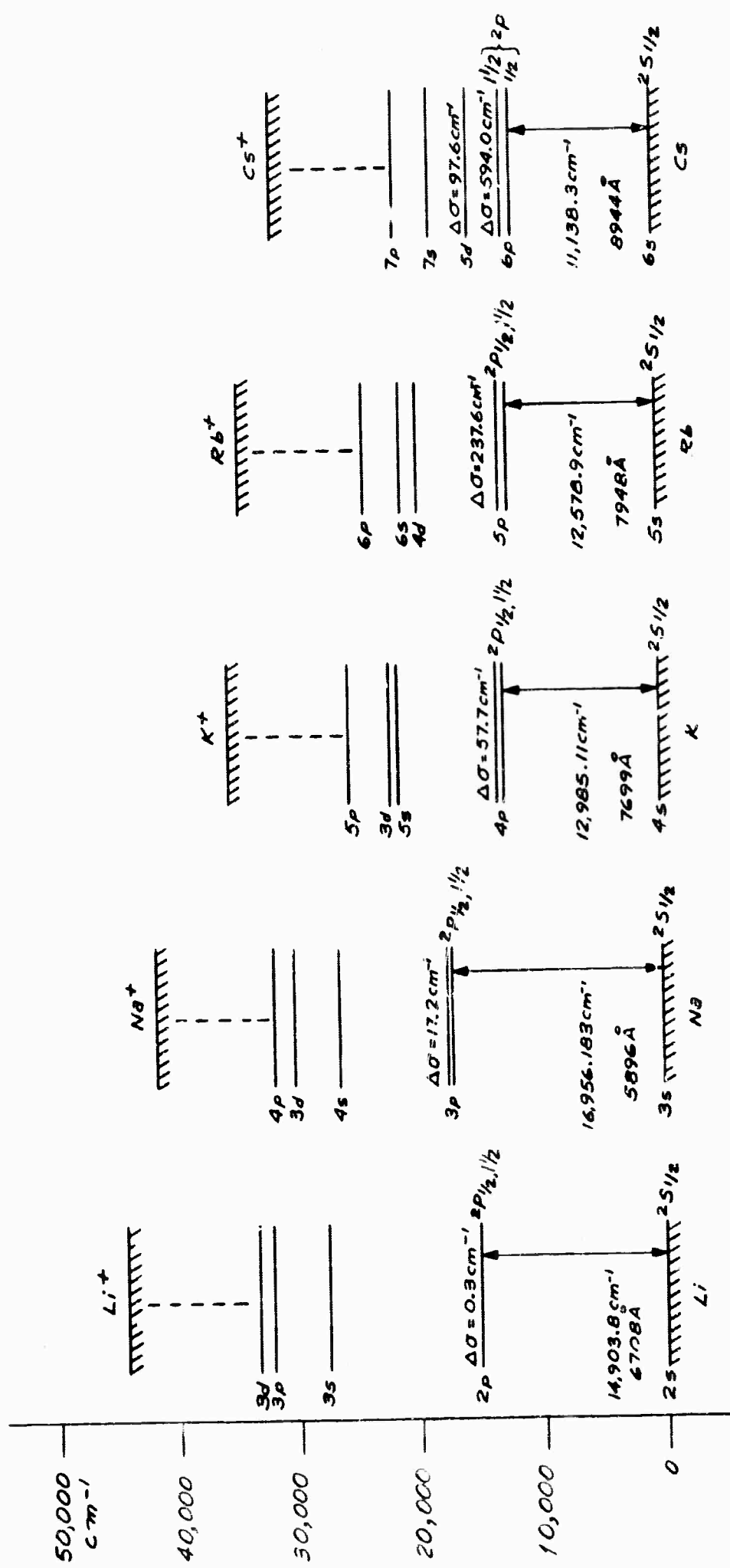
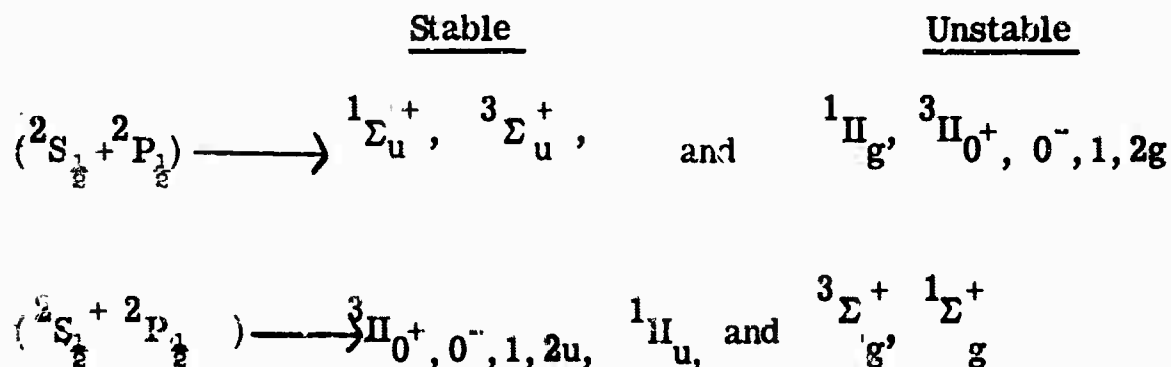


Figure 2.
Lower energy levels of the alkali atoms.

Of these, the $^1\Sigma_g^+$ is the lowest in energy and is the observed ground state, labelled X $^1\Sigma_g^+$, for each of the alkali molecules. The $^3\Sigma_u^+$ is theoretically expected to be unstable in all the alkalis — that is, the two atoms repel each other at all distances when they happen to approach with spins parallel.

The first excited states of these homonuclear molecules arise from the union of an s ground state atom and an atom in its first excited p states.



Theoretical calculations* show the first two multiplets listed in each of the above sets of four to be stable, and the other pairs to be unstable. Since the ground states of the alkali molecules are $^1\Sigma$'s, the absorptive transitions from these to the above stable singlets are highly allowed. The standard labels of these first observed excited states are A $^1\Sigma_u^+$ and B $^1\Pi_u$. But intersystem transitions are usually forbidden, and so the stable triplet

* See Mulliken (1932).

levels have never been directly observed, at least in the lighter molecules of the series.

In addition to the homonuclear diatomic alkalis—the series from Na_2 to Cs_2 — it is well known that vapors of the mixed metals contain important percentages of such combination molecules as NaK , NaCs , KRb , RbCs , etc. These molecules possess all of the above types electronic levels as well as a few more, due to the removal of the homonuclear degeneracy restrictions.

Figure 3 sketches the locations of all known electronic levels of the alkali molecules, together with all of the identifications which are accepted by Barrow (1963) in his recent surveys of these spectra.

The stable triplets are not shown in Figure 3 since they are not directly observable through absorption from the ground state. However, the reality and approximate location of the $^3\Pi_u$ can be inferred from the perturbation which it causes in state A for at least three of the alkali molecules. Through the arrangement called the "magnetic resonance spectrum", the presence of a perturbing effect can be seen for several of the rotational levels in each of several of the vibrational levels of $A^1\Sigma_u^+$ in Na_2 , NaK , and K_2 . The cause of this can be understood theoretically as due to very close coincidences between these levels and similar rotation-vibration levels

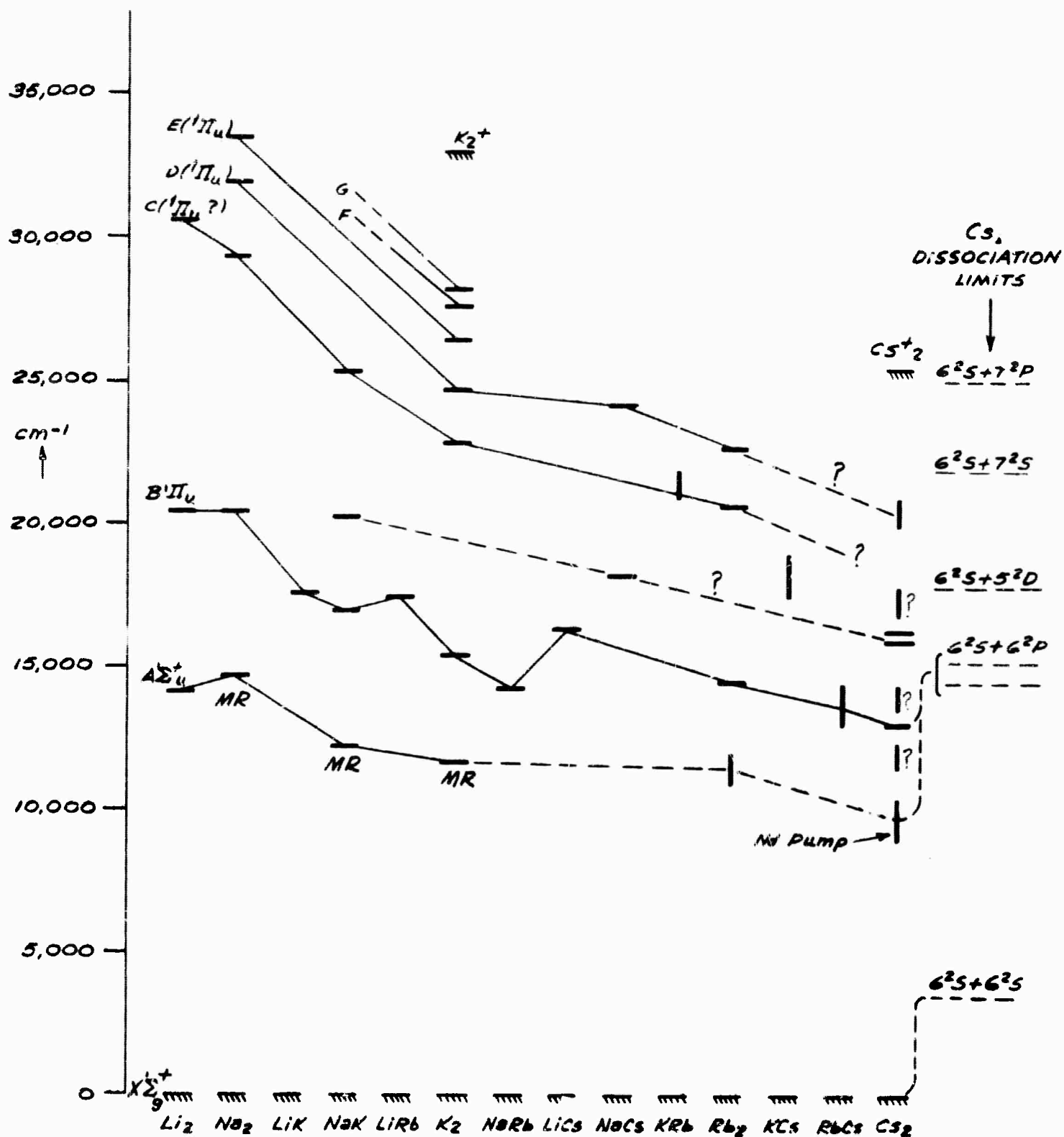


Figure 3.

Electronic levels of the alkali molecules. MR indicates levels whose magnetic resonance spectra are ascribed to perturbation. Vertical bars indicate absorption band regions where the exact electronic level position is uncertain.

of $^3\Pi_0^+u$, which must be very close to $A^1\Sigma_u^+$ in all of these molecules.

The coincidences mix the wavefunctions and cause these particular singlet levels out of the A complex to take on a partial triplet character. Among other results, transitions from these particular levels to the singlet ground state X become weaker than the transitions from the other neighboring rotation - vibration components of state A.

Let us now consider the spectrum of Cs_2 more particularly. Some of its bands were first recorded in absorption by Dunoyer (1912) and in (weak) fluorescence by McLennan and Ainslie (1923). Various later workers extended the spectra until absorption bands had given indication of probable electronic states in at least all the locations marked in Figure 3. The number of probable levels makes it clear that in a molecule as heavy as Cs_2 the prohibition against singlet-triplet transitions has been removed, and some of these levels must be observable members of the stable triplets. Since the molecule has such a large moment of inertia, its rotational levels are very close together. Complete experimental resolution of the band structure, which would probably permit identification of the electronic states, is usually not possible.

Another possible reason for the occurrence of more low levels in Cs_2 than in the lighter members of the series may be seen from Figure 2. In the Cs atom the 5d level occurs almost as low as the 6p. Cs_2 molecules built upon ($^2S_{1/2} + ^2D$) would have a large number of electronic states intermixed in location with those arising from ($^2S_{1/2} + ^2P$).

The particular absorption band system which is probably pumpable by Nd glass laser light lies in the infrared beyond about 8735\AA . It was first noted by Matuyama (1934) and by Loomis and Kusch (1934), independently. Finkelburg and Hahn (1938) extended the measurements of what are probably unresolved vibration band heads as far as $11,292\text{\AA}$, completely overlapping the position of the Nd glass laser emission band.

By extrapolation in Figure 3, it seems reasonable to conclude that this band system represents primarily the highly allowed transition ($A^1\Sigma_u^+ \leftarrow X^1\Sigma_g^+$). However, Finkelburg and Hahn observed slightly different band head locations than Loomis and Kusch—doubtless because of differences in instrument resolution in dealing with a very complex spectrum — and also saw recurring wavenumber differences and unusual fluctuations in intensity which made them believe that more than one upper electronic level was involved.

In view of the perturbations which have since been explained in the lowest Na_2 , NaK , and K_2 levels, it seems likely that the $^3\Pi_u$ state lies very close to $A\ ^1\Sigma_u^+$ in Cs_2 .

Such complexities do not necessarily preclude successful use of cesium vapor as a transformer medium with Nd glass pumps. However, the probable presence of a large number of unknown, as well as known, levels in the general neighborhood of $18,000\text{ cm}^{-1}$ above the ground state might perhaps do so. Molecules which had absorbed one Nd pump light quantum, and so resided in $\text{Cs}_2 \cdot A (+ ^3\Pi_u ?)$, might then absorb a second quantum to arrive at one of these unknown upper levels. If collisions dissociated the molecule from such a highly excited state before it returned to state A, or if it did not dissociate but merely fluoresced back to some place other than state A, the transformer efficiency could be greatly impaired. It should be noted that even though a high level position has not been indicated by absorption from $\text{Cs}_2 \cdot X$, it might still be very easily reached by second quantum absorption from $\text{Cs}_2 \cdot A (+ ^3\Pi_u ?)$, since the selection rules could be quite different for the two transitions.

In view of this uncertainty, further analysis on Cs_2 has been suspended until other possible transformer media have been investigated to some degree.

2.3 Metastable Nitrogen

During the period covered by this report, recent literature on the spectroscopy and the molecular collision properties of the nitrogen molecule which seemed relevant to its use as a transformer medium has been collected, and has been studied to a limited degree. The number of processes in which this molecule may be involved is quite large, but as the experimental and theoretical information is voluminous, there is some reason to hope that enough data will be available to deal with the complexities. Since it is expected that a considerable analysis of the possible metastable nitrogen transformer may be available for the next Technical Summary Report under this contract, only a very brief sketch of the possibilities will be given at this time.

The most promising transitions to be pumped by Nd glass lasers would be those of the "first positive system" of N_2 , which constitutes the transition $N_2 \cdot (B^3 \Pi_g \longleftrightarrow A^3 \Sigma_u^+)$. A sufficient population of metastable $N_2 \cdot A$ molecules might be prepared by use of an electric discharge through the nitrogen — among other possible methods. If such a discharge was indeed employed, the situation could become complicated by the additional presence of N_2 molecules in several other metastable states, as well as N_2^+ molecular ions, and N atoms and N^+ and N^{++} atomic ions in various states containing stored electronic or vibrational energy. Figure 4 shows the energy locations of these various levels.

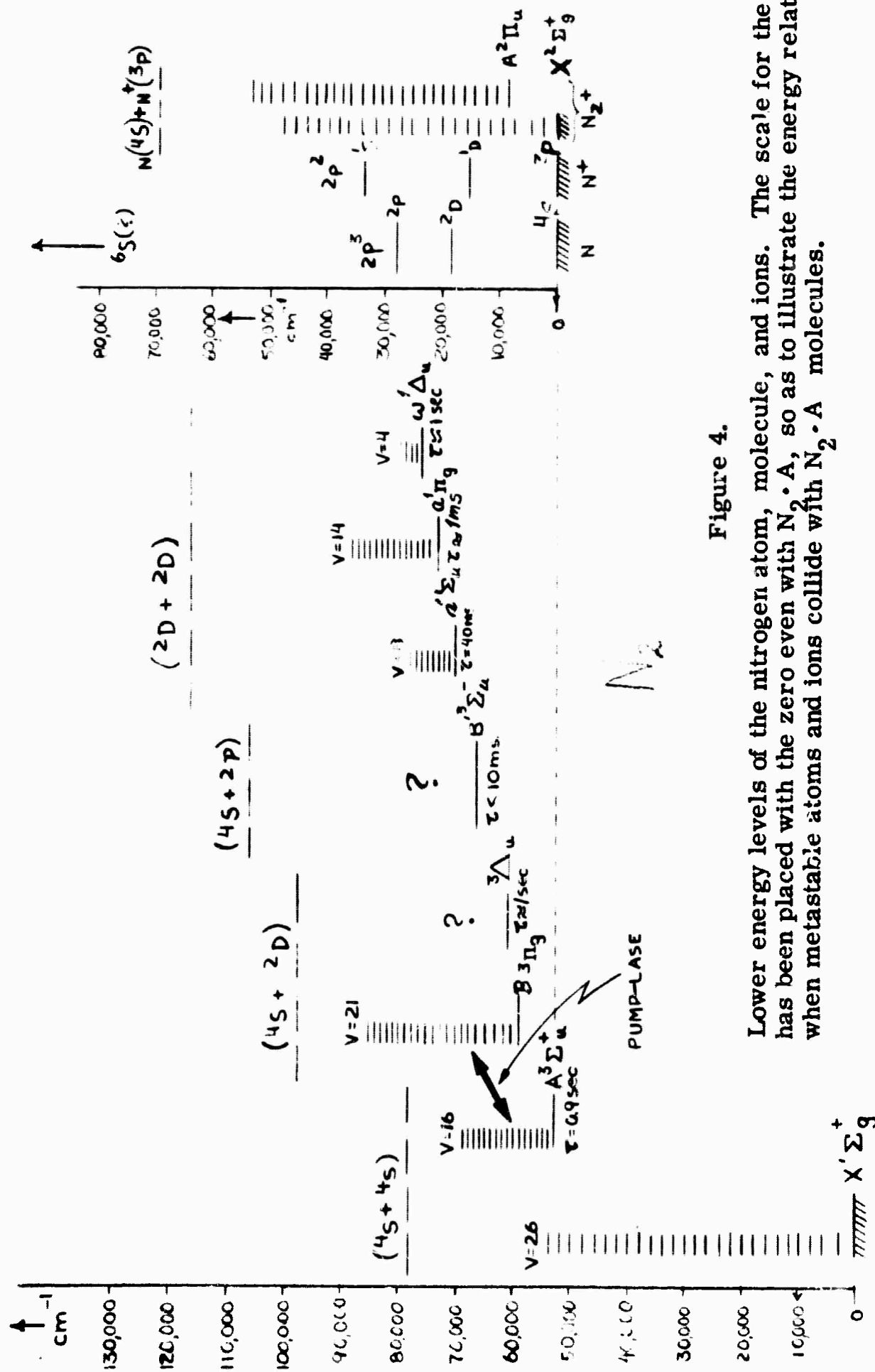


Figure 4.

Lower energy levels of the nitrogen atom, molecule, and ions. The scale for the inset has been placed with the zero even with N₂·A, so as to illustrate the energy relations when metastable atoms and ions collide with N₂·A molecules.

The radiative lifetime of the metastable state $A^3\Sigma_u^+$ ($v = 0$) has been measured as ~ 2 sec (Carleton and Oldenberg, 1962, and Oldenberg, Bills, and Carleton, 1961), and the rate coefficient for destruction of this state by metastable-metastable collisions has been determined as 3.3×10^{-10} cm³/sec, (Zipf, 1965). The radiative lifetime of $B^3\Pi_g$ is about 9.1×10^{-6} sec, (Jeunehomme and Duncan, 1964) Laser oscillations have been produced (Mathias and Parker, 1963) in 28 lines of this system and 7 of these have been assigned to the 0-0 band which lies (Kenty, 1964) near 1.05μ .

Given a sufficient population of $N_2 \cdot A^3\Sigma_u^+$ metastables, it is possible that a laser transformer could then be operated by re-cycling this population between certain rotational sublevels of the upper $B^3\Pi_g$ and the lower $A^3\Sigma_u^+$ states. An analysis of the population inversions obtained by pumping with a Nd^{3+} (or perhaps Pr^{3+}) laser will be more complex than that for Na_2 pumped by a ruby laser since there are 27 rotational branches in each band.

Although our literature search has not been completed, the highest reported population density we have found is 4.5×10^{14} $N_2 \cdot A^3\Sigma_u^+$ molecules/cm³ (Dunford, 1963). It is generally accepted (Mannella, 1963) that these metastables arise from the recombination of N atoms previously dissociated in an electrical discharge through N_2 .

At first glance it might seem that nitrogen should be immediately selected as the leading prospect for a transformer medium, since it is already known to be capable of lasing in the precise bands which could be used with Nd glass

pumping. However, this fact actually has little relevance to the high power transformer problem. In the experiments referenced the preparation of the N_2 metastable molecules was by means of an electric discharge, and the lasing was at low power and of very short pulse duration. There was no necessity in that work to maximize power efficiency and minimize gas heating, by close control of all the possible relaxing and quenching collisions. Also, there was no need to set up a high speed pump-lase-pump-lase repetitive use of the molecules.

A degree of preliminary explaration of the metastable nitrogen transformer laser problem was carried out, sufficiently to make it seem likely that CN would actually be less difficult. The initial serious attack on the problem was therefore begun with that molecule, which will be the subject of the remainder of this report.

3. GENERAL DESCRIPTION OF CN LASER TRANSFORMER CONCEPT

After the consideration of a large number of molecular details during the course of the present report period, a first approximate trial concept for a CN laser transformer design has emerged. This general picture will be presented briefly here, as a background for the more detailed analysis of succeeding sections

Ordinary chemically stable cyanogen gas at temperatures less than 1000°C consists largely of dimer molecules $(\text{CN})_2$. The transformer medium in the suggested design concept will contain about 3cm pressure of cyanogen gas in perhaps 20 cm or more of He, with the mixture at about 210°K . A preparatory flash of fairly monochromatic ultraviolet light with wavelength in the neighborhood of 2000\AA will dissociate the majority of the cyanogen molecules into CN fragments. The CN molecules will be produced in their electronic ground state $\text{CN}^{\cdot}\text{C}$, and may be predominantly in the lowest vibrational level thereof, $\text{CN}\cdot\text{X}(v = 0)$.

There are several regions within the perhaps 700\AA breadth of the Nd-glass fluorescent emission band centered near 1.06μ which are absorbable by $\text{CN}\cdot\text{X}$ molecules. Two of these represent particularly interesting situations. It is at present uncertain at which of these regions within the fluorescent band Nd glass pump lasers can be made to operate most efficiently. In the two cases the pumping would be in either the (0, 0) band or the (6, 5) band of the

CN· (A ← X) absorption system, near 1.090μ or near 1.045μ , respectively. For the latter arrangement, the necessary population of CN· X molecules in their ($v = 5$) vibration state would be produced by including flux near 3900\AA in the preparatory ultraviolet flash. The effect of this near UV radiation will be to transfer a major fraction of CN· X molecules from ($v = 0$) to higher vibration states, by a two-step process to be discussed in a later section.

During the Nd glass laser power pumping flash, collisions with the He atoms will be striving to maintain Boltzmann equilibrium population distributions among the rotation levels of all the vibration states of both CN· X and CN· A. It will be shown that the steady state rotational distributions will produce strong inversion in numerous P-branch lines of the (0, 0) and/or (6, 5) bands, whenever intense pumping of the R-branch lines is being maintained. The result will be to carry perhaps 1% of the CN molecules very rapidly around a pump-lase-pump-lase cycle within one of these bands. At a location in the gas medium where the lasing flux in suitable P-branch lines has been built up to very high levels—under the initial stimulus of flux at the desired wavelengths from the "trigger section"—and whenever Nd glass laser pumping is also very intense, an average molecule will be carried around this cycle many hundreds of times during a perhaps one millisecond power flash. Output wavelengths would be near 1.12μ and/or 1.07μ .

* We will not be interested in such high levels that the rotational spacing becomes larger than kT where equilibrium would be slow of attainment—as in the HCl molecule.

In order to achieve a diffraction limited plane wavefront output beam, great attention must be placed on maintaining closely isothermal conditions throughout the gas medium during the preparatory and power flashes. After the flashes are over, the gas is to be circulated through a heat exchanger before the next flashes. Actually, the gas would probably be circulated continuously at high velocity, so that conditions would be suitable for a pulse every second or so. Detailed consideration of heating conditions has not yet been undertaken; however, features are apparent which could — in principle — maintain constant temperature. As will be discussed in later sections, these include (a) control of dissociation waste heat by careful choice of the wavelength of the preparatory flash, (b) minimization of vibrational relaxation and electronic quenching by operating with He gas at low temperature and not too great a pressure, and (c) adjusting the output flux density so as to balance thermal effects from the input-output quantum size difference against those from the input-fluorescence quantum size difference — the principle of "molecular refrigeration".

Adjustment of these parameters to maintain practically constant temperature will almost automatically lead to minimum wastage of energy throughout the system, so that over all transformer efficiency of 80-90% can reasonably be sought for.

In the next section, detailed consideration of the molecular properties underlying this first design concept, for a transformer laser to be pumped by Nd glass lasers, will be started with a background description of the CN molecular spectrum.

4. ENERGY LEVELS OF THE CN MOLECULE

Consideration of the CN molecular energy levels is most easily begun with a listing of the C and N atomic levels with which they can be approximately correlated.

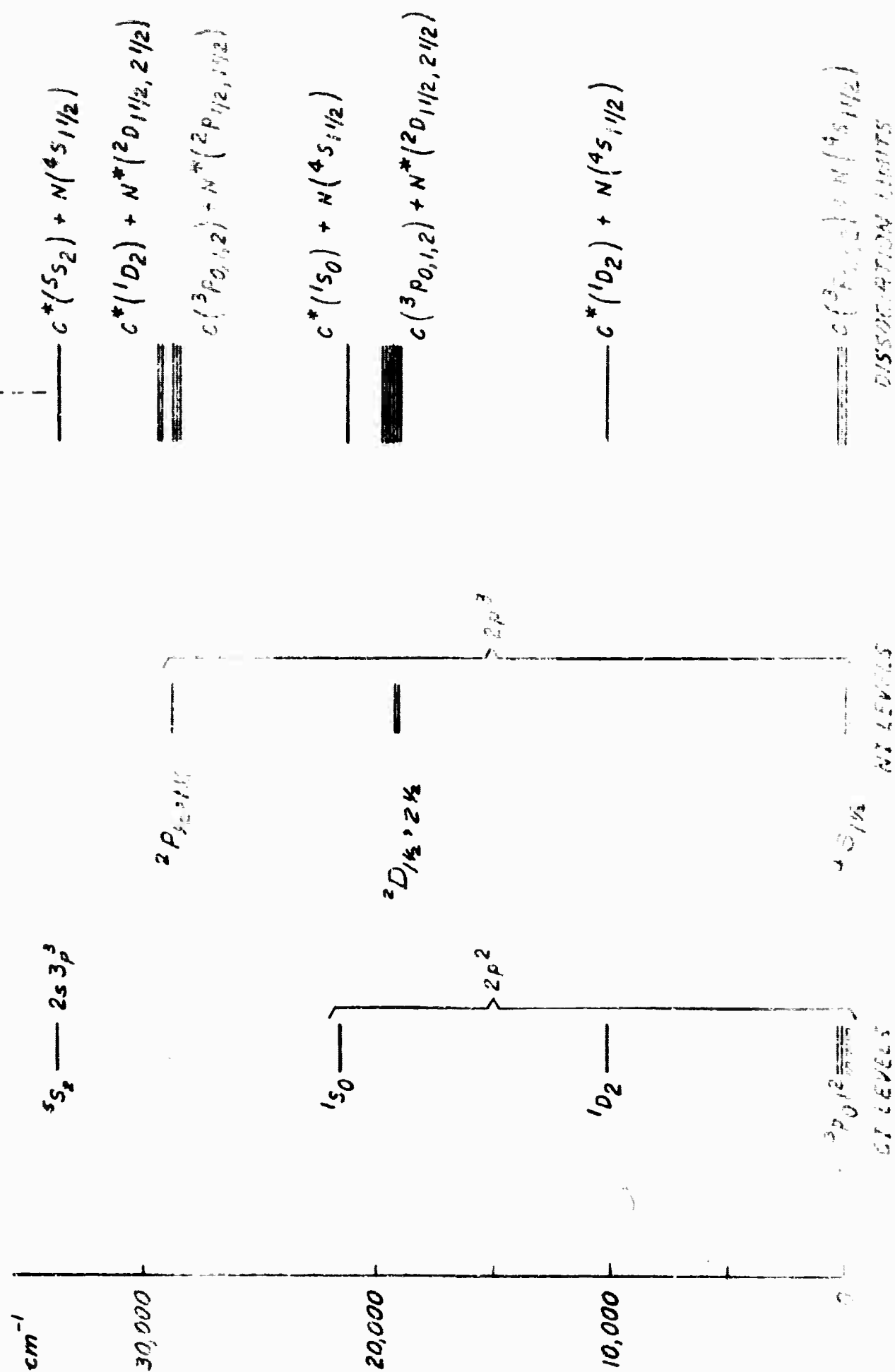
4.1 Lowest Levels of the C and N Atoms

The ground electronic configuration of the neutral carbon atom is $1s^2 2s^2 2p^2$. This $2p^2$ configuration yields the multiplets $^3P_{0,1,2}$ and 1D_2 and 1S_0 . The first excited electronic configurations are $1s^2 2s 3p^3$, whose only really low multiplet level is 5S_2 , and $1s^2 2s^2 2p 3s$, which yields $^3P_{1,0,2}$ and 1P_1 . Figure 5 shows the level spacing. Other configurations follow upward in the usual manner.

The carbon in natural carbonaceous materials consists 98.9% of C^{12} , which has nuclear spin $I = 0$ and so shows no hyperfine structure. The spectrum lines of the rare isotope C^{13} are observable very weakly in the usual sources, but they would not be expected to affect the laser transformer.

The ground electronic configuration of the neutral nitrogen atom is $1s^2 2s^2 2p^3$. This lowest configuration leads to the multiplets $^4S_{1\frac{1}{2}}$, $^2D_{1\frac{1}{2}, 2\frac{1}{2}}$ and $^2P_{\frac{1}{2}, 1\frac{1}{2}}$. The first excited configuration lies quite high, and is not likely to be involved in the laser transformer. These N levels shown in Figure 5 are the same as in Figure 4.

The lower energy levels of neutral carbon and nitropane and the dissociation limits for the CN molecule.



Nitrogen as found in nature consists 99.6% of N^{14} . The spectrum lines of the rare isotope N^{15} are observable very weakly in the usual sources, but they would not be expected to affect the laser transformer. The N^{14} nucleus has spin $I = 1$, with magnetic moment $\mu = +0.4065\text{nm}$, which leads to observable hyperfine structure in the nitrogen atomic spectrum, as well as in the cyanogen molecular spectrum. However, this hfs splitting is so small in CN ($\sim 10^{-4}\text{cm}^{-1}$) that it seems likely it can be ignored for the present transformer laser problem.

4.2 Electronic States of the CN Molecule

To a fair approximation, each electronic state of a lightweight, 13-electron, diatomic molecule such as CN can be characterized in terms of a pair of specific states of the C and the N atoms into which that molecular state would dissociate, if the internuclear separation were to be continuously increased.

The energy separations of these possible dissociation limits, with which various electronic states of CN might be correlated, are easily determined by making various combinations of those states of the separate atoms just listed.

4.2.1 The CN Dissociation Limits and Theoretical States

The lowest such limits, energetically, arise when each of the separated atoms is to be left in its ground multiplet, which means $C(^3P_{0,1,2}) + N(^4S_{1\frac{1}{2}})$. Higher dissociation limits correspond to separating the molecule into a pair of atoms of which one or both is left in an excited state. Figure 5 shows the energy relations among the various combinations.

The electronic states of the CN molecule which are expected to be correlatable with each of the dissociation limits were derived years ago from the quantum theory of such molecules, as listed in the following table.

<u>Dissociation Limit</u>	<u>Correlated Molecular States</u>
$C^*(^5S_2) + N(^4S_{1\frac{1}{2}})$	$^2\Sigma, ^4\Sigma, ^6\Sigma, ^8\Sigma$
$C^*(^1D_2) + N^*(^2D_{1\frac{1}{2}, 2\frac{1}{2}})$	$^2\Sigma, ^2\Pi, ^2\Delta, ^2\Phi, ^2\Gamma, \text{ (some repeated)}$
$C(^3P_{0,1,2}) + N^*(^2P_{\frac{1}{2}, 1\frac{1}{2}})$	$^2\Sigma, ^2\Pi, ^2\Delta, ^4\Sigma, ^4\Pi, ^4\Delta, \text{ (some repeated)}$
$C^*(^1S_0) + N(^4S_{1\frac{1}{2}})$	$^4\Sigma$
$C(^3P_{0,1,2}) + N^*(^2D_{1\frac{1}{2}, 2\frac{1}{2}})$	$^2\Sigma, ^2\Pi, ^2\Delta, ^2\Phi, ^4\Sigma, ^4\Pi, ^4\Delta, ^4\Phi, \text{ (some repeated)}$
$C^*(^1D_2) + N(^4S_{1\frac{1}{2}})$	$^4\Sigma, ^4\Pi, ^4\Delta$
$C(^3P_{0,1,2}) + N(^4S_{1\frac{1}{2}})$	$^2\Sigma, ^2\Pi, ^4\Sigma, ^4\Pi, ^6\Sigma, ^6\Pi$

4.2.2 The Observed Electronic States of CN

In so light a molecule as CN, the selection rule forbidding intersystem transitions is expected to be fairly rigorously obeyed. Since the ground state of the molecule must surely be a $^2\Sigma$, at least the absorption spectrum should consist almost wholly of transitions among doublet states, with all levels of higher multiplicity remaining practically invisible.

Actually, this is found to be the case both for the absorption spectrum and for all CN emission spectra. There is no evidence that any manner of chemical or electrical excitation used so far, or any collision process observed so far, has placed CN molecules in other than doublet states. If any molecules have ever been placed in the quartet and higher groups — as may indeed have happened — no detectable effect has yet been seen from them.*

Neglecting fine structure for the moment, the observed electronic states of CN are as given in the following table. These values, collected by Carroll (1956), include new high levels found since publication of Herzberg's book.

* Perhaps the majority of these are unstable states, with repulsive potential curves.

Probable <u>State</u>	Observed <u>Energy</u>
J $^2\Delta$	65,274 cm $^{-1}$
H $^2\Pi$	\sim 61,050 cm $^{-1}$
F $^2\Delta$	\sim 59,750 cm $^{-1}$
D $^2\Pi$	54,501 cm $^{-1}$
B $^2\Sigma^+$	25,752 cm $^{-1}$
A $^2\Pi$	9,242 cm $^{-1}$
X $^2\Sigma^+$	0 cm $^{-1}$

The molecular ground state X $^2\Sigma^+$ obviously arises from the union of the single atoms in their ground multiplets, C (3P) + N (4S). The vibrational sublevels of the lowest electronic states have been explored to high enough J-values, by Jenkins, Roots and Mulliken (1932), for example, to be certain that A $^2\Pi$ dissociates into the same constituents as X $^2\Sigma^+$. Only two doublet levels are expected to be associated with this limit, and they surely must be X and A. The vibrational analysis shows that B $^2\Sigma^+$ correlates with a dissociation limit about 20,000 cm $^{-1}$ higher than the limit for X and A; so CN· B is very likely one of the states expected from C (3P) + N* (2D).

The amount by which the molecular ground state $X^2\Sigma^+$ is energetically stabilized below the dissociation limit $C(^3P) + N(^4S)$ has been a matter of uncertainty for many years. The most recent studies, by Knight and Rink (1961), Berkowitz (1962), and Kudryavtsev, Gippius, Derbeneva, Pechenov and Sobolev (1963), seem to indicate that this energy of stabilization of $CN^* X$ is about 7.5 or 7.6 eV, which would be around $61,000 \text{ cm}^{-1}$. We have the situation that the pattern of all the possible dissociation limits is quite exactly known, and the pattern of the experimentally found molecular states given above is known with considerable exactness, but the connecting energy location link between them may still admit of appreciable adjustment. Assuming for the time being that the ground state dissociation energy is $D_0^0(CN) \approx 61,000 \text{ cm}^{-1}$, the energy level diagram for the known electronic states of CN becomes as shown in Figure 6 — omitting all fine structure in the levels and in the limits.

Those transitions which have been observed to date are indicated by arrows on the diagram. The two very well known band systems lying principally in the visible region of the spectrum are the "Violet Cyanogen Bands", which constitute the (B-X) transition, and the "Red Cyanogen Bands", which are (A-X). Some of the latter fall in the region pumpable by Nd glass lasers, and are the ones to be employed in the laser transformer under discussion here.

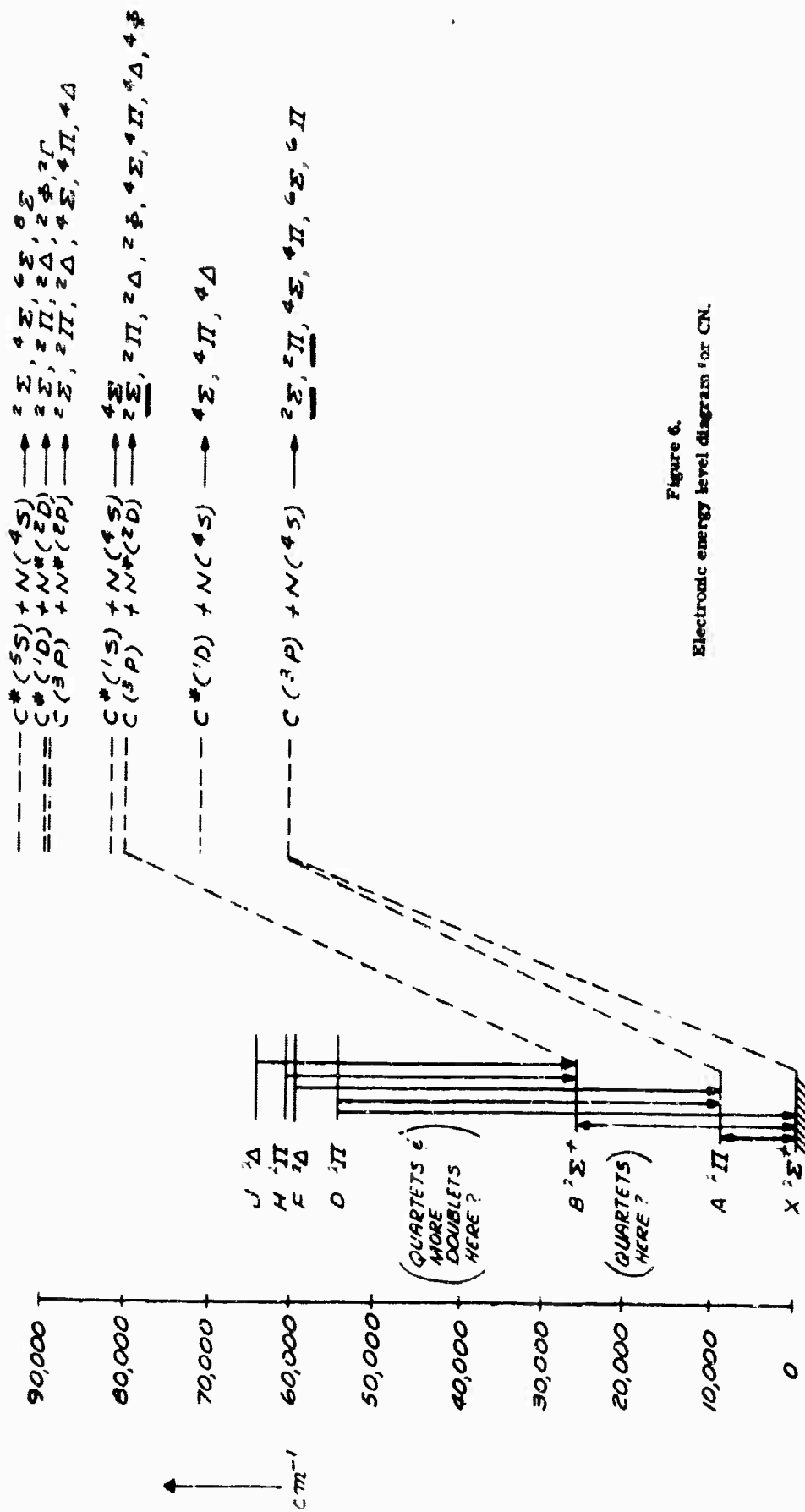


Figure 6.
Electronic energy level diagram for CN.

The diagram indicates that there are doubtless a number of still unobserved doublet levels to be found between the locations of B and D, although it would seem unlikely that any more doublets will be lower than B. The invisible quartets are probably strewn over a wide region from the neighborhood of A upwards. Just as with the Cs_2 molecule, the presence of these still unknown levels is important for its bearing on the possibility of absorption of a second Nd pump laser quantum, by molecules which have already been excited into $\text{CN} \cdot \text{A}$. However, the location of the higher dissociation limits shown in Figure 6, with their remaining doublet states, makes it appear that the region of $18,000 - 20,000 \text{ cm}^{-1}$ is probably free of additional doublet levels. The presence of missing quartets in this region should not cause trouble in the laser transformer. Absorption to such a quartet state should be no more likely from $\text{A } ^2\Pi$ than from $\text{X } ^2\Sigma$. And, collisional transfer of molecules from A to a quartet must be quite unlikely, or its effects would have been observed before now.

4.2.3 Fine Structure of the Three Lowest CN Electronic States

The largest fine structure splitting occurring in any of the three lowest electronic levels X, A, and B is the 52.2 cm^{-1} separation

between $A^2\Pi_{1/2}$ and $A^2\Pi_{3/2}$. The $^2\Pi_{1/2}$ state lies at the lower energy of the two. Because of this 'inversion' from the more usual pattern, the state is sometimes given the label $A^2\Pi_i$. The doublet separation is basic to the $^2\Pi$ electronic levels themselves, arising from electron spin-orbit coupling.

In addition, each of the electronic states $A^2\Pi_{1/2}$ and $A^2\Pi_{3/2}$ is itself inherently doubly degenerate. If the molecule was non-rotating, this electronic degeneracy would not be removed and the two components of $^2\Pi_{1/2}$, for example, would have identical energy. This degeneracy occurs because the vector component of electronic orbital angular momentum can be either parallel or anti-parallel to the net electric field vector along the internuclear axis of the molecule, with no difference in energy between the two cases whenever the molecule is not rotating. Molecular rotation will lead to two separated energy states whose wavefunctions correspond to different probability combinations of these two vector orientations. This small energy splitting in each $^2\Pi$ state, caused by rotation, is known as Λ -type doubling. Its amount varies with the degree of rotation, as will be discussed later.

The two $^2\Sigma^+$ states are single and non-degenerate whenever the molecule is not rotating.

4.3 The CN Vibrational Levels and the Potential Curves

As an average figure, one can say that the spacing between the vibrational levels associated with each of these electronic states is about 2000 cm^{-1} . This figure is much larger than kT under most circumstances, so that thermal collisions alone will not produce much population above $v = 0$ for each state. A long vibrational ladder stretches upward in each state toward its dissociation limit, with each vibrational ladder following approximately the formula

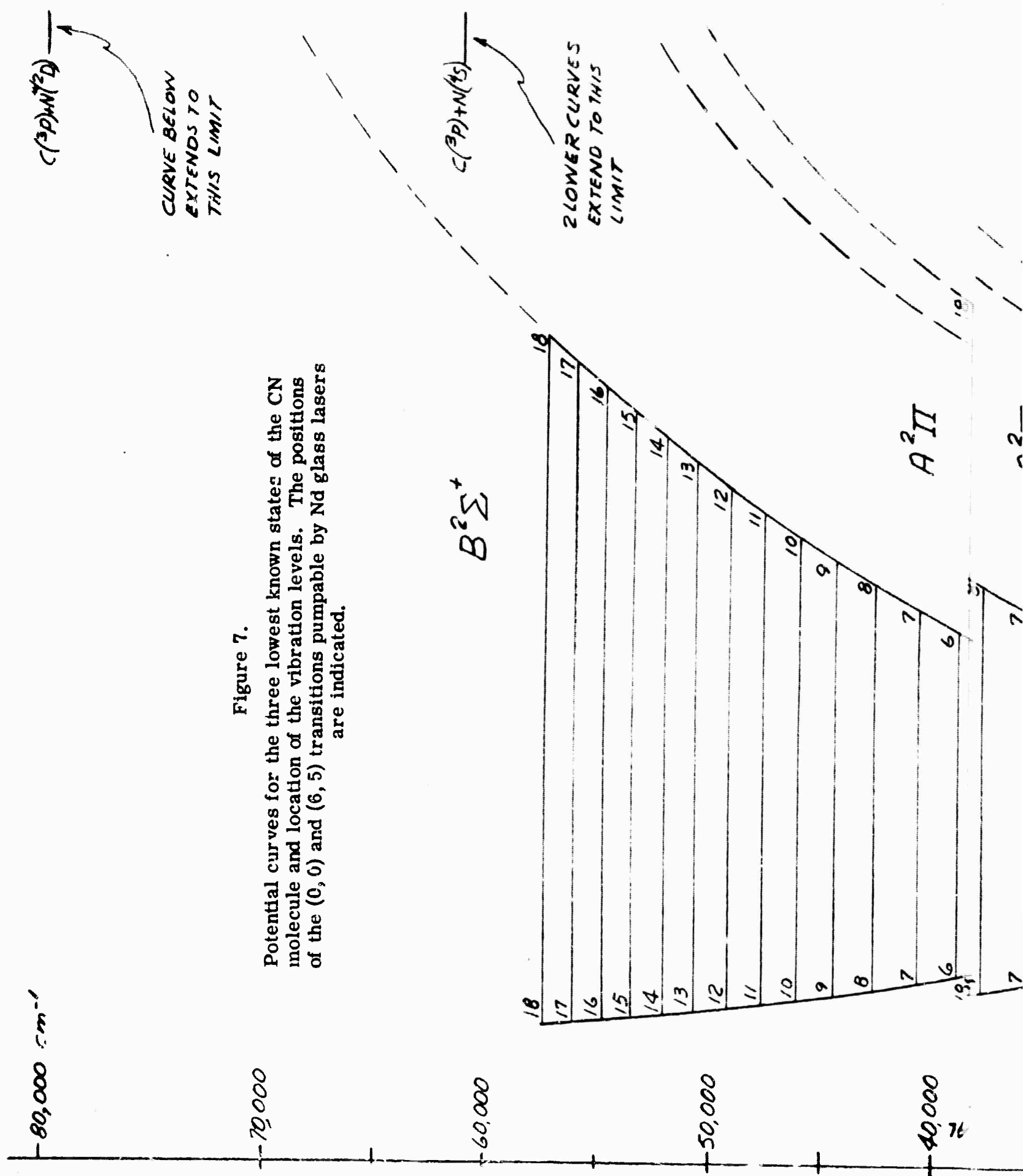
$$E_v = \omega_e \left(v + \frac{1}{2}\right) - \omega_e x_e \left(v + \frac{1}{2}\right)^2 + \omega_e y_e \left(v + \frac{1}{2}\right)^3.$$

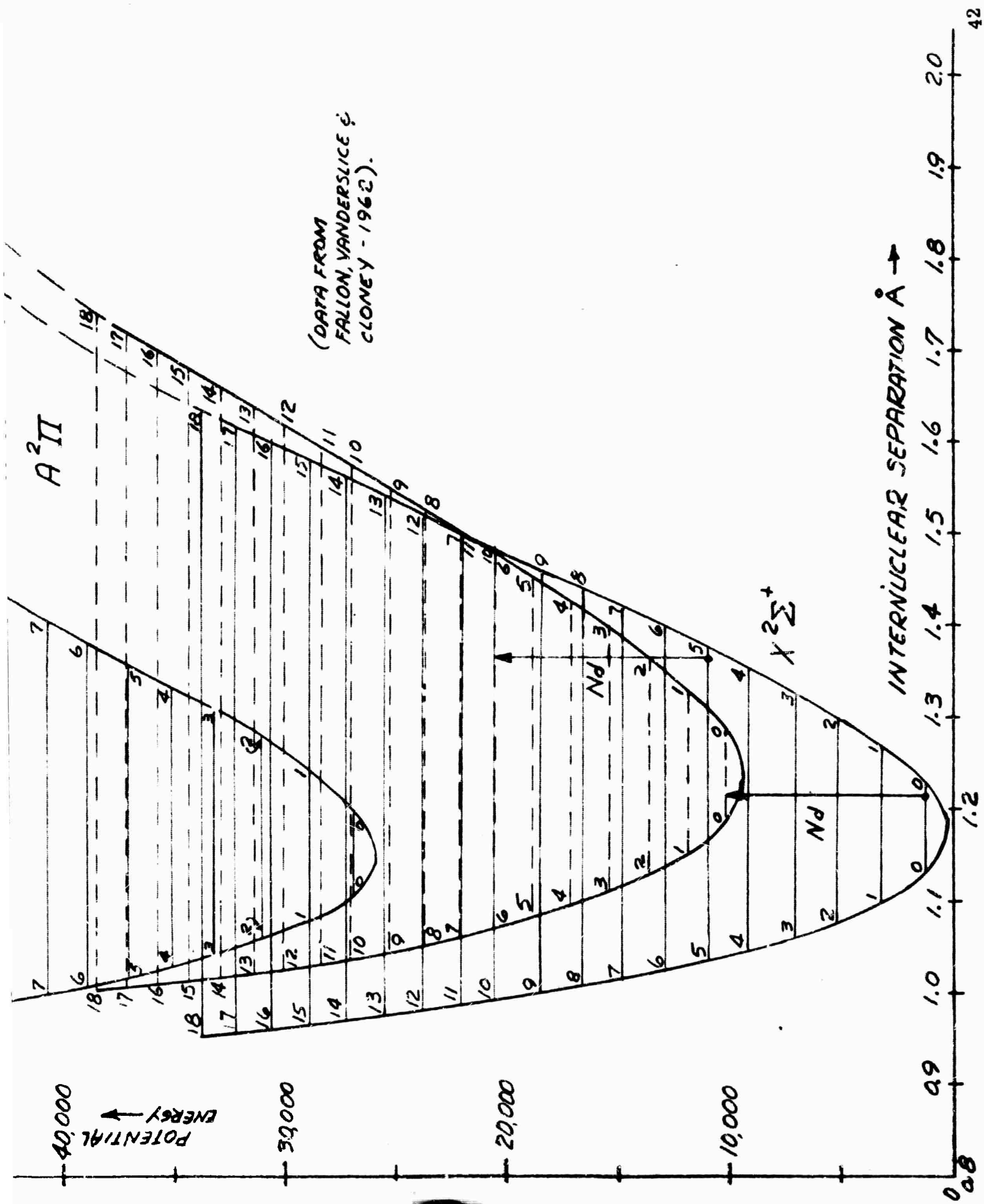
The most recent values for these constants, by Rigutti (1962), for states X and A, and as quoted in Herzberg's book for state B, are shown in the following table.

State	ω_e	$\omega_e x_e$	$\omega_e y_e$
B $^2\Sigma^+$	2164.13 cm^{-1}	20.25 cm^{-1}	
A $^2\Pi$	1812.564 cm^{-1}	12.578 cm^{-1}	-0.013 cm^{-1}
X $^2\Sigma^+$	2068.705 cm^{-1}	13.144 cm^{-1}	

In state B this approximate formula is not very accurate beyond $v = 3$, due to perturbations. The two components of $A^2\Pi$ have practically identical vibrational spacings, and so are not listed separately.

Potential energy curves deduced for these states by Fallon, Vanderslice and Cloney (1962) are shown in Figure 7, with the vibrational ladder indicated on each curve. The separations between the two sets of vibrational levels and potential curves for $A^2\Pi_{1\frac{1}{2}}$ and $A^2\Pi_{\frac{1}{2}}$ are too small to be shown on this scale. The (0, 0) and (6, 5) transitions, which are pumpable by Nd glass laser light, are shown on the diagram.





4.4 The CN Rotational Levels: Theory of Expected Patterns

4.4.1 The Unperturbed Rotational Levels of $A^2\Pi$

With each vibrational level of each of the $A^2\Pi$ states there is associated a set of rotational levels. These are describable in terms of J , the total angular momentum of the molecule. For $A^2\Pi_{1\frac{1}{2}}$, J starts with $J = 1\frac{1}{2}$ (corresponding to zero molecular rotation, when the only angular momentum is that of the electron spin-orbit resultant, which is $1\frac{1}{2}$), and J then takes all half-integral values proceeding upward. For $A^2\Pi_{\frac{1}{2}}$, J starts with $\frac{1}{2}$ and takes all larger half-integral values. The first 38 rotational levels in each set for ($v = 6$) are shown in Figure 8.

In both cases, each of the rotational levels except the lowest is actually a close doublet. This is the Λ -type doubling already mentioned as occurring in all the levels of electronic state A whenever the molecule is rotating. The two members of each Λ -type doublet have the same total angular momentum J , but they differ very slightly in energy, because of the differences in their wavefunctions. This doubling usually amounts to no more than a few tenths of a cm^{-1} , at least in the first 30 rotational levels of the CN-A vibration states. An estimate of its value for each of the lower levels of CN-A ($v = 6$) is included in Figure 8, from the experimental data of Jenkins, Roots and Mulliken (1932).

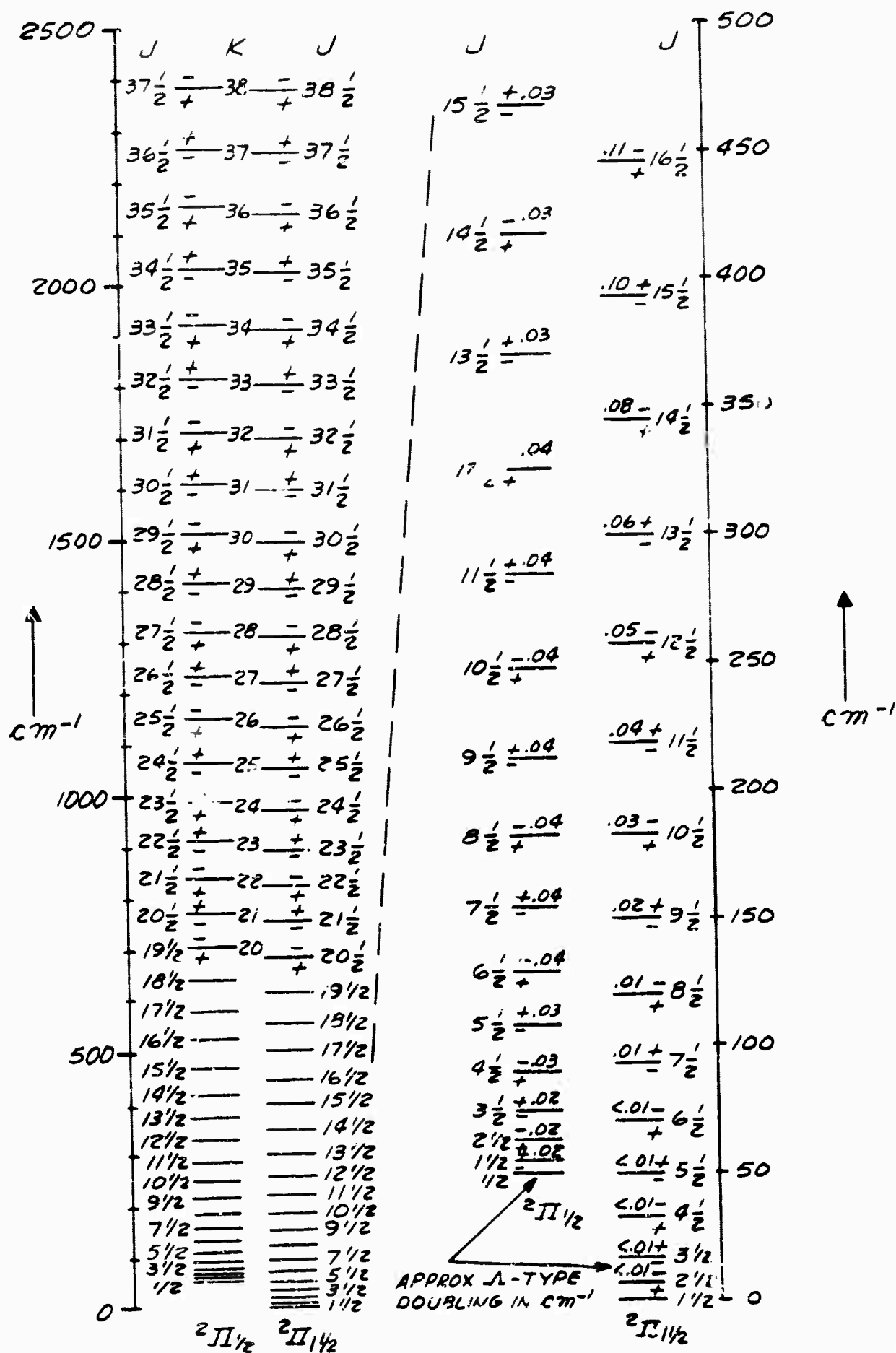


Figure 8
The Rotation Levels of $\text{CN}\cdot\text{A}(v=6)$.

Each A-type component carries a plus or minus sign. This is an indication of the symmetry of the molecular wavefunction of the level with respect to inversion in the origin of coordinates — a property which is of importance for selection rules governing optical transitions between CN· A and other states*.

For low J values, the rotational levels of $^2\Pi_{1/2}$ and $^2\Pi_{1/2}$ follow separately, to first approximation, energy formulas of the type

$$F(J) = B'_v J(J+1) + \dots$$

This pattern of energy levels exemplifies what is known as "Hund's coupling case (a)".

For high J values — fast rotation of the molecule — the total number of levels of a given J belonging to the sum of $^2\Pi_{1/2}$ and $^2\Pi_{1/2}$ is the same as at low J, but the level location pattern is different, as may be seen from Figure 8. At sufficiently high J, that the spacing between levels of adjacent J-values becomes comparable with the 52 cm^{-1} separation between the electronic states $^2\Pi_{1/2}$ and $^2\Pi_{1/2}$, the pattern begins to depart from the

*In various molecules which possess a $^2\Pi$ electronic state, the pattern of the \pm symmetry characters for the assemblage of low rotational levels may either be as shown in the diagram or else it may have + and - for all the levels reversed from the pattern illustrated. Jenkins, Roots and Mulliken (1932) demonstrated from their analysis of the (A-X) bands that the pattern illustrated in Figure 8 is the one appropriate to CN· A levels.

$B'_v \cdot J(J+1)$ formula. Sequences of rotational levels which at low J belonged to either ${}^2\Pi_{1/2}$ or ${}^2\Pi_{3/2}$ begin to regroup into a different pattern in such a way that the actual distinction between the two electronic states becomes lost.

Fairly close level pairs whose two members have consecutive J -values now become evident. Each member of the pair is still a close doublet, with \pm character as before*, since the small Λ -type doubling of each J level always persists. Quantum theory shows that each such pair can now be described in terms of a new quantum number K , where the members of the pair are $J = K + \frac{1}{2}$ and $J = K - \frac{1}{2}$.

*In the CN· A level patterns for low rotation, those levels of ${}^2\Pi_{1/2}$ whose J -values are even integers plus $\frac{1}{2}$ have the + member of the Λ -type doublet below and the - member above; and vice versa for alternate levels. On proceeding toward larger rotation, a continuous sequence of levels may be identified which will form a logical extension of the low- J ${}^2\Pi_{1/2}$ set, even though the label ${}^2\Pi_{1/2}$ has now lost its meaning. In the high rotation pattern for CN· A shown here, this sequence contains the lower J -values associated with each K -value. The property of having the + number of the Λ -type doublet below and the - member above for J equal to an even integer plus $\frac{1}{2}$ persists into the high- J regime, and the magnitude of the doubling increases monotonically with J .

In the CNA· ${}^2\Pi_{1/2}$ low-rotation patterns, the same rule on \pm character holds; however the magnitude of the splitting now at first increases with J and then decreases to zero again and eventually reverses its sign. In CNA($v = 6$), for example, Root and Mulliken found that the Λ -type doubling for the sequence of levels based on ${}^2\Pi_{1/2}$ fell to zero at about $J = 18\frac{1}{2}$. For larger J 's in this sequence, the absolute magnitude of the doubling increases again, but levels having J an even integer plus $\frac{1}{2}$ now have the + member above and the - below; and vice versa for the other levels of the sequence. The symmetry characters in Figure 8 illustrate this case of $v = 6$.

The quantum number J is still the measure of the total angular momentum of the molecule. The quantum number K describes the sum of all the constituent angular momenta of the molecule except those arising from electron spin. The total angular momentum J is computed as the vector sum of K and of the resultant-spin vector, which latter is $\frac{1}{2}$ for a ${}^2\Pi$ state.

Vectorially, it appears that the fast rotation of the molecule has broken that electronic spin-orbit coupling which differentiated the states ${}^2\Pi_{1\frac{1}{2}}$ and ${}^2\Pi_{\frac{1}{2}}$. It has allowed the electronic orbital angular momentum to be coupled independently to the molecular rotation angular momentum, so as to form the vector K , before the electron spin momentum adds to K to form the total J . Some recent authors use the letter N instead of K as the symbol for this quantum number.

Aside from the change in pattern of the rotational levels which results, the important point is that K is now a "good quantum number", and so becomes involved in the selection rules for allowed optical transitions at high rotation. This causes major differences in intensity for some analogous transitions, when comparing low-rotation cases and high-rotation cases, as will be discussed later.

The high-level pattern corresponds to what is known as "Hund's coupling case (b)". In this regime, to first approximation the energies of the centers of the pairs are describable by formula

$$F(K) = B''_v \cdot K(K+1) + \dots$$

That is, the K-pairs now proceed upward in much the same fashion as did the J-levels separately for ${}^2\Pi_{1\frac{1}{2}}$ and ${}^2\Pi_{\frac{1}{2}}$ in the low rotation region.

Hill and Van Vleck (1923) derived theoretical formulas which locate the centers of gravity of the Λ -type doublets for all the rotation regions—small, large and intermediate. In the case of the $\text{CN} \cdot A {}^2\Pi$ state these take the form:

$$F(J)_{2\Pi_{1\frac{1}{2}}} = B_v \left[(J + \tfrac{1}{2})^2 - 1 - \tfrac{1}{2} \sqrt{4(J + \tfrac{1}{2})^2 + \frac{A}{B_v} (\frac{A}{B_v} - 4)} \right] - D_v \cdot J^4 + \text{const.}$$

$$F(J)_{2\Pi_{\frac{1}{2}}} = B_v \left[(J + \tfrac{1}{2})^2 - 1 + \tfrac{1}{2} \sqrt{4(J + \tfrac{1}{2})^2 + \frac{A}{B_v} (\frac{A}{B_v} - 4)} \right] - D_v \cdot (J + 1)^4 + \text{const.}$$

The additive constant is the same for both equations, and so it may be adjusted to make the calculated value for the lowest level equal to zero, or equal to its true value with respect to the ground state of the molecule, as desired.

The values of the constants in the Hill and Van Vleck formulas are given for $\text{CN} \cdot A {}^2\Pi$ by Rigutti (1962) as follows:

$$A = -52.20 \text{ cm}^{-1}$$

$$B_v = B_e - \alpha_e (v + \tfrac{1}{2}) + \gamma_e (v + \tfrac{1}{2})^2 + \dots$$

$$D_v = D_e + \beta_e (v + \frac{1}{2}) + \dots$$

$$B_e = 1.7161 \text{ cm}^{-1}$$

$$\alpha_e = 0.01717 \text{ cm}^{-1}$$

$$\gamma_e = -3.15 \times 10^{-5} \text{ cm}^{-1}$$

$$D_e = 6.0717 \times 10^{-6} \text{ cm}^{-1}$$

$$\beta_e = 1.255 \times 10^{-8} \text{ cm}^{-1}$$

For $v = 6$, the constants may be calculated as

$$B_6 = 1.6032 \text{ cm}^{-1}$$

$$D_6 = 6.1533 \times 10^{-6} \text{ cm}^{-1}$$

$$\frac{A}{B_6} = -32.56$$

$$\frac{A}{B_6} \left(\frac{A}{B_6} - 4 \right) = 1190.4$$

These values were used to compute the level locations displayed in Figure 8.

4.4.2 The Unperturbed Rotational Levels of $X^2\Sigma^+$ and $B^2\Sigma^+$

All molecular $^2\Sigma$ states correspond to Hund's coupling case (b) at all speeds of rotation. The quantum number K takes all integral values from zero upward, and for each K there exists a very close pair of levels $J = K + \frac{1}{2}$ and $J = K - \frac{1}{2}$ (except for $K = 0$ which is single, since J cannot be $-\frac{1}{2}$). These close pairs of consecutive J -values are usually known as "spin doublets". Additional Λ -type doubling does not occur with Σ states; only for states with Π and higher multiplicity.

Now, actually, in the ground state of cyanogen $CN \cdot X^2\Sigma^+$ the spin-doublet separation is so minute that it is not completely resolved with a 21-foot grating. Only single levels are observable. In the upper cyanogen state $B^2\Sigma^+$ spin-doubling is observable at high resolution, although in some levels it is only comparable with and is intermixed with, hyperfine structure separations. (See Radford, 1964).

Figure 9 shows the rotational levels of $CN \cdot X(v = 5)$. The centers of the case (b) unresolved spin doublets are given approximately by formulas of the type

$$F(K) = B_v(K + 1) - D_v K^2 (K + 1)^2 + \dots$$

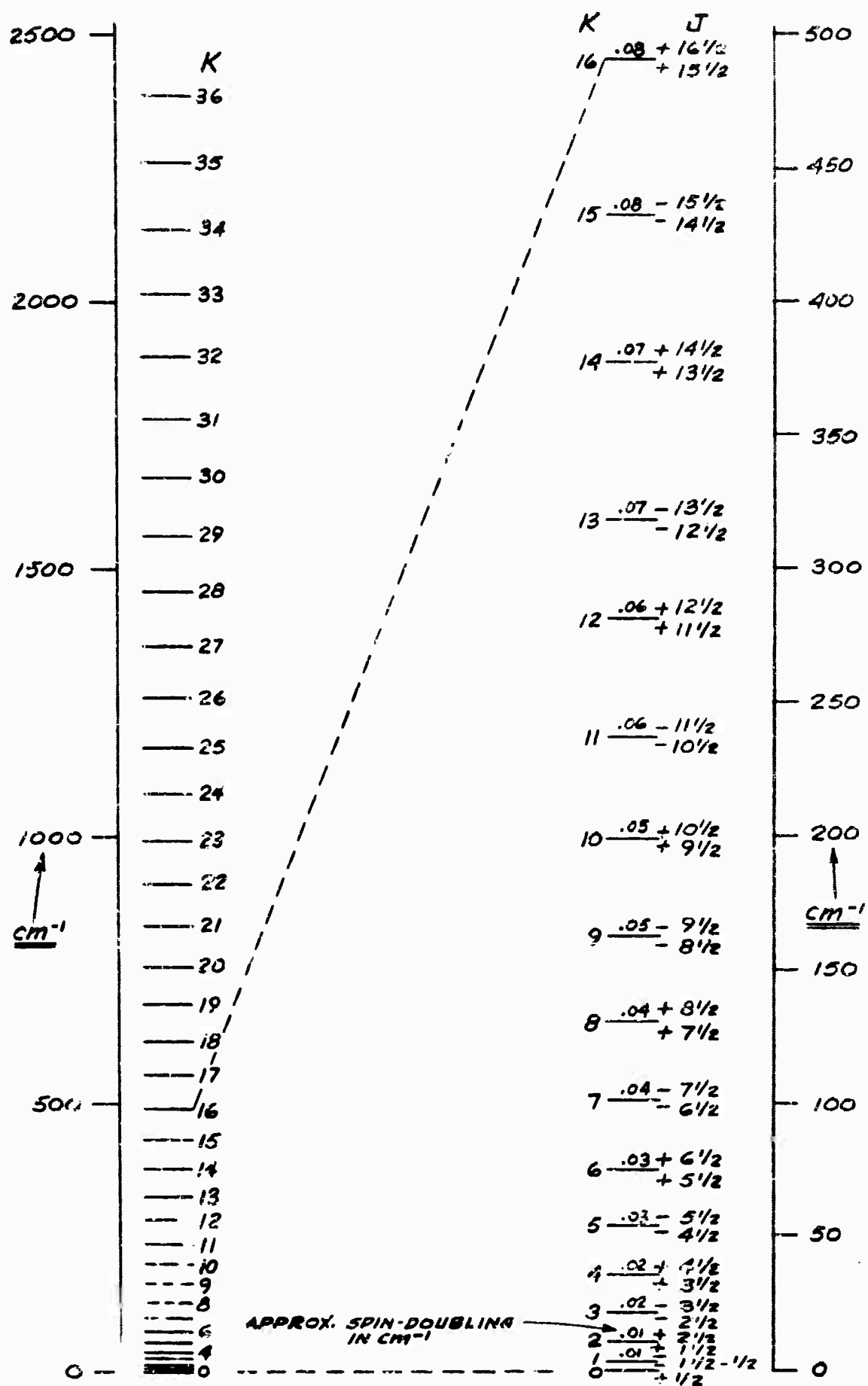


Figure 9.
The rotation levels of $\text{CN}\cdot \text{X}(v=5)$.

where

$$B_v = B_e - \alpha_e(v + \frac{1}{2}) + \gamma_e(v + \frac{1}{2})^2 + \dots$$

$$D_v = D_e + \beta_e(v + \frac{1}{2}) + \dots$$

Rigutti's analysis yields for CN^{*} X the constants

$$B_e = 1.8997 \text{ cm}^{-1}$$

$$\alpha_e = 0.01750 \text{ cm}^{-1}$$

$$\gamma_e \approx 0$$

$$D_e = 6.400 \times 10^{-6} \text{ cm}^{-1}$$

$$\beta_e = 1.000 \times 10^{-8} \text{ cm}^{-1}$$

From these, one may calculate for the state ($v = 5$) the values

$$B_5 = 1.8034 \text{ cm}^{-1}$$

$$D_5 = 6.455 \times 10^{-6} \text{ cm}^{-1}$$

These constants were used in computing the level locations shown in

Figure 9. The \pm symmetry pattern indicated there is the one common to all $^2\Sigma$ states.

Jenkins, Roots and Mulliken found some indirect evidence as to the probable magnitude of the spin doubling in the $\text{CN}\cdot\text{X}$ states, even though the levels were not actually resolved. Estimates from their data are indicated in Figure 9.

4.4.3 Perturbation Effects in Rotation Levels

None of the rotational levels shown in Figures 8 and 9, or any of the rotation levels involved in the (0, 0) or (6, 5) bands shows any perturbation effects. However, in $\text{CN}\cdot\text{X}$ ($v = 11$ and 12), in $\text{CN}\cdot\text{A}$ ($v = 7, 8$ and 10), in several vibration states of $\text{CN}\cdot\text{B}$, a few individual rotation levels are displaced out of the regular positions to be expected from the simple formulas. All of these levels occur where the potential curves of two electronic states lie very close together and where particular rotational levels from each of these states almost coincide in energy.

For such coincidences, mixing of the wavefunctions of the two electronic states occurs and the two perturbing rotation levels are displaced in their energy location and mix their characteristics somewhat — with consequent spectrum line location and intensity anomalies. However, a feature other than the spectrum line characteristic is of some potential importance for a laser transformer design. Since such a rotation level has some of the character of two different electronic states, and it occurs where the two potential curves are close together, a collision can fairly easily transfer a molecule in this rotation level from one electronic state to the other.

Thus, CN collisions with N_2 molecules usually have very little tendency to transfer a molecule from CN· A to CN· B, or to CN· X. But Radford and Broida (1963) found that when a molecule was in one of the particular perturbed rotational levels of CN· A($v = 10$) the probability was about 1% that a N_2 collision would transfer it over to CN· B($v = 0$).

Processes of this type would not be involved in the transformer laser here under discussion unless significant numbers of CN molecules came to reside in vibrational levels higher than those associated with the (0, 0) and (6, 5) bands.

5. THE ALLOWED OPTICAL TRANSITIONS IN CN

5.1 The Electronic Selection Rules

Recapitulating, the three lowest doublet electronic states of CN are of the type $^2\Sigma^+$, $^2\Pi$, and $^2\Sigma^+$, with all three displaying either Hund's vector coupling case (a) or coupling case (b). Some quartets may also lie nearby.

The most general optical selection rules in these types of coupling would predict good probability for all three possible transitions among these doublet levels, but no optical transitions whatever between doublets and quartets in such a light molecule as CN.

If the molecule had been homonuclear, such as C_2 or N_2 , each state would possess a special type of even or odd symmetry character which is labelled with a subscript \underline{g} or \underline{u} . Then there would have been an additional selection rule: "optical transitions have appreciable probability only from \underline{g} to \underline{u} states, or vice versa; never between two states of the same symmetry." The net effect of this rule in a group of three states would be that if two of them both combined with the third, then these first two would necessarily be of the same symmetry, and so a transition between them could not occur.

Now, the CN molecule has nuclei whose electric charges differ by only one unit, and so this special selection rule for molecules with equal charged nuclei applies in the case of CN to a certain degree. It is experimentally found that both of the upper doublet states $B^2\Sigma^+$ and $A^2\Pi$ yield strong band systems in transitions to the ground state X^{2-+} , with radiative lifetimes of the order of 0.1 μsec (Bennett and Dalby, 1962) and 3 μsec (Wentink, Isaacson and Morreal, 1964), respectively. Therefore, any (B-A) optical transition is expected to be a great deal weaker than these.

In fact, no normal (B-A) bands have ever been experimentally observed so far in CN, although they would lie in a well-investigated part of the visible spectrum. Their transition probability must be negligible in comparison with that of (B-X), or else they would have been seen in emission spectra from some of the many kinds of CN sources which have been studied.

This matter of (B-A) absorption is of importance for the laser transformer as it affects the possibility of second pump quantum absorption, as in Cs_2 . A molecule which had been excited to $\text{CN}\cdot\text{A}$ might absorb another quantum of Nd glass laser light and perhaps arrive at a level from which wasteful collision or fluorescence processes

might be too probable, if the (B-A) transition were a strong one.

One slight exception exists, which in itself emphasizes the weakness of the normal (B-A) transition. At the crossing of potential curves near the internuclear separation 1.5\AA , a few rotational levels from each of a few of the vibration states of $A^2\Pi$ are perturbed by close rotation levels of $X^2\Sigma^+$, as just mentioned. Because of the mixing of the wave functions of the respective states, these particular A rotational levels take on some partial characteristics of X levels. Therefore, the prohibition against the (B-A) transition breaks down for any (B-A) spectral line which would involve one of these perturbed rotational levels of state A. Such a line has a partial (B-X) character and so becomes of appreciable intensity. Two or three of these weak rotational lines at (B-A) wavelengths are observed near each of the [A, X] rotational perturbations. However, their number and intensity are too small to absorb very much Nd pump light in a transformer arrangement, unless a major population density in the perturbed levels of $CN\cdot A$ was present.

5.2 The Vibrational Transitions and the Nd Glass Laser Spectrum

The relative intensities of the possible transitions between vibration states of CN· A and CN· X is governed in the usual way by the Franck-Condon principle as regards wavefunction overlap, together with the ν^4 dependence on the frequency. Each such transition gives rise to a complete electronic-vibration-rotation band, such as the (0, 0) or (6, 5) bands.

Wyller (1958) and Nicholls (1964) have made theoretical calculations of expected relative intensities for many possible vibrational transitions. Figure 10 is Wyller's block diagram of the relative Franck-Condon factors, which display the usual "parabolic" type of magnitude distribution in such a quadratic array. Nicholls' results are quite similar. Since the vibrational energy steps are so large in CN, the bands are spread over a large range of the spectrum and the ν^4 factor will have considerable influence on relative intensities of bands in different locations. However, along any line in Figure 10 roughly parallel to the $\Delta v = 0$ diagonal the bands indicated will all fall in about the same place in the spectrum and so their intensities will be approximately proportional to the Franck-Condon factors alone. Wyller calculates that the (6, 5) band will have 6.6% of the intensity of the (0, 0) band.

Dixon and Nicholls (1958) made experimental measurements on the integrated relative intensities at low dispersion of 28 of the CN· (A \leftarrow X) bands, with the results shown in Table 2. Comparison with the relative

ν_A	0	1	2	3	4	5	6	7	8
0									
1									
2									
3									
4									
5									
6									
7									
8									

Figure 10.
Theoretical relative values of I/ν^4 for the CN· (A-X) bands,
where I is integrated band intensity and ν is the frequency
location of the band.

v_A	v_X							
	0	1	2	3	4	5	6	7
0		1.72						
1	0.798		0.936					
2		0.535		0.512				
3		0.395	0.265	0.286				
4		0.249	0.425		0.397			
5		0.115	0.403	0.365		0.572		
6		0.049	0.242	0.497	0.256	0.154	0.484	
7			0.086	0.299	0.366			0.243
8				0.102	0.225			
9				0.018				

Table 2. Experimental Values of Integrated Relative I/ν^4 For Bands of the CN.(A \leftarrow X) System, by Dixon and Nicholls (1958)

theoretical values indicates that I/ν^4 for the (0, 0) band might be about 1.5 on the scale of Table 2. This would mean that the (6, 5) band was about $0.154/1.5 \approx 10\%$ as strong as the (0, 0) band.

The rotational structure within any one of the bands is moderately complex, involving 12 rotational branches, as will be discussed in the next section. A distinctive feature of each branch is the so-called " R_2 head". In each band, most of the structure stretches off toward lower wavenumbers from the R_2 head. The quadratic array in Table 3 shows all the experimentally found locations of R_2 heads, together with calculated locations for a number of bands which have not yet been experimentally measured. The sources of the data are shown in the Table.

Let us now consider the ability of Nd glass lasers to pump into various ones of these bands. Figure 11 shows the fluorescent emission band near 1.06μ of Nd in a soda lime glass at 300°K and at 80°K , as given by Maurer (1963). Superimposed in Figure 11 are schematic diagrams of all the $\text{CN}^*(\text{A-X})$ bands which fall within or near the outline of the Nd band. The R_2 heads are plotted at the wavenumbers listed in Table 3. The extent of the bands toward lower cm^{-1} away from the heads is estimated from the structure of the specific bands described in following sections. The relative band intensities are made to approximate the results of Wyller and of Dixon and Nicholls.

TABLE 3. - LOCATION OF

v_A	v_X	0	1	2	3	4	5	6
0		9150.38 DP	7108.0 FWER					
1		10837.24 DP	8891. HP	6875. HP				
2		12698.7 DP	10656.82 DP	8634.1 C	6645. HP			
3		14434.7 DP	12392.7 DP	~10300 DN 10371.2 C	~8300 DN 5381.8 C			
4		16145.2 DP	14103.1 DP	12087.3 DP 12055.5 G	10093.1 C	~8000 DN 8130.2 C		
5		17830.1 DP	15788.0 DP	13772.2 DP	11782.7 DP 11751 G	9815.3 C	~7800 DN 7873.4 C	
6		19489.2 DP	17447.4 DP	15431.5 DP	13442.0 DP 13438.4 C	11479.0 DP 11475.5 C	~9500 DN 9539.1 C 9542.41 E	~7600 7629.1 C
7			19081.3 DP	17065.4 DP	15075.9 DP 15072.7 C	13112.7 DP 13110.0 C	11173.3 C 11144.5 G	9263.3 C
8			20687.9 DP	18672.1 DP	16682.6 DP	14719.4 DP	12782.7 DP	10870.2 C 10842.1 G
9			22271. DP	20255.1 DP	18265.5 DP	16302.7 DP	14365.5 DP	12453.6 C
10					19822.2 DP	17858.9 DP	15922.0 DP	14010.4 C
11					21532.79 JRM	19389.55 JRM	17452.8 DP	15542.5 C
12					22857.87 JRM	20894.72 JRM	18956.5 C	17047.2 C
13								
14								
15								
16								
17								
18								

DP = GRATING MEASUREMENTS OF R_2 HEADS BY DAVIS AND PHILLIPS (1963).

FWER = GRATING MEASUREMENTS OF R_2 HEADS BY FISHER, WEINSTEIN, EDE AND RAO (1964).

JRM = GRATING MEASUREMENTS OF R_2 HEADS BY JENKINS, ROOTS AND MULLIKEN (1932).

HP = PRISM MEASUREMENTS OF R_2 HEADS BY HERZBERG AND PHILLIPS (1946).

DN = APPROX. VALUES FOR MOST INTERIOR PART OF BAND, READ FROM A LOW DISPERSION PRISM RECORDING PUBLISHED BY DIXON AND NICHOLLS (1932).

C = COMBINATIONS FROM COMPUTED ELECTRONIC-PLUS-VIBRATION TERM VALUES ($J_A = J_X = 0$) GIVEN BY JENKINS, ROOTS AND MULLIKEN (1932).

THEY SHOULD BE WITHIN A FEW cm^{-1} FROM THE EXPECTED R_2 HEADS.

G = ESTIMATES OF BAND ORIGIN BY GOODRINE (1959).

E = R_2 HEAD COMPUTED FOR PRESENT REPORT.

P

5) GIVEN BY JENKINS, ROOT AND MULLIKEN (1932).

-X) HANDS

8 9 10 11 12 13 14 15 16

DN

C

C 8713.2 C

C 10270.0 C 8349.6 C

C 11800.9 C 9880.4 C 8165.4 C

DP 13306.1 C 11385.7 C 9671.7 C 7894.2 C

14725.6 C 12865.1 C 11151.1 C 9373.7 C 7822.6 C

735 14318.8 C 12604.9 C 10827.4 C 9076.4 C 7351.8 C

877 17663.9 DP
17667.2 C 12255.3 C 10504.28 C 8779.8 C

1010 11906.5 C 10181.9 C 8483.9 C

1155 11558.3 C 9860.3 C 8188.8 C

11211.0 C 9539.4 C 7894.4 C

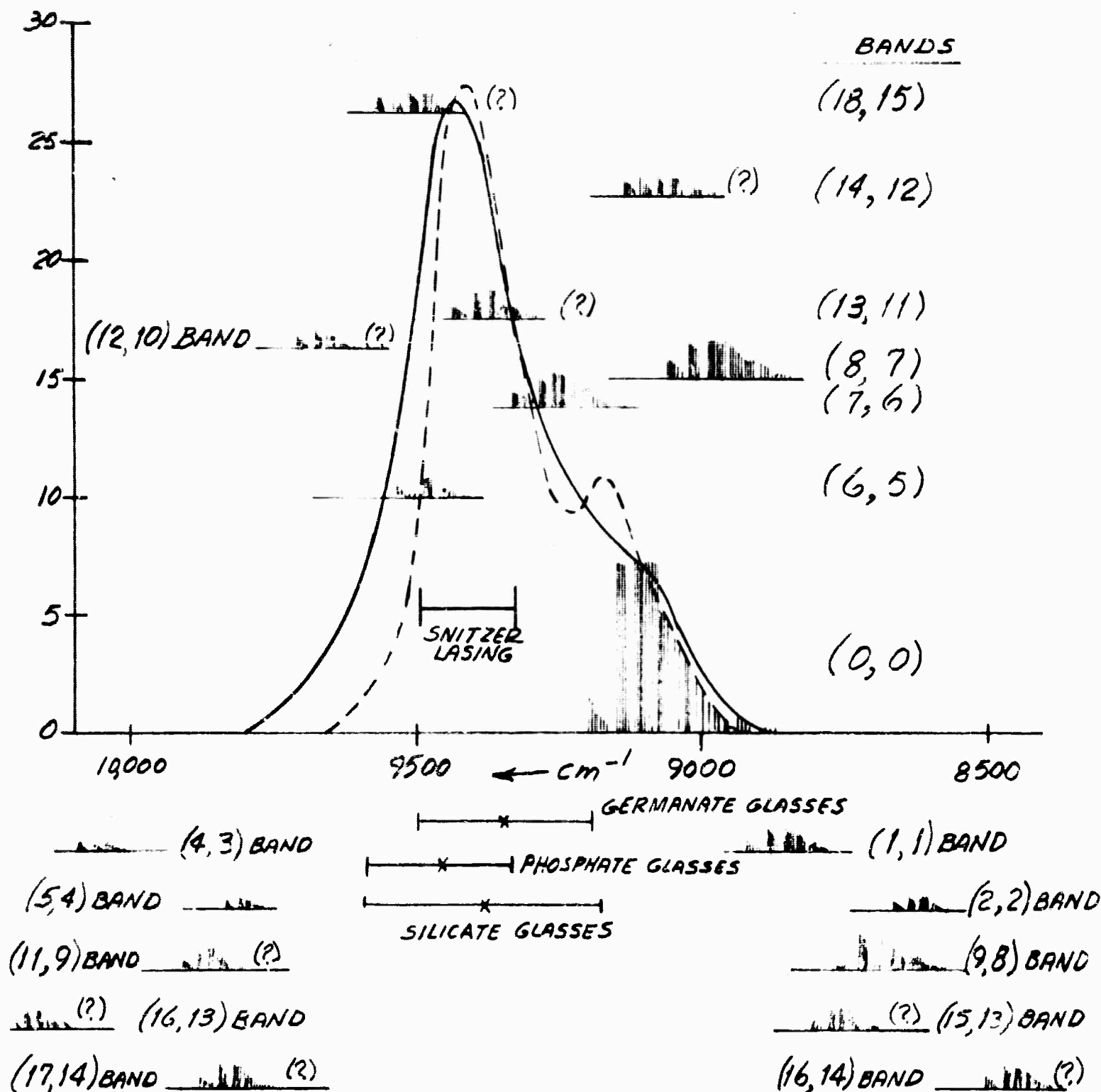


Figure 11.

Fluorescence band of Nd glasses, and location of CN (A-X) bands. The solid curve is for a typical soda lime glass at room temperature; the dotted curve is for 78°K. The various CN bands are correctly placed with respect to the wavenumber axis and their relative intensities are shown according to the theoretical calculations, where available. Question marks refer to band intensities, not band locations. The vertical placing of the various CN band sketches on the diagram is arbitrary. Also shown are the ranges of fluorescence for three general types of glasses, and the region in which Dr. E. Snitzer has found Nd glass lasers to be most efficient, so far.

The most obvious place to pump CN with Nd glass lasers would appear to be in the (0, 0) band. However, if bands involving absorption from an excited vibrational level of CN·X have to be used, the one requiring the least preparatory excitation energy would be (6, 5).

No experimental data have been published to show how efficient Nd glass lasers may be made when emitting near the wings of the Nd fluorescence band. Work to date has involved lasing chiefly near the center of the band. Dr. E. Snitzer says that he has not tried lasing at locations outside the central region indicated in Figure 11. There is some indirect indication that lasing in the wings of the Nd band might be hampered by self-absorption of the output frequency within the glass laser. However, Dr. Snitzer has not yet been able to experimentally demonstrate any such absorption. *

In this situation, one cannot be sure whether it would be best to try to pump the CN in the (0, 0) band or the (6, 5) band, or both. Further research on Nd-bearing glasses might favor either one or the other. Thus MacAvoy, Charters and Maurer (1963), from a study of some 500 glasses, tabulate the center and edge locations of the Nd fluorescent bands for typical germanate, phosphate and silicate glasses — as also indicated on Figure 11.

*-----
Personal communication from Dr. E. Snitzer to C. B. Ellis 15 April 1965.

With the germanate glasses the CN (0, 0) band falls appreciably closer to the band center than it does with the silicates, while with phosphate glasses the (6, 5) band is closer to the center of the Nd fluorescence.

Considerable work is now underway in various laboratories on the exploration of many kinds of Nd glasses. Thus the Centre National d'Etudes des Telecommunication (1963) is working on 150 of the more unusual Nd glass types, such as those based on beryllium fluoride.

Similarly, definitive work still remains to be done on the relative efficiencies of lasing when a Nd glass laser is constrained to emit in selected bandwidths at a chosen mean wavelength.

For the present, this report will simply give preliminary explorations of the behavior of the CN medium when pumped in either (0, 0) or (6, 5).

5.3 The Rotational Branches of the (A-X) Band

For small rotation, CN•A follows Hund's coupling case (a), while CN•B follows case (b) as always. In this regime, only two selection rules govern optical transitions among the rotational sublevels of the various vibration states.

- A. Transitions occur only for $\Delta J = 0$ or ± 1 .
- B. Transitions occur only between levels of opposite symmetry character, $+\longleftrightarrow -$.

Application of these rules to the rotational level patterns already illustrated yields, in principle, 12 branches for each vibration-rotation band. The system for labelling these is illustrated in Figure 12.

Now, although all these branches occur in ($^2\Pi - ^2\Sigma$) transitions in some molecules, in the special case of CN the spin-doubling for CN•X is so small that the separate members of the pairs are not experimentally resolvable, even with a 21-foot grating. Inspection of Figure 12 will show that if this splitting of the CN•X levels is negligible, then all the lines of the Q_{12} branch will fall on top of lines of the P_1 branch. Similarly, the R_{12} branch will be merged with the Q_1 branch, the P_{21} branch with the Q_2 branch, and the Q_{21}

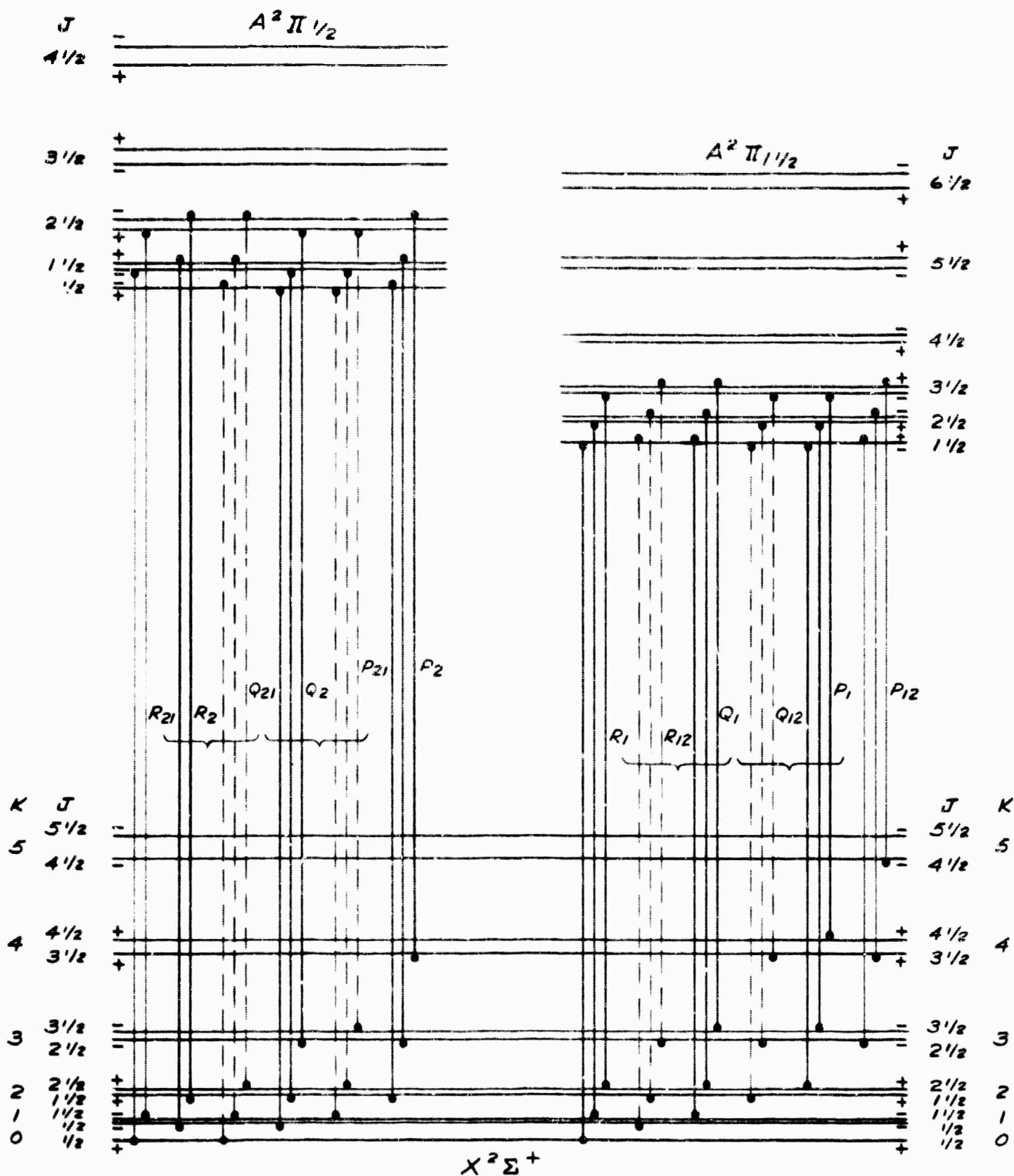


Figure 12.

The system of labelling for the twelve rotational branches of each CN(A-X) band. Dotted transitions bracketed with heavy-line transitions represent pairs of branches which are experimentally unresolved, to date.

branch with the R_2 branch. Branches which are not resolvable in CN for this reason are shown as dotted lines in the diagram. Thus, experimentally, each of these cyanogen bands consists of 8 resolvable rotation branches associated with each vibrational transition.

The way the low-J level spacing patterns happen to occur, it turns out that 4 heads have an obvious appearance in each band. That is, the R_{21} branch, the R_2 branch ($+Q_{21}$), the R_1 branch, and the Q_1 branch ($+R_{12}$), give patterns of lines which form recognizable heads, while the other four do not. Of these, the R_2 head contains the most intense lines, and so can be used as a rough indicator for the wavelength location of each band.

On proceeding toward large J-values, the state $A^2\Pi$ changes to coupling case (b) and the quantum number K becomes defined for both $A^2\Pi$ and $X^2\Sigma^+$. Thereupon, an additional selection rule appears. Now $\Delta K = 0$ or ± 1 , in addition to the regular $\Delta J = 0$, or ± 1 . This causes the R_{21} and P_{12} branches to disappear at high rotation, since ΔK would equal 2 for such transitions.

As K becomes more and more clearly defined, another selection rule also takes on more and more force: branches for which $\Delta K \neq \Delta J$ have much lower transition probabilities than those for which

$\Delta K = \Delta J$. Finally, above about $K = 20$ in $CN(A-X)$, the intensity of those branches with $\Delta K \neq \Delta J$ has diminished effectively to zero. Experimentally, these branches—which are Q_{21} , P_{21} , R_{12} and Q_{12} —just disappear at high rotation, as do R_{21} and P_{12} . Thus, the six disappearing branches are the ones with the double subscript indices in the previous diagram. Only the six bands with single indices (P_1 , Q_1 , R_1 , P_2 , Q_2 , and R_2) continue with good intensity into high J -values.

5. 4 Intensity Relations for Rotation Lines

Earls (1935) has provided theoretical formulas for the relative intensities of all the rotational spectrum lines within an unperturbed band of the CN \cdot (A-X) type, at any equilibrium temperature. The theory is in reasonable agreement with experimental data, such as that of Jenkins, Roots and Mulliken (1932), whose photographic densities measured in the (9, 3) band in absorption at room temperature are shown in Figure 13. The Q₁ and Q₂ branches are the strongest, followed by P₁ and R₂ and R₁ and P₂.

Figure 13, of course, is mainly useful as an indication of relative strengths of corresponding low-J lines in the various branches. The actual shapes of the branch intensity curves are dependent on the relative molecular population densities in the various levels. For Boltzmann equilibrium at 210°K, the lines involving higher J would be less prominent than in Figure 13.

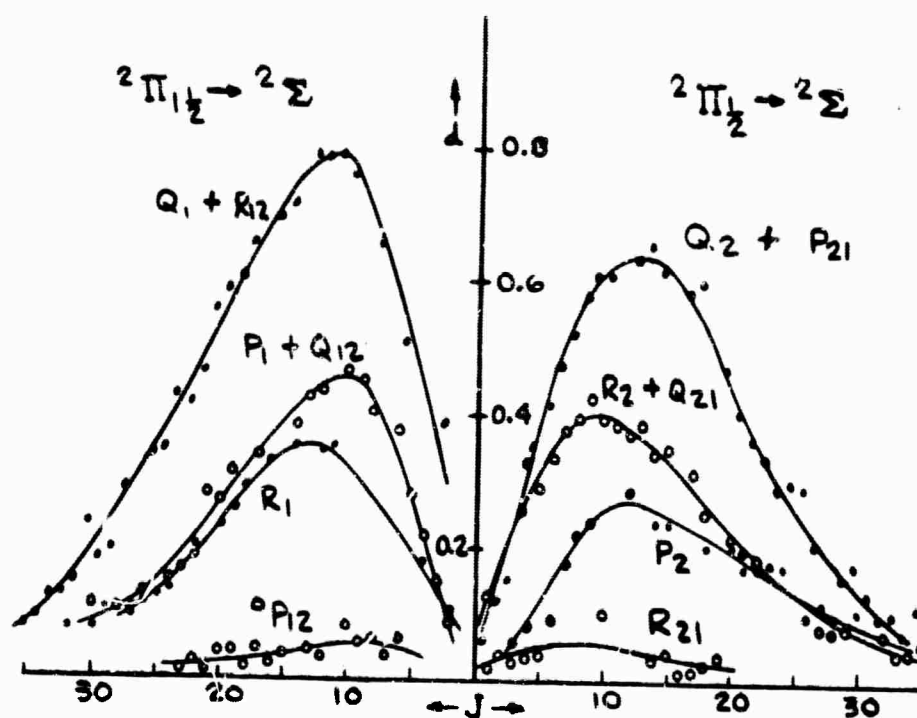


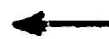
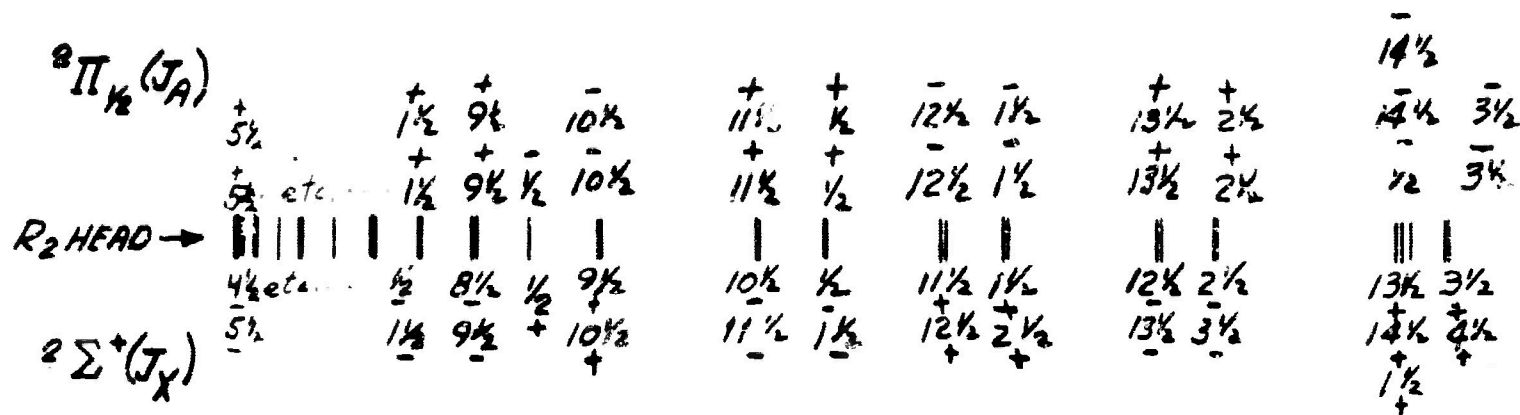
Figure 13.
Experimental values for the relative intensities of rotation lines
of the (9, 3) band.

6. STRUCTURE OF THE (6, 5) AND (0, 0) BANDS

6.1. The (6, 5) Band.

Figures 8 and 9 showed the rotational levels of CN: A(v=6) and CN: X(v=5) as calculated under the present contract from the level formulas published by Rigutti (1962). Subtractions among these level values, according to the pattern illustrated in Figure 12, yield the spectrum line locations for the various branches. As a typical sample such a calculated map for the lines up through K=17 of the $R_2(+Q_{21})$ branch, up through K=8 of the $Q_2(+P_{21})$ branch, and up through K=5 in the P_2 branch, all of which fall in the region 9509-9543 cm^{-1} , is shown in Figure 14. This includes the R_2 head and some of the strongest lines of the band.

It may be assumed that all measured line positions existing in the literature refer to the single-index-labelled ("main") branches only. The double-index ("satellite") branches are both theoretically and experimentally a great deal weaker, and so presumably they have not greatly affected the measured line positions. Rigutti deduced his level positions chiefly from these measured main branch lines, plus only a few quite weak lines of the R_{21} and P_{12} branches. Since all the R_2 , Q_2 and P_2 lines arise from the lower members of the CN: X spin-doublets, these lower levels are most probably the ones which are yielded by computations with Rigutti's constants for CN: X.



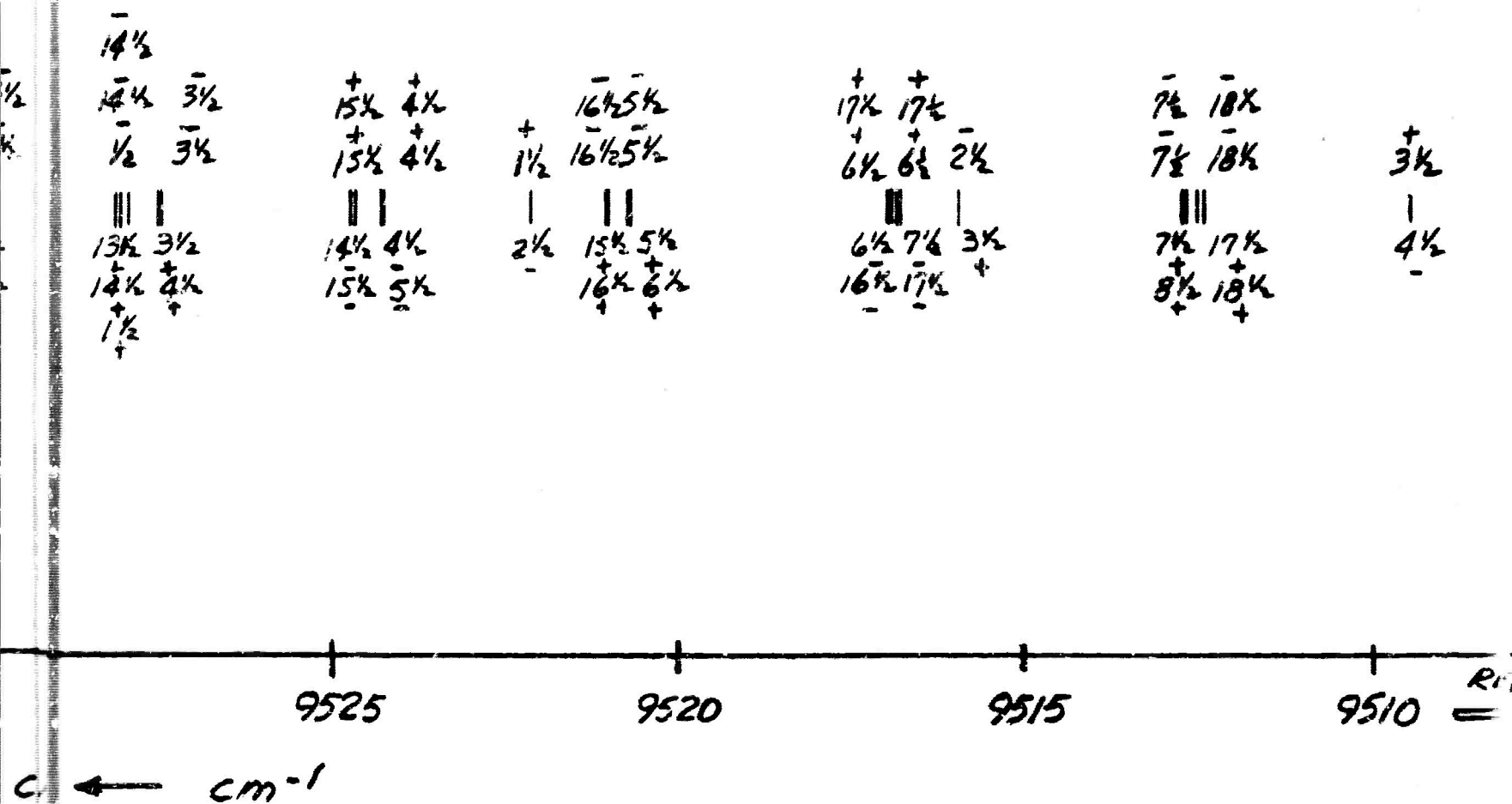


Figure 14.

Calculated (6, 5) line position
in the range 9509-9543 cm⁻¹

In $^2\Pi$, the R_2 and P_2 lines involve only the upper members of the $CN \cdot A$ $^2\Pi_{1/2}$ Λ -type doublets, while the Q_2 lines involve only the lower members of these doublets. Presumably, therefore, the level locations in $CN \cdot A$ $^2\Pi_{1/2}$ which result from use of the Rigutti constants represent more or less the center of gravity of the Λ -type doublets. Estimates of the amounts of the Λ -splitting of these levels, and of the spin-doubling in $CN \cdot X$, can be taken from the work of Jenkins, Roots and Mulliken as shown in Figures 8 and 9, so that a more enlarged approximate map can be calculated which will distinguish between the nearly-coincident lines of main and satellite branches. Although previous experiments have not resolved these close doublets, a CN laser might well be emitting under various conditions in only one member at a time.

As a typical sample, Figure 15 is such an enlarged approximately calculated map for a 4 cm^{-1} region including the R_2 head. In the present state of knowledge, an arbitrary shift of the scale in this Figure by a few hundredths of a wavenumber would be possible. All lines were given an arbitrary half-width of 0.02 cm^{-1} ,

 = MAIN BRANCH = R_2

 = SATELLITE BRANCH = Q_{21}

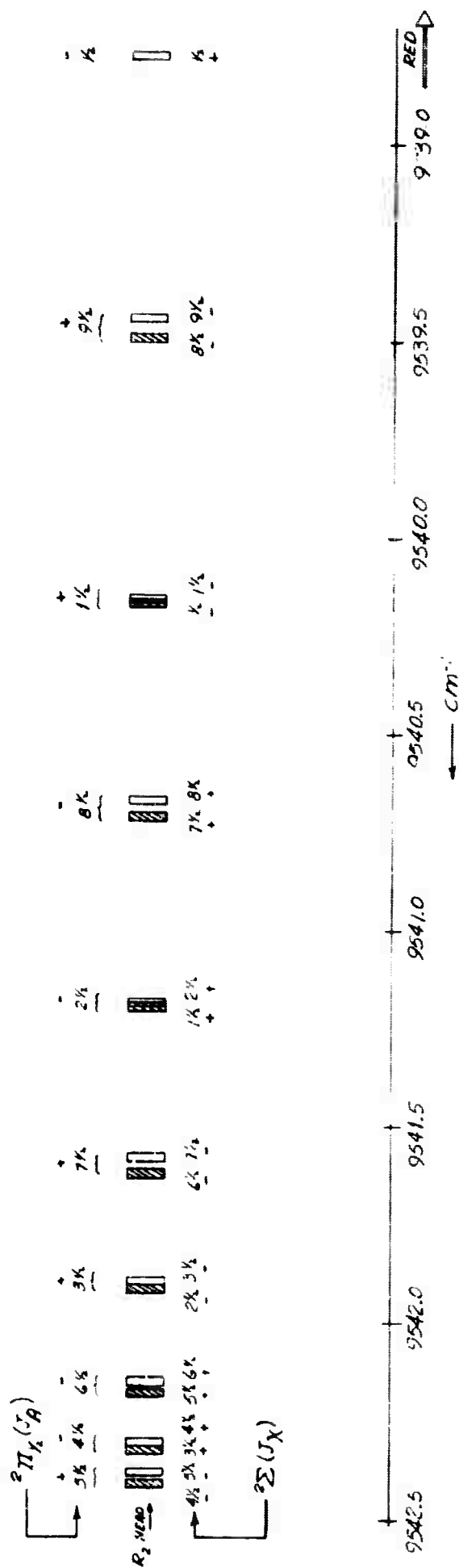


Figure 15.
Calculated (6, 5) lines near the R_2 head.

which is the computed pure Doppler halfwidth* in CN near 9500 cm^{-1} , when the gas is at 210° K . This temperature was chosen for initial laser transformer calculations because it is about the lowest temperature at which cyanogen can have a vapor pressure as great as several cm Hg. No allowance was made for pressure broadening, so the map will not be strictly applicable at total pressures in the transformer medium above perhaps a few cm Hg.

The rotational structure of the (6, 5) band has not yet been mapped experimentally. However, semi-experimental locations for its lines can be found by applying the combination principle to selected lines of other bands of the CN·(A-X) system for which high resolution experimental data are available.

Davis and Phillips (1963) resolved the rotational structure and provided complete analyses for 39 of these bands, with measurements to 0.01 cm^{-1} . The bands studies are indicated in the following quadratic array. **

* The well-known spectrum line Doppler halfwidth formula for gas of molecular weight M at an absolute temperature T is $\Delta\sigma/\sigma = \Delta\lambda/\lambda = 7.16 \times 10^{-7} \sqrt{T/M}$. For $\sigma = 9500\text{ cm}^{-1}$, $M = 26$, and $T = 210^\circ\text{ K}$, this gives $\Delta\sigma = 0.019\text{ cm}^{-1}$.

** Davis and Phillips reference earlier analyses by various workers on twelve of these thirty nine bands. In addition to those mentioned by Davis and Phillips, see analyses of the (10, 3) and (10, 5) bands by Kiess and Broida (1961), and of the (10, 4) band by Wager (1943).

		V_X								
		0	1	2	3	4	5	6	7	8
V_A	0	X								
	1	X								
	2	X	X							
	3	X	X							
	4	X	X	X						
	5	X	X	X	X					
	6	X	X	X	X	X				
	7		X	X	X	X				
	8		X	X	X	X	X			
	9			X	X	X	X			
	10				X	X	X			
	11						X	X		
	12							X	X	
	13									
	14									
	15									X

The wavenumbers of any four lines having identical labels in each of four bands will satisfy a simple combination relation, whenever the designations of the four bands occupy vertices of any rectangle in the above quadratic diagram. Thus, as a typical example, the following holds for each value of K.

$$R_2(K)_{6,2} - R_2(K)_{6,5} = R_2(K)_{8,2} - R_2(K)_{8,5}$$

The entire R_2 branch of the (6, 5) band may be mapped out in this way by adding and subtracting the experimental wavenumbers for corresponding lines in the (6, 2) (8, 2) and (8, 5) bands. Inspection of the quadratic array shows a total of nine different ways in which the Davis and Phillips data can be combined to yield the wavenumber of a (6, 5) band line. The same kind of relation holds for lines from each of the other branches of the (6, 5) band as for the R_2 lines.

Figure 16 shows most of the complete (6, 5) band, as derived under the present contract in this semi-experimental fashion from the Davis and Phillips data. They were not able to resolve any of the spin doublets. The line locations agree with those calculated from the Rigutti constants to within a few hundredths of one cm^{-1} for the initial lines of a branch, and within a few tenths of one cm^{-1} for high members of each series.

P_{12} →

$\frac{1}{2}$
| — — — — etc.
 $\frac{2}{2}$

R_{21} --- etc. --- $\begin{array}{c} +2\frac{1}{2} \quad -1\frac{1}{2} \\ | \quad | \\ -1\frac{1}{2} \quad +1\frac{1}{2} \end{array}$

P_2 →

$Q_2(+P_{21})$ →

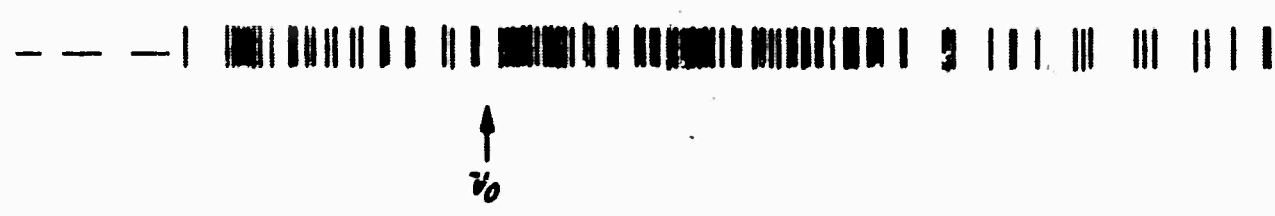
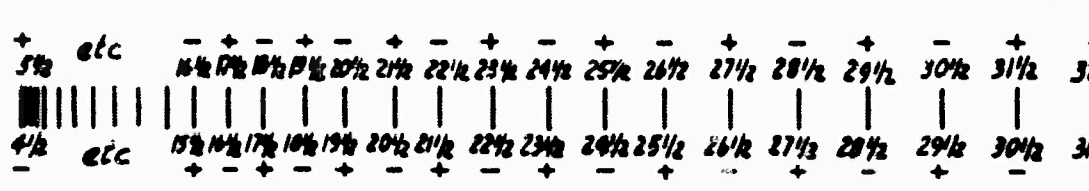
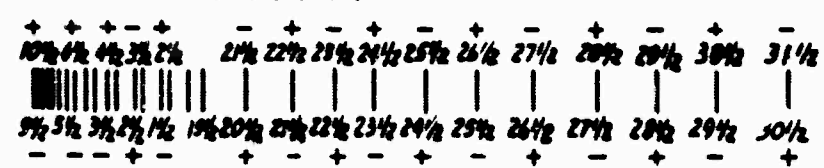
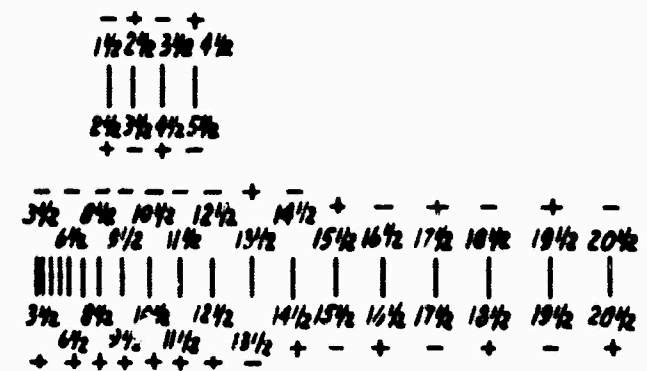
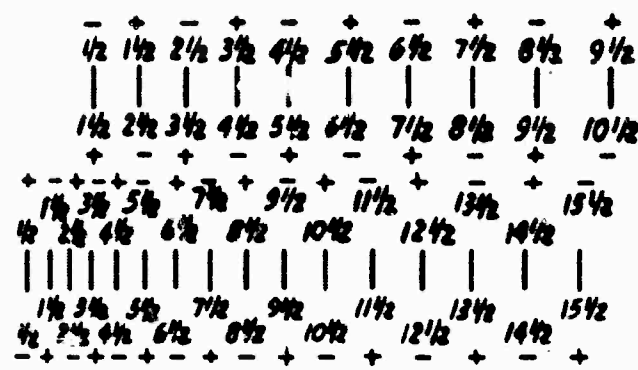
$P_1(+Q_{12})$ →

$Q_1(+R_{12})$ →

R_1 →

$J_A \rightarrow$
 $R_2(+Q_{21})$ →

$J_X \rightarrow$

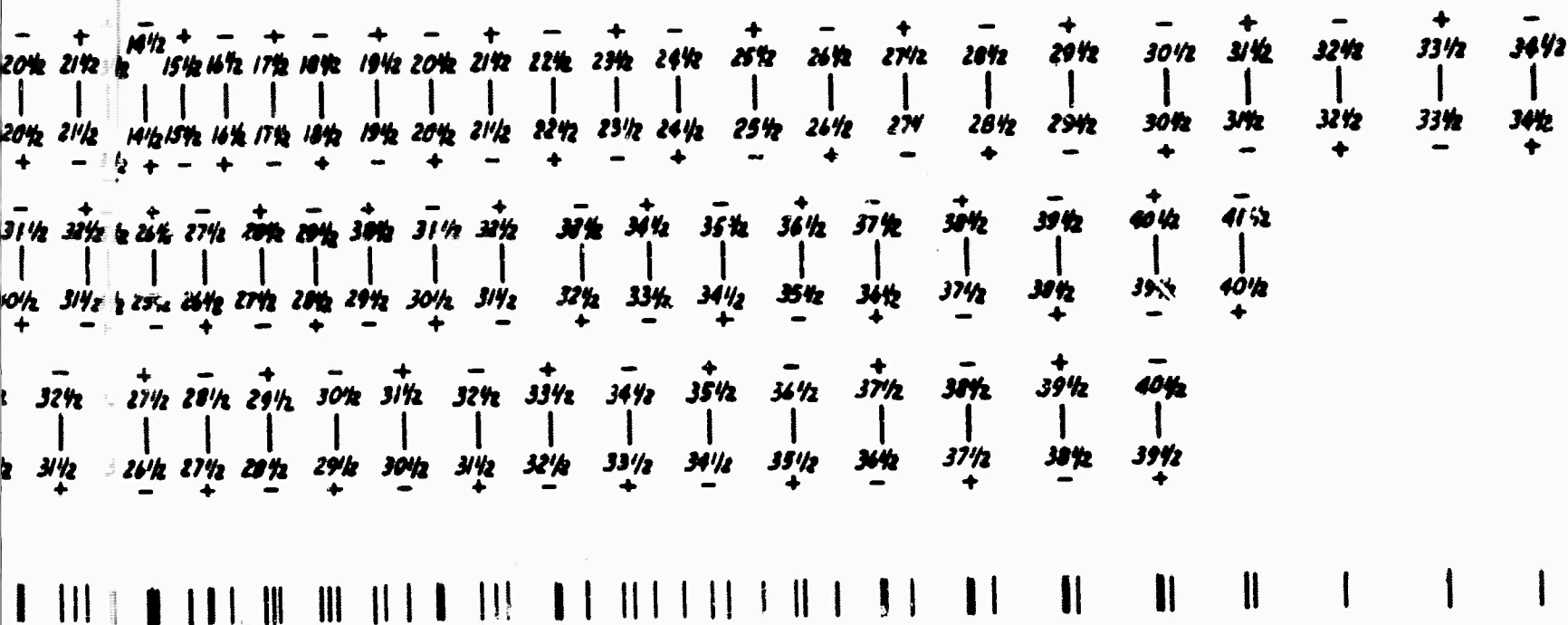


9550 9500 9450

\uparrow
 ν_0



— etc.



9450 9400 9350 9300
← cm⁻¹

The complete list
as deduced from

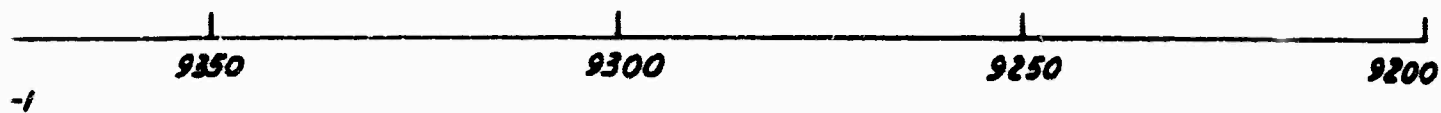
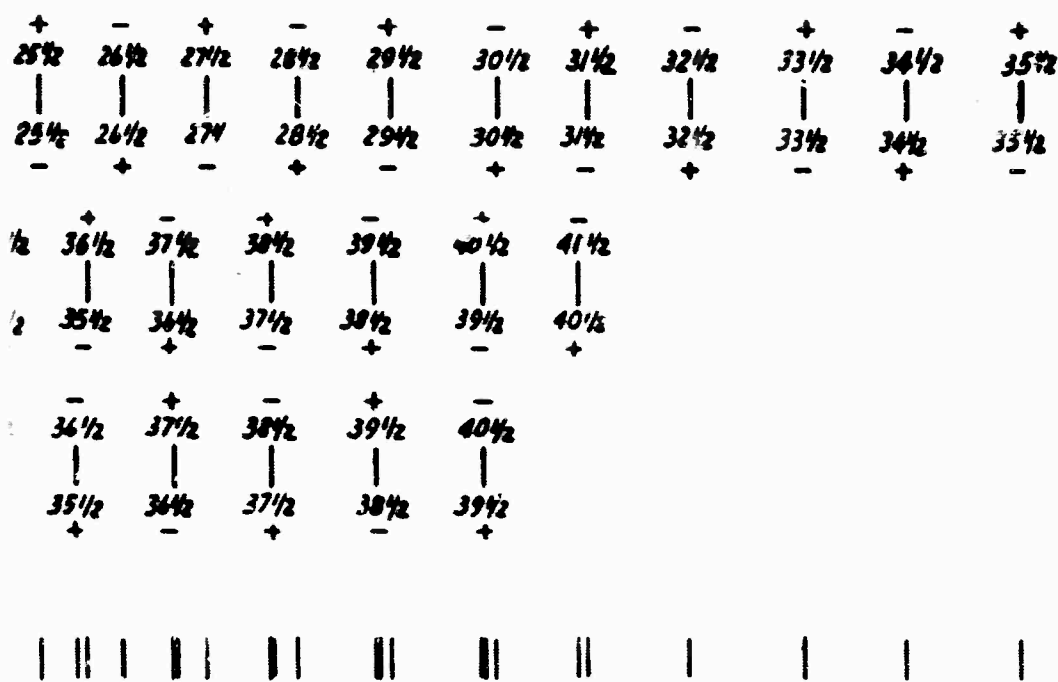


Figure 16.
The complete lower-J end of the (6, 5) band
as deduced from experimental data.

6.2 The (0, 0) Band

The (0, 0) band is among those measured with precision and analyzed by Davis and Phillips. Figure 17 is drawn from their tabulated wavenumbers. More detailed calculated maps could also be made if needed from the Rigutti constants. The relative line spacings obtained from such a calculation might be slightly more accurate than the existing experimental data on the (0, 0) band, since the formulas resulted from a synthesis of experimental data from many bands, smoothed according to our present understanding of molecular structure.

Before proceeding to a discussion of the lasing possibilities in these bands, it will be convenient to devote Sections 7 and 8 to the question of how to prepare CN from the starting $(\text{CN})_2$ gas, and how to specify the CN-He mixture.

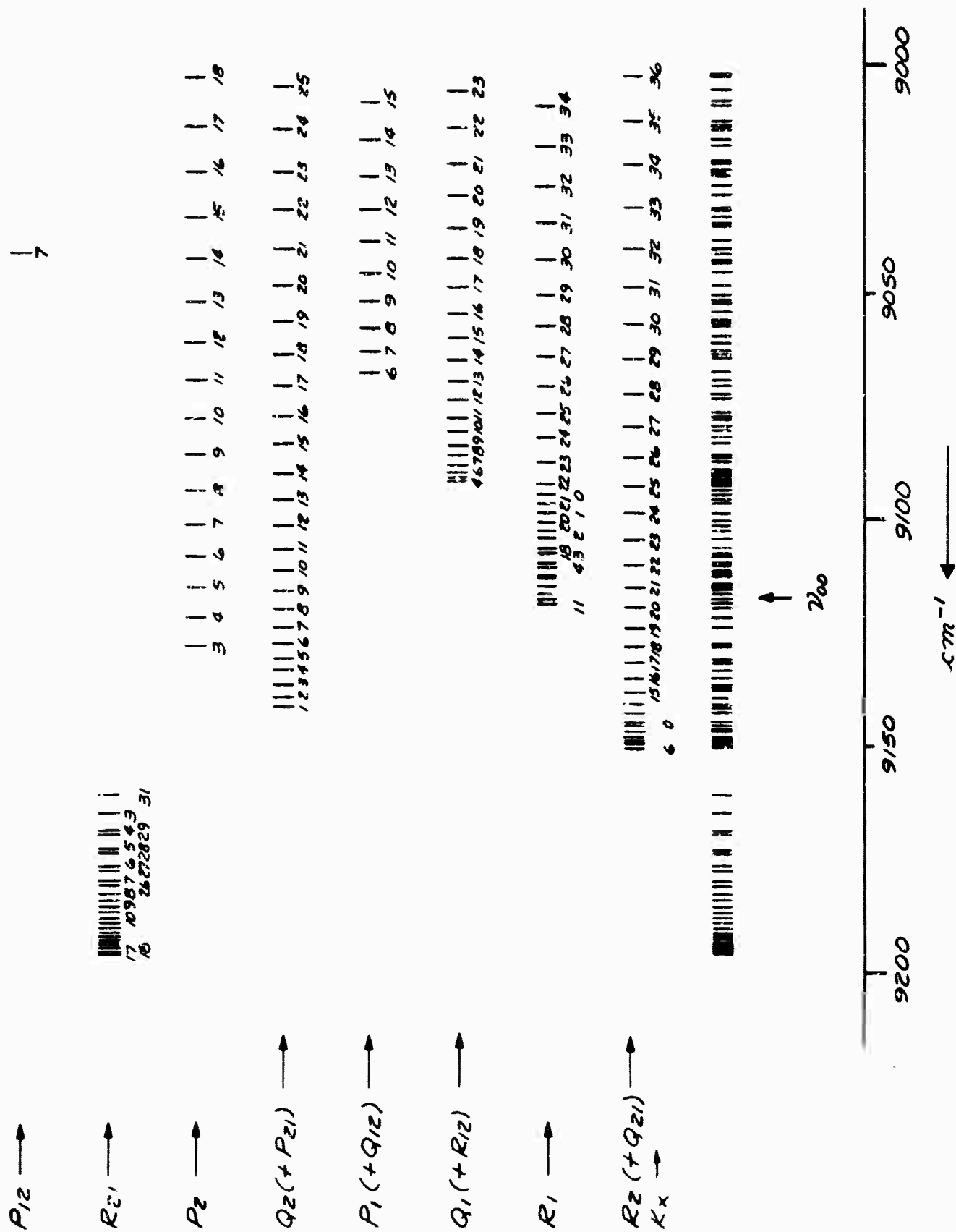


Figure 17.
The (0,0) band, as measured by Davis and Phillips.

7. WAYS OF PREPARING CN • X

The monomer CN is not a stable entity having permanent normal existence in any practical amount, since it is quite reactive and will disappear by chemical reaction with many things. The usual cyanogen gas at ordinary temperatures consists chiefly of the dimer $(\text{CN})_2$.

7.1 Thermal Dissociation of $(\text{CN})_2$

Collisions between two or three $(\text{CN})_2$ molecules must always have some non-vanishing probability of disrupting one of them, so that a few CN's are doubtless present in cyanogen gas at room temperature. This probability increases with rising temperatures, and the equilibrium concentration of CN rises, until at 1000°C Kistiakowsky and Gershinowitz (1933) were just able to see the $\text{CN} \cdot (\text{B} \leftrightarrow \text{X})$ absorption bands in a volume of $(\text{CN})_2$ gas. At 1515° , White (1940, b) could measure the intensity of these CN absorption bands in cyanogen gas at roughly one atmosphere pressure, and calculated the equilibrium partial pressure of CN present then as about 7×10^{-4} mm. From the variation of band intensity with temperature, White extrapolated back and estimated that in normal gas at 375°C there should be an equilibrium concentration of about 0.03 CN molecules per cm^3 , while at 475°C there should be about $300/\text{cm}^3$. Brewer, Templeton and Jenkins (1951) carried such studies up to 2900°K . Above this range CN itself

begins to decompose, by the reaction $2\text{CN} \rightarrow \text{C}_2 + \text{N}_2$.

At high temperatures, either occasional single collisions or two successive collisions can provide enough energy to yield CN molecules in the first excited electronic state, CN-A, which lies about 9200 cm^{-1} above CN-X. Thus, in a furnace at 2500°C , Ballik and Ramsay (1958) found that cyanogen gas was fluorescing near 1.09μ and 1.41μ — emitting the (0, 0) and (0, 1) bands of CN (A \rightarrow X). Knight and Rink (1961) also found CN fluorescence from shock waves in cyanogen gas at temperatures above about 2000°K .

7.2 Electric Discharges for Preparing CN

A great many varieties of electric discharges, in either pure $(\text{CN})_2$ gas, or in mixtures of cyanogen with the noble gases, or in any of numerous carbon- and nitrogen-bearing vapors, will yield the emission spectrum of the CN molecule. For example, Herzberg and Phillips (1948) studied the CN spectrum from a discharge in a mixture of argon, nitrogen and benzene. This means that numerous collision mechanisms can either split off or synthesize the CN molecule from the original constituents, and either in the initial process or by subsequent collision can produce this CN in various excited electronic states — from which subsequent fluorescent emission serves to indicate the existence of the processes.

As probably the best-known example, White (1940, a) estimates that the flame of "an ordinary carbon arc in air" must often contain a population of about 2×10^{16} CN/cm³. This number would correspond to a partial pressure of about 1/2 mm of CN at room temperature.

7.3. Value of the Heat of Dissociation of (CN)₂

Various methods are available for estimating the heat of dissociation of cyanogen. In a thorough survey of numerous earlier measurements, Gaydon (1953) suggested that the value of $D^0_{\text{NC-CN}}$ most probably lies in the range 115-146 kcal/mole = 40,200 - 51,100 cm⁻¹. From the work available at that time, Gaydon recommended the lower value, about 115 kcal/mole. However, two recent researches by Knight and Rink (1961), and Berkowitz (1962), have yielded 145 and 143 kcal/mole, respectively.

Probably all that can be certain yet is that the first dissociation limit of (CN)₂ lies in the range of about 40,000 cm⁻¹ to 50,000 cm⁻¹, producing two CN·X molecules. *

*Proof that the methods alluded to here are really measuring the dissociation limit to the lowest electronic state, i. e. $(\text{CN})_2 \rightarrow 2\text{CN}\cdot\text{X}$, is probably provided by the fact that the work of White (1940, b), whose thermal dissociation researches at relatively low temperatures were surely dealing with the least energetic process, could be correlated with a dissociation energy of about 146 kcal/mole. However, such checks are not sufficiently accurate to be sure that all methods are measuring dissociation to the (v=0) level of CN·X, rather than sometimes to CN·X (v=1), for example, which lies 3042 cm⁻¹ higher.

7.4 Photodissociation of $(\text{CN})_2$; Experiments

It is well known that very shortwave ultraviolet light will dissociate $(\text{CN})_2$. However, most experimenters have used sources with a continuous spectrum, so that the minimum photon energy able to cause dissociation cannot be pinned down exactly.

Ramsay (1953) used a special thin-walled quartz mercury discharge tube which emitted the $1849\overset{\text{O}}{\text{\AA}} = 54,100\text{ cm}^{-1}$ line. This lamp, operating continuously at 100w electrical input and completely immersed in the gas, caused the cyanogen to display the absorption band (0, 0) of the $\text{CN}\cdot (\text{B}\leftarrow\text{X})$ system, when the volume was traversed by an auxiliary light beam. Such a result would be expected, from the above work on the dissociation energy needed to produce $\text{CN}\cdot \text{X}$ from $(\text{CN})_2$. The absorption measurement required 4 meters path length of gas at a few mm pressure, so the $\text{CN}\cdot \text{X}$ concentration was not very great in this low power steady-state experiment.

Paul and Dalby (1962) used a 100 joule "flash photolysis lamp" of much greater instantaneous power than the Hg lamp, but having a broad-band UV spectrum. Probably the usual quartz envelope of such a lamp would not transmit much light of shorter wavelength than about $1900\text{-}1850\overset{\text{O}}{\text{\AA}}$, or $52,800\text{-}54,000\text{ cm}^{-1}$. They made quantitative measurements of the intensity of the (0, 0) absorption band of

CN· (B←X) which the cyanogen gas displayed within microseconds after irradiation, and calculated that they were producing an initial density close to 10^{14} CN· X/cm³. The pure cyanogen gas was at 18.3 mm pressure and 175°C.

Basco, Nicholas, Norrish and Vickers (1963) used a flash lamp of similar properties, but still more powerful—about 1600 joules electrical input. They did not try to make absolute measurements of the resulting CN· X concentration. However, they were able to show that at least 96% of their (CN)₂ dissociation processes initially yielded CN· X in its lowest vibrational level, $v = 0$. As the additional excitation energy of CN· X ($v = 1$) is only 2042 cm^{-1} , if light quanta with energies up to the neighborhood of $53,000\text{ cm}^{-1}$ were thus not found to produce many ($v = 1$) dissociation fragments, perhaps this may be indirect evidence that $D^0_{\text{NC-CN}}$ actually lies closer to $50,000\text{ cm}^{-1}$ than to the lower end of Gaydon's suggested range. However, the dissociation mechanism is not sufficiently well understood for this to constitute definite proof.

In any case, these authors also found that pre-irradiated (CN)₂ gas had no detectable absorption spectrum at longer wavelengths than $2200\text{Å} = 45,500\text{ cm}^{-1}$, for their pressures and path lengths—up to 27 mm(CN)₂ mixed with up to 1 atm N₂, with 16 to 50 cm paths—so $D^0_{\text{NC-CN}}$ seems probably higher than $45,500\text{ cm}^{-1}$.

Basco, et al, furthermore demonstrated through the use of various filters that $\text{CN} \cdot \text{X}$ ($v = 0$) was being produced in sufficient amount in the first few microseconds of their flash duration for these molecules to absorb strongly at the $\text{CN} \cdot (\text{B} \leftarrow \text{X})$ wavelengths out of the continuous flash spectrum in subsequent microseconds. Following which, the $\text{CN} \cdot \text{B}$ molecules presumably fluoresced back down to those various higher vibration states of $\text{CN} \cdot \text{X}$ to which transitions are permitted by the Franck-Condon principle; so that by the end of the UV flash at least the first four vibrational levels of $\text{CN} \cdot \text{X}$ were observed to be almost equally populated, as checked by the absorption spectrum. Heavy population of considerably higher vibrational levels could also be predicted, from the known fluorescent intensities of the various $\text{CN} \cdot (\text{B} \rightarrow \text{X})$ bands.

Paul and Dalby had also observed this $\text{CN} \cdot (\text{B} \rightarrow \text{X})$ fluorescence arising from their irradiations. It surely could not have resulted immediately from the dissociation process. The state $\text{CN} \cdot \text{B}$ lies $25,750 \text{ cm}^{-1}$ above $\text{CN} \cdot \text{X}$, and so it presumably could not have been populated directly from dissociation of $(\text{CN})_2$ by light of lesser energy than $(40,000 \text{ to } 50,000) + 25,750 = (65,750 \text{ to } 75,750) \text{ cm}^{-1}$, which corresponds to $1420\overset{\text{O}}{\text{\AA}}$ to $1320\overset{\text{O}}{\text{\AA}}$.

Another research on photodissociation of $(\text{CN})_2$ was by Jakovleva (1939, b). Here, no search was made for $\text{CN} \cdot \text{X}$ absorption, but $\text{CN} \cdot (\text{B} \rightarrow \text{X})$ fluorescence

resulted from irradiation of cyanogen gas with the continuous spectrum of a steadily operated hydrogen discharge tube having a fluorite window. Depending on the thickness of window used, fluorite is known to transmit to various limits reaching to the neighborhood of $1250\text{-}1200\text{\AA}$ ⁰; and, under some circumstances, hydrogen discharge tubes can be made to emit wavelengths at least as short as 1300\AA ⁰. * Therefore, the primary process $(\text{CN})_2 \xrightarrow{\text{O}} \text{CN}\cdot\text{X} + \text{CN}^*\cdot\text{B}$ might have been energetically possible with an assumption of $\text{D}_{\text{NC-CN}}^{\text{O}}$ anywhere in Gaydon's range.

Jakovleva did not find the $(\text{B} \rightarrow \text{X})$ fluorescence when irradiating the cyanogen through a quartz window—such light being surely unable to produce $\text{CN}\cdot\text{B}$ initially. This also indicates that the 4400\AA ⁰- 3600\AA ⁰ region of the steady hydrogen discharge tube was not powerful enough to cause the sequential absorption and fluorescence processes $\text{CN}\cdot(\text{B} \leftrightarrow \text{X})$ observed with the flash lamps of Paul and Dalby, and of Basco, et al; or else that the 2000\AA ⁰ region of the H_2 tube was not strong enough to produce sufficient $\text{CN}\cdot\text{X}$ molecules for observing the sequential process.

*See, for example, Robinson (196?).

Basco, et al, furthermore demonstrated through the use of various filters that $\text{CN} \cdot \text{X}$ ($v = 0$) was being produced in sufficient amount in the first few microseconds of their flash duration for these molecules to absorb strongly at the $\text{CN} \cdot (\text{B} \leftarrow \text{X})$ wavelengths out of the continuous flash spectrum in subsequent microseconds. Following which, the $\text{CN} \cdot \text{B}$ molecules presumably fluoresced back down to those various higher vibration states of $\text{CN} \cdot \text{X}$ to which transitions are permitted by the Franck-Condon principle; so that by the end of the UV flash at least the first four vibrational levels of $\text{CN} \cdot \text{X}$ were observed to be almost equally populated, as checked by the absorption spectrum. Heavy population of considerably higher vibrational levels could also be predicted, from the known fluorescent intensities of the various $\text{CN} \cdot (\text{B} \rightarrow \text{X})$ bands.

Paul and Dalby had also observed this $\text{CN} \cdot (\text{B} \rightarrow \text{X})$ fluorescence arising from their irradiations. It surely could not have resulted immediately from the dissociation process. The state $\text{CN} \cdot \text{B}$ lies $25,750 \text{ cm}^{-1}$ above $\text{CN} \cdot \text{X}$, and so it presumably could not have been populated directly from dissociation of $(\text{CN})_2$ by light of lesser energy than $(40,000 \text{ to } 50,000) + 25,750 = (65,750 \text{ to } 75,750) \text{ cm}^{-1}$, which corresponds to $1420\overset{\text{O}}{\text{\AA}}$ to $1320\overset{\text{O}}{\text{\AA}}$.

Another research on photodissociation of $(\text{CN})_2$ was by Jakovleva (1939, b). Here, no search was made for $\text{CN} \cdot \text{X}$ absorption, but $\text{CN} \cdot (\text{B} \rightarrow \text{X})$ fluorescence

resulted from irradiation of cyanogen gas with the continuous spectrum of a steadily operated hydrogen discharge tube having a fluorite window. Depending on the thickness of window used, fluorite is known to transmit to various limits reaching to the neighborhood of $1250\text{-}1200\text{\AA}$; and, under some circumstances, hydrogen discharge tubes can be made to emit wavelengths at least as short as 1300\AA . * Therefore, the primary process $(\text{CN})_2 \xrightarrow{\text{O}} \text{CN}\cdot\text{X} + \text{CN}^*\cdot\text{B}$ might have been energetically possible with an assumption of $\text{D}^{\text{O}}_{\text{NC-CN}}$ anywhere in Gaydon's range.

Jakovleva did not find the $(\text{B} \leftrightarrow \text{X})$ fluorescence when irradiating the cyanogen through a quartz window—such light being surely unable to produce $\text{CN}\cdot\text{B}$ initially. This also indicates that the $4400\text{\AA}\text{-}3600\text{\AA}$ region of the steady hydrogen discharge tube was not powerful enough to cause the sequential absorption and fluorescence processes $\text{CN}\cdot (\text{B} \leftrightarrow \text{X})$ observed with the flash lamps of Paul and Dalby, and of Basco, et al; or else that the 2000\AA region of the H_2 tube was not strong enough to produce sufficient $\text{CN}\cdot\text{X}$ molecules for observing the sequential process.

*See, for example, Robinson (1962).

7.5 The Absorption Spectrum of (CN)₂

It is necessary to use the less direct methods discussed above for deducing the minimum dissociation energy of (CN)₂, because the spectrum of this polyatomic molecule is not yet sufficiently understood to permit reliable extrapolation of its vibrational sequences to any dissociation limits.

The molecule of (CN)₂ is linear, and so it has a single rotational frequency. In its ground state the rotational energy levels are given by the usual formula, with the constants

$$B_0 = 0.15752 \text{ cm}^{-1} \text{ and } D_0 = 4 \times 10^{-8} \text{ cm}^{-1},$$

as measured in the rotational Raman effect by Møller and Stoicheff (1954).

This four-atomic symmetrical linear molecule will have seven fundamental modes of vibration, of which two are doubly degenerate. Of these, one of the single and one of the double frequencies as well as a number of combination and harmonic frequencies, are expected to be active in the infrared spectrum.* All of the seven fundamentals may possibly appear as vibrational level separations in the ultraviolet electronic bands.

*See, for example, Nielsen (1962).

Nixon and Verderame (1964) have found the following four strong infrared (electronic ground state) vibrational frequencies

732 cm^{-1}
2158 "
2563 "
2663 "

as well as five other weaker ones, of which the lowest is 615 cm^{-1} . It should be noted that White (1940, b) has quoted some indirect thermochemical evidence which indicates that one of the vibrational frequencies inactive in the infrared may be as low as about 230 or 240 cm^{-1} .

Callomon and Davey (1963) found that the ground state* of $(\text{CN})_2$ is $X^1\Sigma_g^+$, and what is presumably the first excited electronic state is $A^3\Sigma_u^+$ at about $33,290 \text{ cm}^{-1}$. The very weak, singlet-triplet intercombination band system connecting these levels lies in the region $3100 \text{ \AA} - 2400 \text{ \AA}$. Its absorption

*Mulliken (1962) and Clementi and McLean (1962) have made theoretical studies on the nature of the electronic configuration and on relative chemical bond strengths in this ground state of $(\text{CN})_2$.

bands cannot be seen except with path lengths of about 2 meter-atmospheres of $(\text{CN})_2$. The only vibrational frequencies identified so far in this upper state are about 895 cm^{-1} and about 2049 cm^{-1} , which are of the same order of magnitude as the ground-state frequencies identified in the infrared. The upper level rotational constant is very similar to that of the ground state: $B_0 = 0.1536 \text{ cm}^{-1}$. This causes the rotational lines to be quite close together, since their spacing depends on the difference in B_0 between upper and lower states. Similar earlier work on these bands, but at lower dispersion, was done by Woo and Liu (1937).

The stronger absorption of $(\text{CN})_2$ consists of a collection of bands beginning about 2400 \AA , or $41,700 \text{ cm}^{-1}$, where the $A \leftarrow X$ system merges into them, and stretching on into the far ultraviolet. They have been mapped as far as 1820 \AA , or $55,000 \text{ cm}^{-1}$, by Woo and Badger (1932). Similar results were found by Mooney and Reid (1932) and by Jonescu (1937).

In the neighborhood of 2000 \AA , or $50,000 \text{ cm}^{-1}$, Woo and Badger found that a path length of 75 cm at 10 mm $(\text{CN})_2$ pressure was adequate for mapping these absorption bands with a steady hydrogen discharge tube light source. Hogness and Tsai (1932) made quantitative absorption measurements with the undispersed light of a H_2 discharge tube and found that between 2240 \AA and 2145 \AA these bands absorbed 9% of the continuous incident spectrum, in one passage through a mass thickness about the same as used by Woo and Badger; i. e., 2.5 cm path length at 1 atm pressure of $(\text{CN})_2$. Thus, these bands are

not extremely strong, but it may be remembered that the 100-joule flash lamp used by Paul and Dalby caused enough $(\text{CN})_2$ dissociation by absorption at these wavelengths to produce a CN density of about $10^{14}/\text{cm}^3$.

The bands are sufficiently complex that they probably consist of overlapping systems involving several upper electronic states. Some evidence can be seen for two of these states, separated by about 2100 cm^{-1} , which might be components of an electronic II state—such as Callomon and Davey thought was probably present in this location. There are varying indications of the following vibrational level spacings involved in the spectrum in some fashion:

230 cm^{-1}
508 " (double)
766 "
2149 "
2355 "

The rotational structure has not been resolved, but all the bands degrade toward the red.

The absence of obvious convergence of any vibrational sequences would make it seem that at least most of these bands must correlate with dissociation limits above the end of the experimentally accessible region at $55,000 \text{ cm}^{-1}$ —probably with $(\text{CN} \cdot \text{X} + \text{CN} \cdot \text{B})$ and higher limits.

All of the facts discussed so far are at least consistent with the rough sketch of a suggested energy level diagram for $(\text{CN})_2$ given in Figure 18,

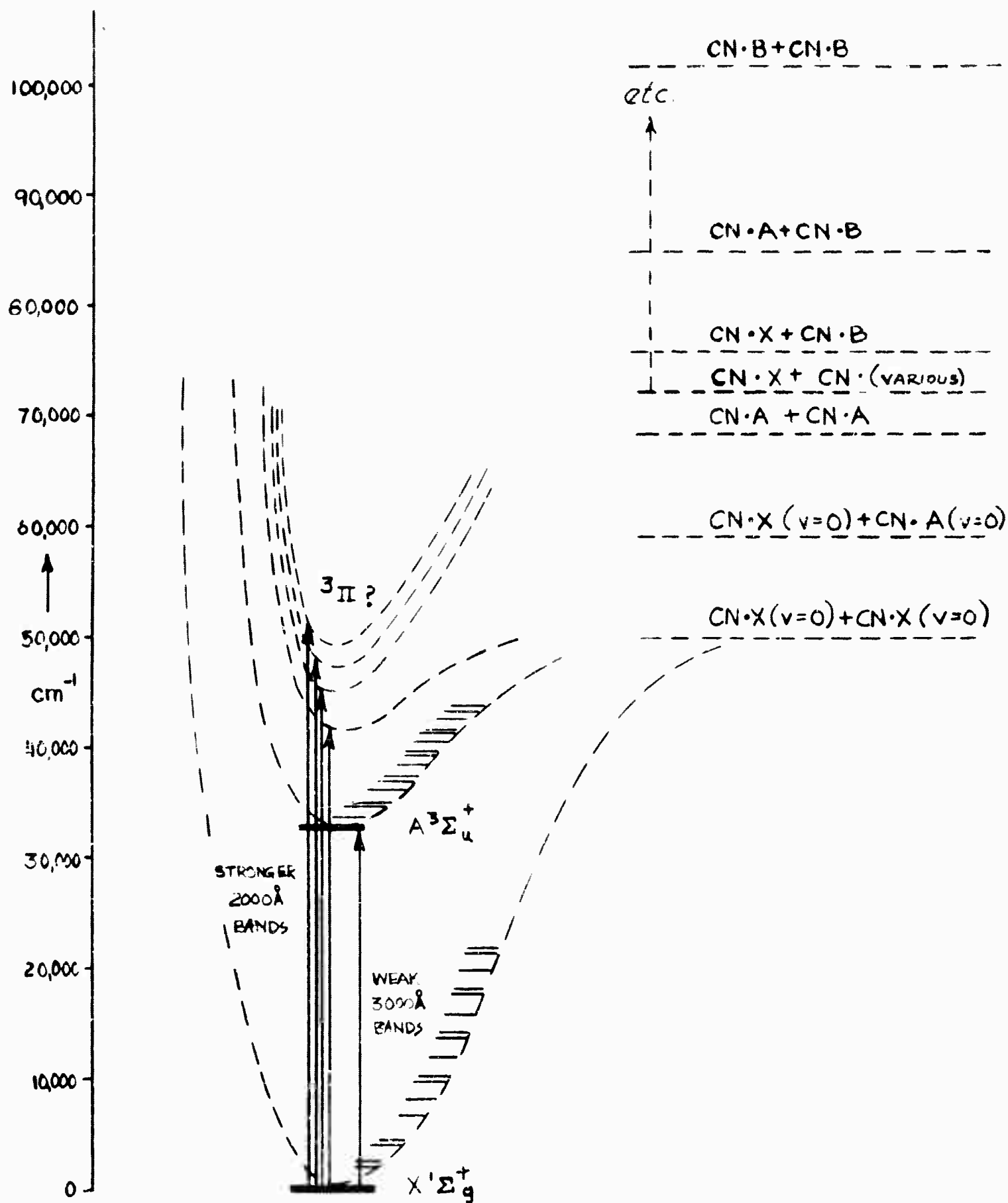
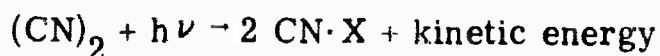


Figure 18.
Suggested electronic states and dissociation limits of $(CN)_2$;
schematic only.

although few details are definite. In this diagram the value of $D^0_{\text{NC-CN}}$ has been arbitrarily set at exactly $50,000 \text{ cm}^{-1}$, and the assumption that dissociation is always to ($v=0$) of every state has also been made, rather arbitrarily.

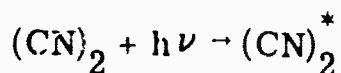
7.6 Photodissociation of (CN)₂ as a Two-Stage Process.

One of the most important facts which emerges from these various fragmentary investigations is that dissociation of the (CN)₂ molecule is probably not the initial result of the absorption of light near 2000Å. That is, for example,

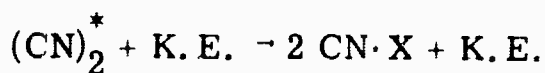


is probably not the first thing which happens when a light quantum is absorbed.

This reaction would require the presence of an absorption continuum. Yet none of the experimenters have observed any continuous absorption by cyanogen gas. Therefore, the first process must be absorption by the discrete spectrum lines ** of the UV bands into definite excited levels of (CN)₂:



After such an absorption has placed the molecule in some level near one of the dissociation limits, then thermal collisions or spontaneous radiationless transitions can quite readily cause the actual dissociation,



** Ramsay's attempt at photodissociation of (CN)₂ with monochromatic light was successful doubtless because the 1849Å Hg line happens to fall within one of the definite (CN)₂ vibration-rotation absorption bands whose head lies at 1846.7Å.

If the probability for spontaneous dissociation from most of the levels above the first limit D^0_{NC-CN} was quite high, then the absorption lines involving these levels would be broad and diffuse, because of the shortened lifetime of the states. This is the phenomenon usually called "predissociation." It is true that many, but not all, of the bands in the $\lambda < 2400\text{\AA}$ region mapped by Woo and Badger are rather diffuse—and all the bands look diffuse at low dispersion, so that Hogness and Tsai (1932) believed these bands indicated predissociation throughout. However, much of this diffuseness can probably be ascribed to unresolved close rotational structure. It seems likely that at total gas pressures of a few cm or more, most dissociations of the excited $(CN)_2$ molecules are caused by thermal collision.

Now, in the design of a high-power laser transformer it is necessary to reduce the production of sensible heat in the gas to an absolute minimum. Therefore, the fraction of the absorbed photon energy which gets converted into kinetic energy in these dissociations becomes of great importance. Clearly, the wavelength of any light to be used for photoproduction of CN from $(CN)_2$ must be chosen to place the excited $(CN)_2$ molecules in a level just as close to the D^0_{NC-CN} dissociation limit as possible. Fortunately, the closer the level lies to this limit the more readily the collisions will complete the dissociation process. All energy transfers by molecular collisions in

gases have greatest probability when the discrepancy ΔE between initial and final discrete level sums — that energy which has to be transferred into or out of the translational form — approaches zero.

It is simplest to assume that the cyanogen gas must be operated at just as low a temperature as possible, possibly about 210°K , where the saturated vapor pressure over the solid state is about 3 cm Hg*. This will reduce the probability for production of sensible heat during pumping because of collision relaxation of the vibrational levels of excited $(\text{CN})_2$. As most of the excited $(\text{CN})_2$ molecules may be expected from the above data to have vibrational energies greater than about 500 cm^{-1} , a value of kT of 145 cm^{-1} for the gas should make the ΔE for vibrational relaxation large enough to keep the relaxation probability fairly low. (Although there would still be a possibility of heating trouble if the presumed vibrational frequency near 230 cm^{-1} is actually very important.)

If the collision dissociation probability is to be made high at such a small kT , then the pumping process must be very accurate in placing the excited $(\text{CN})_2$ molecules closely adjacent to the $\text{D}^0_{\text{NC-CN}}$ limit. This means that photoproduction of $\text{CN} \cdot \text{X}$ from cyanogen gas without appreciable heating of the gas will be possible—under the simple considerations discussed above—

* See the compilation of data on $(\text{CN})_2$ by Brotherton and Lynn (1959).

only for a quite narrow and carefully chosen band of pump wavelengths. Because of the present uncertainty in the value of $D^0_{\text{NC-CN}}$, this wavelength position will have to be found from experiment. It seems most likely that it will lie close to 2000\AA , or $50,000\text{ cm}^{-1}$.

Probably production into ($v = 0$) of $\text{CN}\cdot\text{X}$ can be caused to predominate, with very few molecules dissociating into ($v = 1$) or higher vibrational levels. Although perhaps, by a suitable choice of wavelength, dissociation into any chosen higher vibration level could be favored. The results of Ramsay on photodissociation with 1849\AA Hg light, which apparently yielded only $\text{CN}\cdot\text{X}$ ($v = 0$) in the low-power steady state, even though there was surely several thousand cm^{-1} of extra quantum energy available, may or may not argue against this possibility. In his pure cyanogen gas at room temperature and only a few mm pressure, vibrational relaxation of the $(\text{CN})_2^*$ may have occurred before dissociation. Likewise Basco, et al, found that at least 96% of the $\text{CN}\cdot\text{X}$ molecules were produced in $v = 0$ in cyanogen plus about one atmosphere of N_2 , even though the $(\text{CN})_2$ was surely absorbing in many of its lines scattered across the broad spectrum of the flash tube source. Probably, vibrational relaxation of $(\text{CN})_2^*$ before dissociation also predominated in this mixture, since N_2 collisions are well known to favor vibrational relaxation of various molecules. This indicates that there may be an inherent tendency for CN

fragments formed from mostly non-vibrating $(\text{CN})_2^*$ also to be mostly nonvibrating — although this must also depend on whether the nonvibrating level of one of the $(\text{CN})_2^*$ electronic states just happens to have an energy very close to the $\text{D}^\circ_{\text{NC-CN}}$ which yields $2 \text{ CN} \cdot \text{X}$ ($v = 0$). The experiments of Paul and Dalby are not relevant to this point, since they specially looked only for the $\text{CN} \cdot \text{X}$ ($v = 0$) produced by their flash lamp.

7.7 An Analogous Photo-Collision Dissociation in Na₂

Since direct experiments on the proposed process in (CN)₂ are lacking, it may be useful to note the existing data on an analogous process in Na₂. When vapor containing sodium molecules absorbs light in the spectral range from green to near ultraviolet, the molecules are raised from the ground state Na₂X ¹Σ_g to the upper electronic state Na₂B ¹Π_u, as indicated by the partial level diagram in Figure 19. Since the natural lifetime of Na₂B is only about 10⁻⁸ sec, the molecules quickly return to the ground state emitting fluorescent blue-green light.

It is known, however, that any of various impurities included with the sodium vapor will have a quenching action on this fluorescence. Quantitative measurements on this phenomenon were made by Jablonski, Pringsheim and Rompe (1932), who added increasing amounts of He, Ar, or N₂ to the sodium vapor. They found that if (a) the excitation process was by optical pumping up into the v = 1 vibration level of Na₂B only, and if (b) the total gas pressure was kept so low that not enough collisions occurred within the fluorescent lifetime of the excited molecule for it to be shifted to any other vibration state before radiating, then the resulting fluorescence from saturated sodium vapor at 315° was not noticeably weakened by adding 1 mm of He.

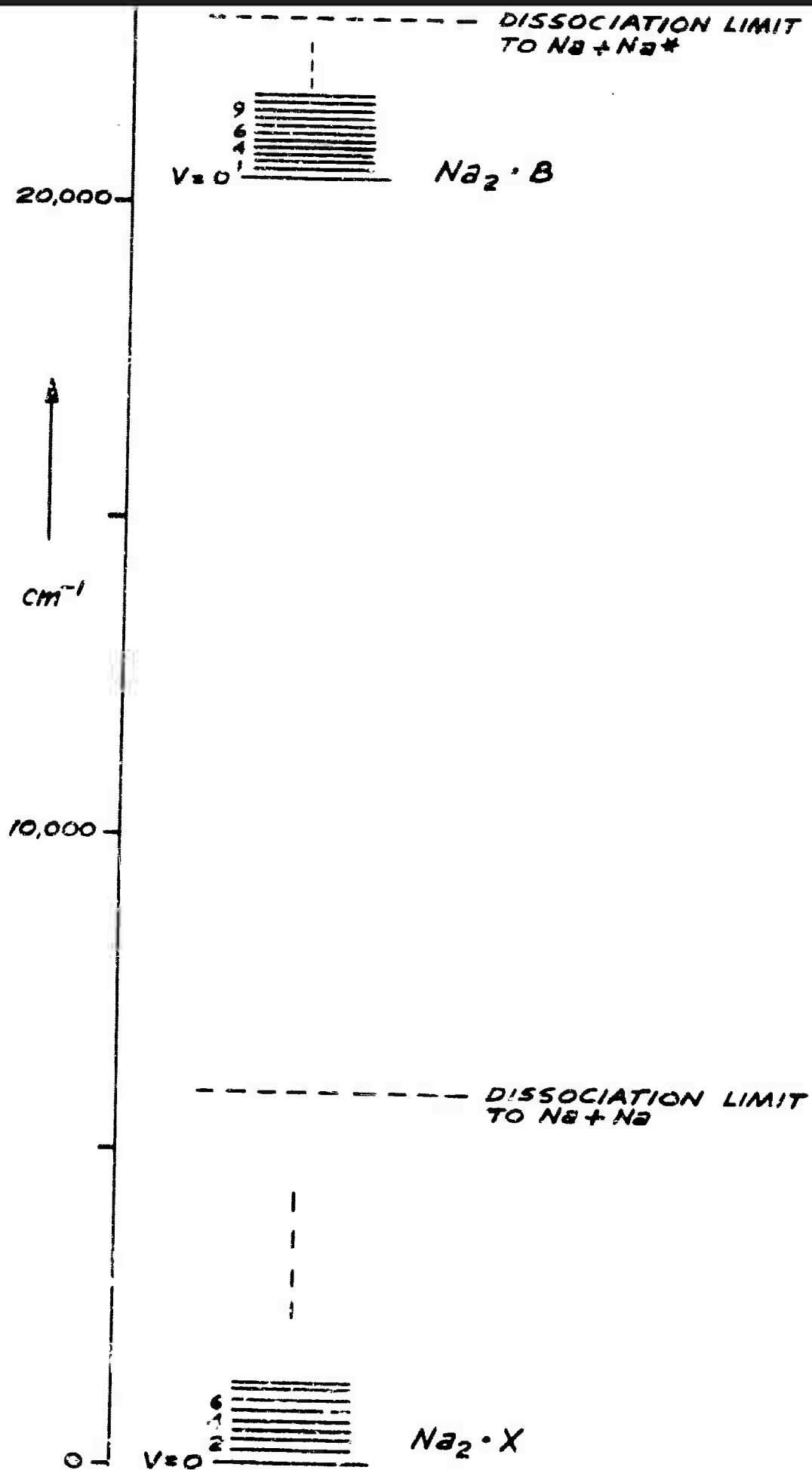


Figure 19
Partial energy level diagram for Na_2 .

But when the pumping quantum energy was gradually increased so as to raise the molecules successively to the $v = 4$, the $v = 6$, or the $v = 9$ vibration level of $\text{Na}_2^+ \text{B}$ with other circumstances the same, then the addition of 1 mm He caused greater quenching of the molecular fluorescence. This could be interpreted as meaning that the quenching process — in at least some cases — was a dissociation of the $\text{Na}_2^+ \text{B}$ molecules, upon collision with those He atoms which happened to be travelling fast enough to provide the amount of kinetic energy needed for dissociation. The closer the pumping light had already raised the molecules toward their dissociation limit, the more frequency of occurrence of He collisions having enough energy to take them the rest of the way.

As shown by Figure 19, the $v = 1$ vibration level of $\text{Na}_2^+ \text{B}$ lies about 2380 cm^{-1} below the dissociation limit of the state, neglecting rotational energies for the moment. But $v = 4, 6$ and 9 lie only about 2021, 1789, and 1454 cm^{-1} , respectively, below the limit and so should require progressively less additional energy from a helium collision to cause dissociation.*

*These figures are based on the analysis of relative level locations by Smith (1924) and by Frederickson and Watson (1927) and on the most recent estimate of the location of the $\text{Na}_2^+ \text{B}$ dissociation limit, by Barrow (1961). The present uncertainty of about $\pm 125 \text{ cm}^{-1}$ in the latter should be applied to the absolute values of ΔE quoted above, but this would not affect differences between them, which are known to a small fraction of one cm^{-1} .

The explanation of at least part of this impurity quenching in terms of dissociation receives support from another type of observation. Wood and Kinsey (1928), when using blue-violet light to pump the molecules up into the general region around $v = 5$ of $\text{Na}_2 \cdot \text{B}$, had found that 3mm of either air, H_2 or N_2 caused the appearance of the yellow D lines, which arise from excited Na atoms, in addition to the (weakened) molecular green band fluorescence. With the sodium pressure and temperature and the color of pumping light being used, there had been no trace of D-line fluorescence before the foreign gases were added. Therefore, the pumped sodium molecules were not transferring their excitation energy directly to colliding Na atoms in the pure vapor to any appreciable extent, under these circumstances. But collisions with the foreign molecules did produce excited Na atoms, and indeed this should be expected if some of the pumped molecules in $\text{B } ^1\text{II}_u$ were being dissociated by this type of collision. As indicated in Figure 19, dissociation from the $\text{Na}_2 \cdot \text{B}$ state yields one normal Na atom and one excited Na atom — which latter will then radiate one of the D lines within an average lifetime of about 10^{-8} sec, if it is not de-excited in some other way earlier.

Similarly, Jablonski, Pringsheim and Rompe found that 1 mm of He added to the saturated sodium vapor at 315°C brought out some D-line fluorescence with each of the arrangements for pumping the molecules — even from $v = 1$ where weakening of the molecular fluorescence was too slight to be noticeable. The strongest D lines occurred when the $\text{Na}_2 \cdot \text{B}$ molecules had been optically excited to $v = 9$.

These authors also added argon and nitrogen at 315°C and again got D-line fluorescence, although weaker, when the sodium molecules were being pumped into the B state. The relative weakness in these cases does not necessarily mean that these two additives have less effect on the Na_2 molecule than does He. In fact, it was also demonstrated that 1 cm of nitrogen added to sodium somewhat less than saturated at 290°C had a very strong quenching action on the molecular green-band fluorescence — as Wood and Kinsey had found earlier. But with regard to the D-line fluorescence from excited Na atoms, another process appears in the case of these particular additives. It is well known that nitrogen particularly, and also argon and many other atoms and molecules, are strong quenchers of D-fluorescence. Therefore, many pumped $\text{Na}_2 \cdot \text{B}$ molecules were doubtless indeed being dissociated by fast N_2 collisions, thus weakening the molecular fluorescence; but also many of the resulting excited Na^* atoms were then being de-excited by another N_2 collision before they had a chance to radiate, thus weakening the D-line fluorescence*. When the nitrogen or argon pressures were raised to one or two cm, the D fluorescence practically vanished — as had the band fluorescence from $\text{Na}_2 \cdot \text{B}$.

A process in which the N_2 molecule in one collision simultaneously dissociated the $\text{Na}_2 \cdot \text{B}$ molecule and de-excited the Na^ atom, itself carrying away most of the pumped energy and leaving behind two neutral Na atoms, would be an alternative to the above successive collision mechanism — and would probably be indistinguishable from it in simple experiments.

But in the case of helium, Winans (1930), Hámos (1932) and Duchinsky (1932) have all shown that this gas causes practically no quenching effect on the D-line fluorescence from excited sodium atoms.

This fact, that He has no good mechanism for absorbing $16,965\text{ cm}^{-1}$ of energy from an excited Na^* atom, probably means that it also cannot absorb similar amounts of energy from an excited Na_2B molecule upon collision. Doubtless practically all of the quenching of the sodium green-band fluorescence by He occurs through the fast collision molecular dissociation process already discussed.

These He experiments with Na_2 give considerable indication that He will be the best gas to use in a mixture with cyanogen for a transtormer laser medium. The He should dissociate the $(\text{CN})_2$ with the minimum production of heat through either vibrational relaxation or quenching from the $\text{CN}\cdot\text{A}$ electronic state. As will be discussed later, a considerable amount of this additive gas will be needed to provide collisions with CN which will rearrange the rotational level distribution in a manner suitable for lasing.

Before proceeding to a survey of CN collision processes, let us briefly catalogue the remaining known ways to prepare CN, for the sake of completeness.

7.8 Dissociation of $(\text{CN})_2$ by Chemical Reactions

Steacie(1954) has collected references to various chemical reactions of atomic H, O, and Na with $(\text{CN})_2$ which yield CN as one of the products.

There is a large literature on the occurrence of the CN emission bands in flames of cyanogen plus oxygen or other gases. This subject is reviewed by Gaydon (1957).

So-called "active nitrogen" strongly reacts with cyanogen, in a group of complex processes which include the production of CN. This system has recently been studied by Haggart and Winkler (1960), among others. Active nitrogen gas contains several carriers of potential energy; prominent among these are the N atom in its ground state, and the N_2 molecule in its metastable state $A^3\Sigma_u^+$. For a recent review of the behavior of active nitrogen in many circumstances, see Manella (1963).

Any of these arrangements would seem to the present writer to leave a laser transformer vapor medium in a more complex condition than would the relatively simple photodissociation of cyanogen.

7.9 Ways of Preparing CN from Other Starting Substances

Neujmin and Terenin (1936) showed that the region of the hydrogen discharge tube spectrum near 1400\AA would dissociate acetonitrile,

CH_3CN , in such a manner as to produce the fluorescent $\text{CN}(\text{B-X})$ bands. In a similar manner, Jakovleva (1939, a) observed the CN fluorescence upon photodissociating the cyanogen halides, ICN and BrCN , with far UV light. Basco, Nicholas, Norrish and Vickers, (1963) applied their 1600 joule photoflash lamp to ICN and BrCN through a quartz window and obtained $\text{CN}\cdot\text{X}$, as seen by its absorption bands.

Although it is possible that CN production by almost monochromatic photodissociation of one of these gases instead of cyanogen might perhaps place the necessary light source wavelength in a more convenient region, the resulting fragments other than CN which would be left in the vapor are all known to be highly active in vibrational relaxation collisions, and other complex reactions. They would seem to lead to much more chance of wastage of the prepared CN molecules, and chance of production of sensible heat in the medium.

Such molecules as BrCN will also yield CN in chemical reactions with Na , for example. (See Williams, 1948)

Heavy hydrocarbon vapors can utilize the stored energy of metastable excited mercury atoms in the presence of N_2 to split off fluorescing $\text{CN}\cdot\text{A}$ and $\text{CN}\cdot\text{B}$ fragments. (See page 221 of Pringsheim, 1949).

Wager (1943) studied the CN spectrum very successfully by adding chloroform to active nitrogen, as did Jenkins, Roots and Mulliken (1932) and Dixon and Nicholls (1958) with CCl_4 , and Kiess and Broida (1958) with twenty nine different organic vapors.

However, all these classes of preparation processes would leave a very complex mixture which could have undesirable quenching and heating properties in a high-power laser transformer medium, even though they were satisfactory for simple spectroscopic studies.

In the next sections, some of the important collision processes involving CN will be considered further.

8. MECHANISMS FOR DISAPPEARANCE OF CN AND CN*

8.1 Disappearance of CN through Polymerization of (CN)₂

Cyanogen gas has a very considerable tendency to polymerize. Within an isolated volume of the gas, the polymer is believed to be formed only in the presence of appreciable amounts of CN, with the initial reaction probably being



The (CN)₃ so formed seems to further polymerize rather quickly, so that no detectable equilibrium concentration is built up. The chain has not been followed in detail but the next member (CN)₄ might perhaps be particularly stable, since Henglein, Jacobs and Muccini (1963) found that the ion (CN)₄⁺ was very persistent in cyanogen discharge tubes.

Pure cyanogen gas in a darkened glass or quartz container at one atmosphere pressure or less is rather stable until the temperature is raised to about 400°C, although prolonged heating at 300°C will cause the onset of polymerization. (Quagliano, 1949) It was mentioned earlier that White (1940, b) calculated 400° C as the temperature region where CN concentration from thermal dissociation of (CN)₂ begins to rise rapidly*. At higher pressures, cyanogen begins to polymerize at lower temperatures.

*Even at room temperature some slight polymerization will occur as a result of wall reactions at metal surfaces. Appreciable solid polymer can be observed within stainless steel or Monel cylinders after cyanogen gas at normal pressure has been stored in them for 100 days. (Brotherton and Lynn, 1959).

At elevated temperatures, the observed equilibrium concentration of CN doubtless represents a balance between the dissociation and the polymerization reactions (and the three-body recombination yet to be discussed), with solid polymer gradually accumulating on the container walls. The crystal structure of the solid is assumed to be a continuous molecular lattice of $(\text{CN})_x$. Above 800°C , the polymer slowly breaks apart again and returns to $(\text{CN})_2$. (Robertson and Pease, 1942).

On exposure to sunlight, cyanogen always slowly polymerizes. Hogness and Tsai (1932) found that this photopolymerization is chiefly caused by absorption in the $(\text{CN})_2$ bands at wavelengths less than 2300\AA . From data already presented on photodissociation produced in these UV bands, it is clear that the polymerization is closely associated with the presence of CN. Along the same line, electric discharges—which are well known sources of CN—will also polymerize $(\text{CN})_2$, although other more complex reactions could also be present in this case. Haggart and Winkler (1960) found that active nitrogen also polymerized $(\text{CN})_2$ at any temperature above 80°C .

The polymerization mechanism will therefore be an important contributor to the disappearance of CN, whenever CN is produced in any manner which leaves a considerable remainder of $(\text{CN})_2$ present. The most recent quantitative rate measurements in such circumstances are by Paul and Dalby (1962). They flashed their small continuous-spectrum light source, for measuring the CN

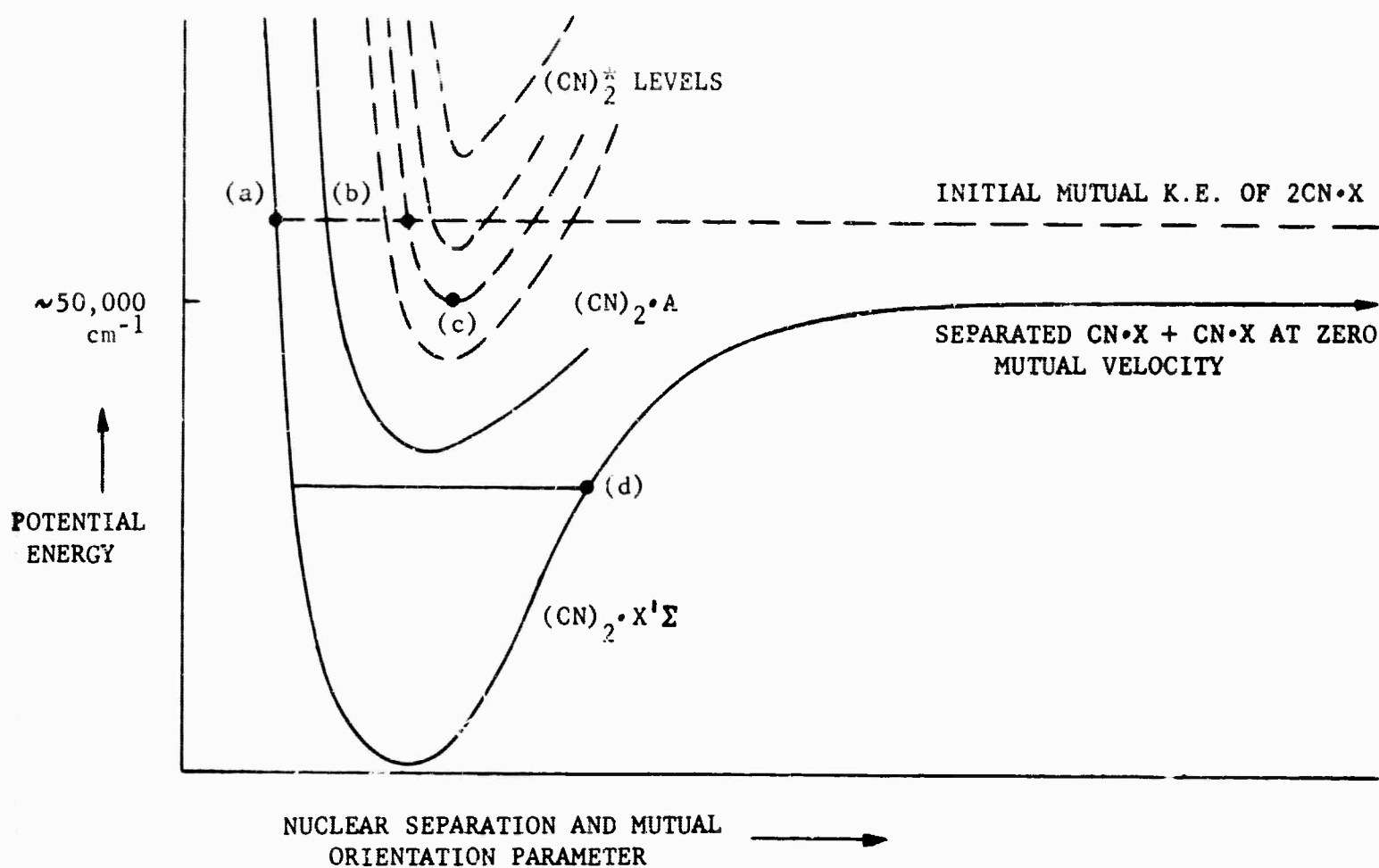
absorption bands, at various short time intervals after flashing their 100 joule photoflash lamp which dissociated the $(\text{CN})_2$. In this way, they could follow the rate of disappearance of the small $\text{CN} \cdot \text{X}$ fraction formed in the mixture by the UV flash. The disappearance of the CN was presumably almost wholly through the polymerization reaction. For example, they found that a moderate amount of CN formed in pure $(\text{CN})_2$ at 18.3 mm pressure and 175°C disappeared exponentially with a half-life of $75 \mu\text{sec}$.

Since the polymer seems quite stable at ordinary temperatures, the polymerization reaction must be exothermic. There do not seem to be data available on how much sensible heat appears in the gas with the removal of each CN.

In different circumstances, if the production process converts a large fraction of the cyanogen to CN — and if a large quantity of some inert gas additive has been included in the mixture — then the major contributor to the disappearance of these molecules will probably be the three-body recombination process, which is discussed in the next section.

8.2 Three-Body Recombination of CN

If two $\text{CN}\cdot\text{X}$ molecules collide head-on, they will probably approach close enough to come to rest momentarily high on the left hand side of the $(\text{CN})_2\cdot\text{X}$ potential curve, at the location corresponding to their initial kinetic energy — such as point (a) in the sketch below.

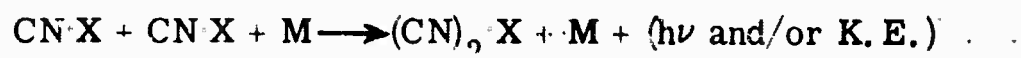


In this case they will almost every time simply reverse their path and separate again along the right hand side of the $(\text{CN})_2\cdot\text{X}$ curve toward infinity. That is,

the two-body stable recombination reaction $2\text{CN}\cdot\text{X} \rightarrow (\text{CN})_2\cdot\text{X}$ practically never occurs.

However, if before the two CN's have time to separate again, an inert third body of any kind impinges upon the combination, its force fields may temporarily alter the potential curves of both $(\text{CN})_2\cdot\text{X}$ and the higher $(\text{CN})_2^*$ states so as to make them intersect. In this case, changes in the electronic quantum numbers will have a good probability, in such a way as to transfer the temporary cyanogen dimer into a level of one of those higher $(\text{CN})_2^*$ electronic states which are responsible for the far UV absorption bands—such as level (b) in the diagram. From there, the $(\text{CN})_2^*$ could—with fairly low probability because of the relative weakness of the UV bands—become stable by fluorescing down to a low vibration level of $(\text{CN})_2\cdot\text{X}$. But at total gas pressures of at least several cm, it is probably more likely that a subsequent collision will either re-dissociate the $(\text{CN})_2^*$ or will drop it to level (c) in a vibration-to-translation relaxation—where it will be stable against collisions for long enough to have time to fluoresce down to $(\text{CN})_2\cdot\text{X}$. Alternatively, in the original three-body collision, there is good probability for the momentum conservation laws to permit the third body to carry more kinetic energy away from the collision that it brought into it. Then, the transient $(\text{CN})_2\cdot\text{X}$ molecule might be left at a point such as (d), from which it could not re-dissociate but would eventually relax down to $(\text{CN})_2\cdot\text{X}$ ($v = 0$) by collision.

The net result is that in any vapor mixture containing a large proportion of CN, these molecules should disappear chiefly by the three-body recombination process



Note that in each case, except the usually less probable one of stabilization by UV fluorescence where the light escapes from the gas volume, every recombination eventually converts into sensible heat the full $\sim 50,000 \text{ cm}^{-1}$ of energy which had been invested in producing the pair of CN's in the first place.

Both polymerization and three-body recombination thus can have a doubly deleterious effect on an efficient high-power laser pulse transformer design—wasting the prepared CN's and heating the gas—if they occur to an important extent just before or during the course of an output pulse. Of course, after the pulse is over the gas medium can be circulated through a heat exchanger to remove waste heat.

To minimize both of these CN consumption processes during a pulse, the laser transformer design should seek to

- (a) achieve the highest possible percentage dissociation of the cyanogen gas during the preparative UV flash, so as to minimize the number of $(\text{CN})_2$ molecules remaining to take part in polymerizing collisions;
- (b) use containers of reasonably low surface-to-volume ratio, avoiding excessive wall area which would favor polymerizing collisions;
- (c) use the lowest practical partial pressure of cyanogen, so as to minimize the frequency of triple-CN collisions, which probably also produce polymer—this means operating at the highest possible pumping and lasing fluxes—and,

- (d) choose the inert gas additive, which will be needed in the laser for increasing the frequency of two-body thermalizing collisions, to consist of a light atom with the weakest possible external force fields — so that most of its inevitable three-body collisions with two CN molecules will not lead to CN recombination.

With regard to the last point, some evidence has already been mentioned that helium gas is the best possible inert additive. Also, for example, Smith (1962) has theoretically calculated the probability that a three-body collision at 293° K between two iodine atoms and a noble gas atom will produce recombination of the iodine atoms to form I_2 . The probability of the process, per collision, becomes less and less upon going from the heavy to the lighter noble gas atoms. Thus, with additive helium the probability is calculated as 1/720 per triple collision, while with additive Xe it is 1/44 per triple collision*.

As has often been pointed out, one reason the process probability is lower with very light additive particles is that then the conservation laws happen to prevent much momentum transfer in a collision, so there is less likelihood for the additive to stabilize the new molecule by carrying away kinetic energy.

As another example, Jablonksi, Pringsheim and Rompe (1932) found that argon atoms had much more effect in quenching molecular sodium fluorescence after pumping than did helium atoms. The effect of added nitrogen molecules,

*These process probabilities per collision would be greater at lower temperatures, because the third body would spend more time in the neighborhood of the transient molecule, and so would have more opportunity to cause an electronic transition which might stabilize it. However, the number of collisions per sec per unit of molecular density would also be less at lower temperatures, so there is not likely to be any net disadvantage in dropping to 210° K for the laser transformer.

which can exchange energy in vibrational as well as translational form, was even more drastic — although parts of the phenomenon in this case might have been chemical reaction and/or quenching of electronic excitation, as will be mentioned in the next sections.

8.3 Chemical Reaction of CN with Additives

A great many entities which might be present in a suggested lasing mixture either as conscious additives or as stray impurities could destroy the CN molecules by reacting chemically with them.

Thus, Bulewicz and Padley (1962) found that NO added to cyanogen-oxygen flames weakened the CN emission bands, probably by the reaction $\text{CN} + \text{NO} \rightarrow \text{N}_2 + \text{CO}$. Haggart and Winkler (1960) observed that adding H_2 to a mixture containing CN also destroyed the latter, probably by a reaction which forms HCN. Paul and Dalby (1962) came to a similar conclusion when they added H_2 to their cyanogen under flash photolysis. They also included, separately, ClCN , H_2O , O_2 , ethylene, and propane—each of which caused accelerated disappearance of the CN absorption bands. Gossikhin and Tsikora (1961) added a solution to a carbon arc which produced the OH molecule, and found that it weakened the cyanogen bands, probably by the reaction $\text{CN} + \text{OH} \rightarrow \text{CO} + \text{NH}$. Ghosh, Nand and Sharma (1963) noted the great weakening of CN emission bands by the addition of CH_2Cl_2 , as did Bayes (1961) upon the admixture of ammonia, and of CCl_4 .

These scattered experiments which happen to exist in the literature are rather random illustrations of the high degree of chemical reactivity of the CN molecule.

In an electric discharge in $(\text{CN})_2$, White (1940), a) found some evidence

that the rate of disappearance of the produced CN molecules was probably being governed by their attachment to various ions in the discharge*—notably to $(\text{CN})_2^+$ to form $(\text{CN})_3^+$. The CN molecule is also known to attach stray electrons to itself very readily, forming the ion CN^- . Herron and Dibeler (1960), Morris (1961), and Napper and Page (1963) have determined values for the electron affinity of CN ranging from 64 to 81 kcal/mole, or $22,400 - 28,300 \text{ cm}^{-1}$. This type of behavior is one reason for wishing to avoid electric discharge methods in the preparation of the molecules for the laser transformer medium, if possible.

8.4 Collision Quenching of CN^*

Pringsheim (1949) mentions that the fluorescence of $\text{CN} \cdot \text{B}$ is seriously weakened by the addition of N_2 ; more so for molecules in ($v = 0$) of $\text{CN} \cdot \text{B}$ than in ($v = 1$). Although this might be evidence of chemical reaction, it could also be an example of collision quenching of electronic excitation, since $\text{N}_2 \cdot \text{X}$ has available vibrational energy levels as far above its ground state as the $\sim 26,000 \text{ cm}^{-1}$ excitation energy of $\text{CN} \cdot \text{B}$. The collision energy exchange $\text{CN} \cdot \text{B}(v = 0) + \text{N}_2 \cdot \text{X}(v = 0) \rightarrow \text{CN} \cdot \text{X}(v = 0) + \text{N}_2 \cdot \text{X}(v = 12)$ would be entirely possible.

* Similarly, Magge (1961) quotes work showing that in a discharge through cyanogen gas plus xenon, the charged dimer shows a tendency for attachment to the noble gas atoms, forming such complexes as $[(\text{CN})_2 \text{Xe}]^+$.

An analogous case is well known in the addition of nitrogen gas to excited atomic sodium vapor. The N_2 molecules strongly quench the emission of the D lines from Na atoms in levels near $17,000\text{ cm}^{-1}$.

Any electronic quenching possibility would be a much stronger consideration in the choice of an additive for the CN in a laser transformer medium than the three-body recombination processes already discussed. The latter depend on relatively rare three-body collisions, but a quenching process could have an appreciable probability of wasting the absorbed Nd-glass laser pump energy at every collision of an excited CN molecule with the additive. Fortunately, both considerations point in the same direction— exclusion of all additives and impurities from the cyanogen except the monatomic noble gases. These have no electronic or vibrational energy levels which can accept $10,000 - 20,000\text{ cm}^{-1}$ in a collision with CN-A, for example; and their acceptance of that much energy as translation in a low-temperature collision is quite unlikely.

Thus Winans (1930), Hámos (1932), and Duschinsky (1932) all found that in contrast to the N_2 case, the addition of helium gas to fluorescing atomic sodium vapor did not weaken the D-line emission to any detectable degree.

Addition of helium to fluorescing CN has apparently not been studied, but

Mertens and Potter (1959) noted that immersing a CN-emitting flame in argon gas did not change the CN spectra in any observable way.

Let us now assume that suitable choices of these parameters of the transformer laser medium can be made in practice, and turn in Section 10 to a consideration of the pumping conditions which will lead to strong inversion in CN. At this time the analysis will deal only with the (6, 5) band, since operation within the (0, 0) band would be quite similar. As a summary, upon which to base the analysis of Section 10, Section 9 first outlines some of the parameter choices.

9. SUMMARY OF CN TRANSFORMER MEDIUM PARAMETERS

All of the last five sections, in effect, constitute background material for a study of the real problem: will CN behave properly in an ultra high flux pump-lase cycle? Before beginning the attack on this question, let us summarize here what has been discussed of the basic properties of the suggested transformer laser medium. Some of these items actually anticipate Section 10.

<u>Item</u>	<u>Remarks</u>
Best method of CN production	Probably, photodissociation of $(\text{CN})_2$ by almost monochromatic light near 2000\AA . Energy requirement: around a milli-joule per cm^3 of gas. Very high flux desired.
Gas heating problem during CN production	Vibrational relaxation and quenching of excited $(\text{CN})_2$ before dissociation. Control by choice of uv wavelength and heavy dilution of gas.
Best additive gas for dilution and rotation-shifting	Almost surely helium.
Worst gas heating problem throughout power pulse	Probably, polymerization of CN. To be minimized by leaving little $(\text{CN})_2$ available.
Desirable CN operating partial pressure	Balance between too high, causing three-body recombination, and too low, requiring excessive additive gas pressure and perhaps excessive pumping and lasing fluxes per unit of desired output. Probably a few cm is best.

ItemRemarks

Desirable additive gas pressure

Sufficient for fast enough rotation-shifting, dilution of waste heat, and collision-dissociation of $(\text{CN})_n^*$, but not so much as to relax or quench CN^* . Possibly somewhat less than 1 atm.

Best operating gas temperature

High enough to have adequate $(\text{CN})_2$ saturated vapor pressure, but low enough to minimize gas heating through relaxation and quenching collisions—although methods can be visualized to counterbalance some of these heating sources. Preliminary suggestion: 210°K .

Best pumping bands

Would be desirable if Nd glass laser efficiency could be verified for pumping into (0, 0) band of $\text{CN} \cdot (\text{A}-\text{X})$; probably best into R_2 branch of this band if the analysis proves promising.

Best lasing spectral range

Probably best into P_1 branch of the band pumped, if later analysis discloses no circulation inefficiencies here. This is at wavelengths to the redward from the pump position.

Mechanism for maintaining quantum energy balance during high power pulse, to avoid gas heating

Chiefly, adjustment of output flux versus fluorescence flux to balance average quantum sizes. Center of intensity of the fluorescence will lie towards the blue from the pump location, because of the ν^4 factor in the transition probabilities.

Limits on power pulse length

Not so short that Nd glass pumps lose efficiency when required to compress their output into so small a bandwidth as the region near a $\text{CN} \text{ R}_2$ head. Not so long that vibration-shifting or vibration-translation relaxation in CN becomes deleterious. Around 1 ms probably all right.

Limit on power pulse repetition rate

Limited only by efficiency in mechanically circulating the cyanogen through a heat exchanger: possibly a sonic velocity limit.

10. LASING POSSIBILITIES IN THE (6, 5) BAND AT 210° K

10.1 Boltzmann Distributions at 210° K in CN·X (v=5)

Let us first calculate the Boltzmann distribution of population among the rotational levels of CN·X (v=5), for a group of CN molecules whose rotational energy is in thermal equilibrium with the translational energy of molecules of the vapor at a temperature of 210° K.

If the total molecular density in the equilibrium distribution over (v=5) is $[N_{X5}]_{210}$ molecules/cm³, and the equilibrium molecular density in any one rotation level J is $[N_{X5}(J)]_{210}$ molecules/cm³, then (as described, for example, in Herzberg's book) the relation between these equilibrium population densities is

$$\frac{[N_{X5}(J)]_{210}}{[N_{X5}]_{210}} = \frac{(2J+1) e^{-F(J)hc/kT}}{\sum_{J=0}^{\infty} [(2J+1) e^{-F(J)hc/KT}]} \equiv [n_{X5}(J)]_{210}$$

That fraction of the total molecules/cm³ in (v=5) which resides at equilibrium in the level J is here labelled with the lower case $[n_{X5}(J)]_{210}$. Population densities and fractional densities under general, non-equilibrium, conditions can be represented by the same label, omitting the square brackets and outer subscript.

Because of the spin-doubling in CN·X there are two different levels for each value of J. These have separate population fractions which are different, because the two levels are associated with different K-values and so have different energies, $F(J)$. We will distinguish these energies and fractional

populations by labels which refer to the uppermost or to the lowermost of the two levels with a given J , as $n_{X5}(5\frac{1}{2}u)$ and $n_{X5}(5\frac{1}{2}l)$.

The sum in the denominator is in every case to be taken over the complete set of levels, including levels of both + and - symmetry character. Although there are symmetry selection rules governing optical transitions between the various levels, these do not apply to collision-induced transitions. There is no solid theoretical or experimental evidence to show that an exchange between translational and rotational energies in a collision cannot move a $CN \cdot X$ ($v=5$) molecule from any initial rotational level to any of the other $CN \cdot X(v=5)$ rotational leads—with the proviso, however, that ΔJ always tends to be rather small in a collision. Therefore, all the levels will form a single set in the establishment of statistical equilibrium*. At 210°K the value of kT/hc is 146.0 cm^{-1} .

Figure 20 shows the Boltzmann rotational distribution of $[n_{X5}(J)]_{210}$ for $CN \cdot X$, based on the energy level positions calculated earlier.

*For a homonuclear molecule such as H_2 , there is an additional symmetry property, usually labeled "a" and "s", which involves the effect on the wavefunctions which would result from an interchange of the two nuclei in the molecule. A selection rule on this symmetry property holds rigorously for collisions as well as optical transitions, in such a manner as to completely divide the H_2 rotational levels into two almost non-interacting sets. This feature is not present for CN .

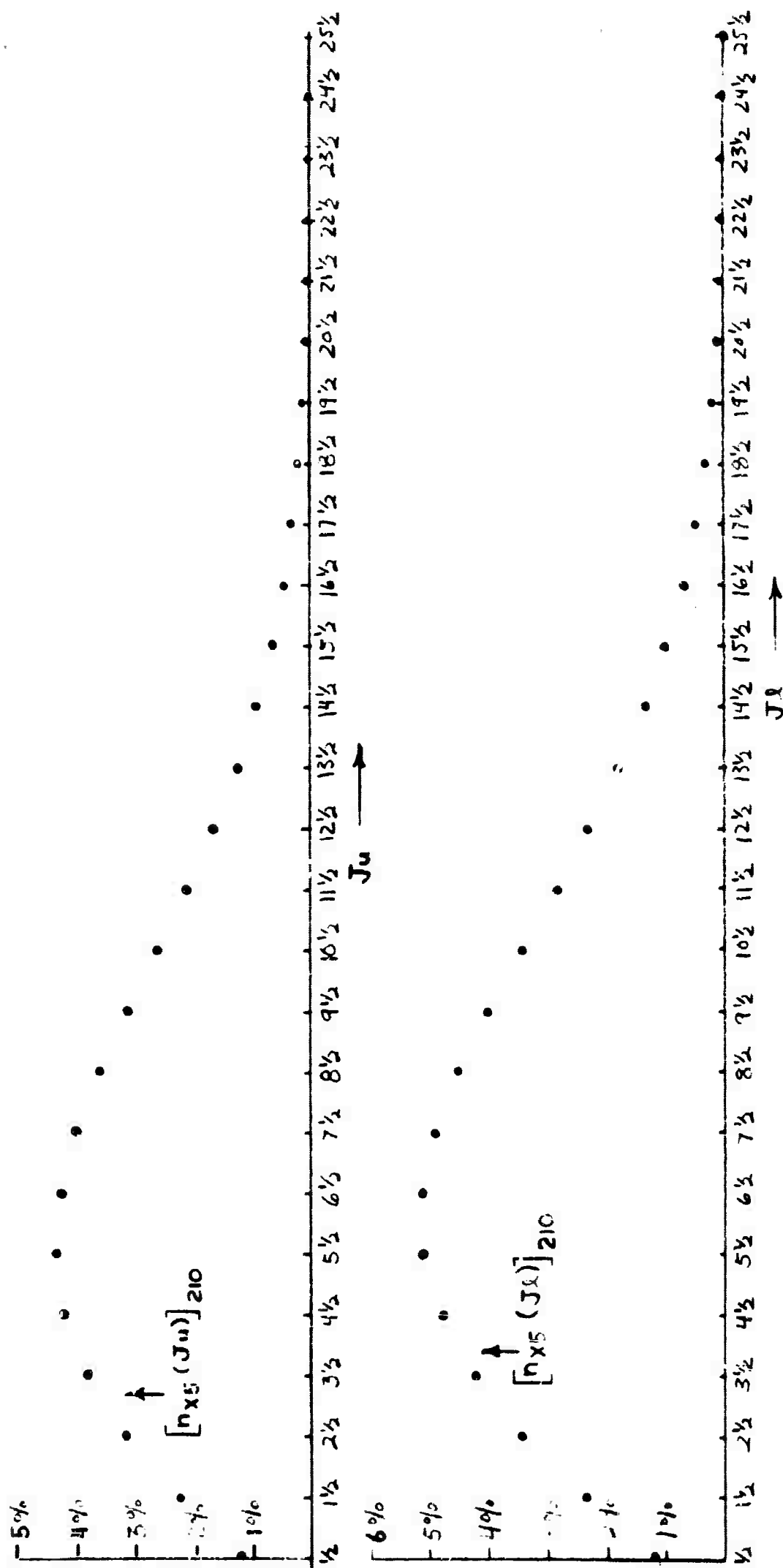


Figure 20
Rotational Boltzmann distribution for $\text{CN}\cdot\text{X}$ ($v=5$) at 210°K .

10.2 Boltzmann Distribution at 210°K in CN·A (v = 6)

The thermal equilibrium Boltzmann molecular density distribution for all the rotational levels of CN·A (v=6) is calculated in the same fashion as CN·X(v=5). Every J-value in ${}^2\Pi_{1/2}$ and ${}^2\Pi_{3/2}$ occurs twice, because of the Λ -type doubling, but this may be ignored in an initial calculation of relative populations, since the factor two will cancel out everywhere. Each member of a Λ -doubling pair will have the practically same equilibrium population, because the energies of the two are almost identical. All the levels of ${}^2\Pi_{1/2}$ and ${}^2\Pi_{3/2}$ are to be taken together as one set, with energies based on zero at the lowest ${}^2\Pi_{1/2}$ level.

There are two Λ -doublet pairs of levels for every J-value except for $J=1/2$, and so the population fractions will be given labels as before, such as $n_{A6}(5\frac{1}{2}^{\pm}u)$ and $n_{A6}(5\frac{1}{2}^{\pm}l)$. A label such as $[n_{A6}(5\frac{1}{2}^{\pm}u)]_{210}$ refers to that fraction of the total molecular density in CN·A (v=6) which resides at equilibrium in the upper pair of the two Λ -doublet pairs with $J=5\frac{1}{2}$. Each separate member of this Λ -doublet will have half the equilibrium population density of the doublet; this latter fractional population for any particular level will be labelled in the manner of $[n_{A6}(5\frac{1}{2}^{\pm}u)]_{210}$. Throughout the low-rotation regime, up to about $J=20$, the upper Λ -doublet pair for each J-value will have a ${}^2\Pi_{1/2}$ character, to a varying degree. And, the lower pair for each J-value will have a ${}^2\Pi_{3/2}$ character, similarly. At high rotation the ${}^2\Pi_{1/2}$ - ${}^2\Pi_{3/2}$ distinction is lost, as has been discussed previously.

Figure 21 displays the equilibrium Boltzmann distribution for CN·A(v=6) at 2100°K, calculated in the manner described.

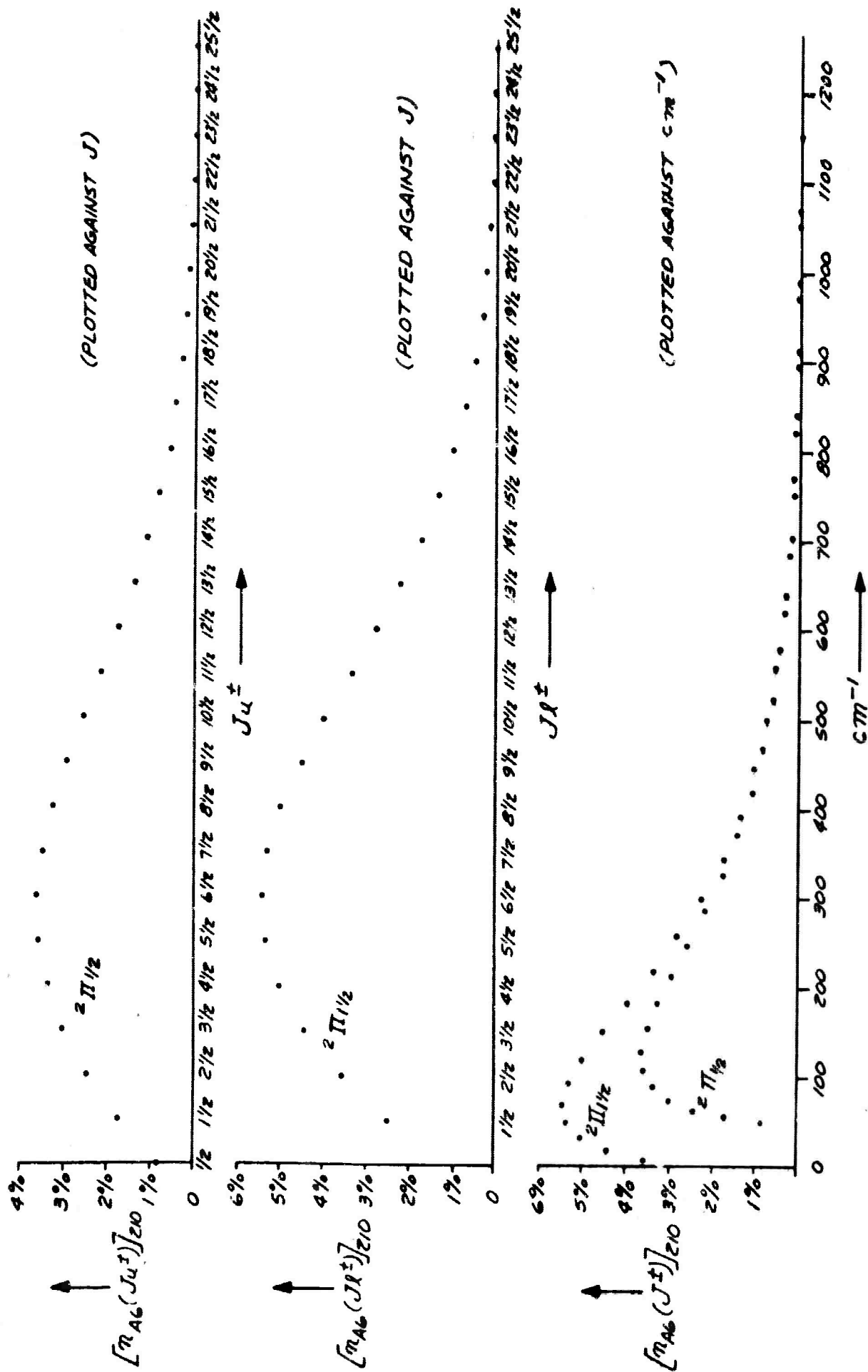


Figure 21.
Rotational Boltzmann distributions for $CN \cdot A(v=6)$ at $210^{\circ}K$.

10.3 Excitation Required for Zero-Gain at Each (6, 5) Line Wavelength

Let us consider first the $R_2(5)$ line, which falls at the edge of the prominent R_2 head of the band, with the calculated wavenumber $\sigma = 9542.410 \text{ cm}^{-1}$. This line is a transition between the plus Λ -doublet component of ${}^2\Pi_{1/2}(J=5\frac{1}{2})$ in $\text{CN}\cdot\text{A}$ ($v=6$), this being the upper $J=5\frac{1}{2}$ level in the $(v=6)$ state, and the upper $J=4\frac{1}{2}$ level in $\text{CN}\cdot\text{X}$ ($v=5$), which is a component of $K=5$. The molecular population densities at any instant in these two levels have been given the labels $N_{A6} \cdot n_{A6} (5\frac{1}{2}^+u)$ and $N_{X5} \cdot n_{X5} (4\frac{1}{2}u)$, respectively. Boltzmann equilibrium is not necessarily assumed, at present.

For each of these levels the statistical weight will be $g = (2J + 1)$. Here, g is the number of virtual sub-components of the level arising from the number of separate quantized space orientations with respect to the Poynting vector of an incident light beam, which the total angular momentum vector of the molecule, J , will have available to it in the presence of such a beam. In the absence of any space-orienting force such as an electric or magnetic field, all directions of space will be alike before any incident beam arrives, and so all virtual sub-components of a rotational level will then contain equal fractions of the molecular density. Let us divide each of the molecular densities noted above by $g=(2J+1)$ to find the population density per virtual sub-component, obtaining

$$\frac{N_{A6} \cdot n_{A6} (5\frac{1}{2}^+u)}{12} \quad \text{and} \quad \frac{N_{X5} \cdot n_{X5} (4\frac{1}{2}u)}{10}$$

Now, let us suppose that a parallel beam of light of wavenumber $\sigma = 9542.410 \text{ cm}^{-1}$ is sent through a cm^3 of gas containing these CN molecules in their various levels. Whenever each virtual sub-component of the lower level of the $R_2(5)$ transition happens to contain a greater molecular density than that of each virtual sub-component of the upper level of the transition, net absorption will occur. The beam will emerge with less intensity than it started. (The absorbed energy will be partly converted into heat in the gas, through relaxation collisions, and partly reradiated in all directions at various fluorescent wavelengths.)

On the other hand, if the population density of each virtual sub-component of the upper level of the transition is greater, then net stimulated emission will occur and the parallel beam will emerge with increased intensity. The boundary line of the excitation region in which inversion occurs is the condition of equality between population densities of the virtual sub-components of upper and lower levels of the transition. As expressed in terms of general labels applicable to any transition, this condition for zero-gain* within a volume of a

 *Mitchell and Zemansky (1934), Chapter V, describe some of the experimental evidence that with a unidirectional monochromatic illuminating beam, the relation between the Einstein coefficients for absorption and stimulated emission in the same transition between levels 1 and 2 is

$$\frac{B_{2 \rightarrow 1}}{B_{1 \rightarrow 2}} = \frac{g_1}{g_2}$$

This same relation between Einstein coefficients is well-known for isotropic black-body radiation impinging on molecules within a cavity having non-conducting walls. The relation leads to the condition stated above for zero-gain. Thus, for a balance between absorption and stimulated emission probabilities: (Level population per cc)₂ x (Stimulated emission probability $B_{2 \rightarrow 1}$ per molecule per unit flux at the transition wavelength) = (Level population per cc)₁ x (Absorption probability $B_{1 \rightarrow 2}$ per molecule per unit flux). This becomes the condition
 $(\text{Pop. Dens.})_2 \times B_{2 \rightarrow 1} = (\text{Pop. Dens.})_1 \times B_{1 \rightarrow 2} = (\text{Pop. Dens.})_1 \times B_{2 \rightarrow 1} \times \left(\frac{g_2}{g_1}\right),$

or

$$\frac{(\text{Pop. Dens.})_2}{g_2} = \frac{(\text{Pop. Dens.})_1}{g_1} .$$

laser medium is

$$\frac{N_{Av} \cdot n_{Av}(J_A)}{g(J_A)} = \frac{N_{Xv} \cdot n_{Xv}(J_X)}{g(J_X)}$$

We shall characterize the degree of excitation of the CN gas required from the Nd-glass pump lasers to produce zero-gain at any chosen (6, 5) band line in terms of the quantity Z , which will be defined as that percentage of those molecules/cm³ in [CN·X(v = 5) + CN·A(v = 6) which resides in CN·A(v = 6) at any instant, whether Boltzmann rotational equilibrium is present or not.

However, it will now be convenient in the analysis to consider, temporarily, circumstances where Boltzmann rotational equilibrium is present. Let us suppose that for some particular value Z_0 of the vibrational population ratio, one line of the (6, 5) band such as $R_2(5)$ is exactly at the zero-gain condition whenever Boltzmann rotational equilibrium at 210°K occurs in both upper and lower states. This value of Z will be given the label $[R_2(5)Z_0]_{210}$. Although $[R_2(5)Z_0]_{210}$ is a ratio between total population densities of vibrational states, it is a characteristic property of the $R_2(5)$ transition alone, and a separate such $[Z_0]_{210}$ value is associated with every line of the (6, 5) band.

From the previous discussion, and inserting the Boltzmann equilibrium values for the population fractions from Figures 20 and 21,

$$\begin{aligned}
 [R_2(5)Z_0]_{210} &= \left\{ \frac{[N_{A6}]_{210}}{[N_{A6}]_{210} + [N_{X5}]_{210}} \right\}_{\text{zero-gain}} = \left\{ \frac{[N_{A6}/N_{X5}]_{210}}{[N_{A6}/N_{X5}]_{210}^{+1}} \right\}_{\text{zero-gain}} \\
 &= \frac{[12n_{X5} (4\frac{1}{2}u)/10n_{A6} (5\frac{1}{2}u)]_{210}}{[12n_{X5} (4\frac{1}{2}u)/10n_{A6} (5\frac{1}{2}u)]_{210}^{+1}} \\
 &= \left[\frac{12n_{X5} (4\frac{1}{2}u)}{12n_{X5} (4\frac{1}{2}u) + 10n_{A6} (5\frac{1}{2}u)} \right]_{210} \\
 &= \left[\frac{12 \times 4.23}{(12 \times 4.23) + (10 \times 1.79)} \right] = 0.739 \approx 74\%
 \end{aligned}$$

The general formula for $[Z_0]_{210}$ is

$$\left[\frac{n_{X5}(J_X) \cdot g(J_A)}{n_{X5}(J_X) \cdot g(J_A) + n_{A6}(J_A) \cdot g(J_X)} \right]_{210}$$

Figure 22 displays such calculated values for each of the stronger lines of the (6, 5) band.

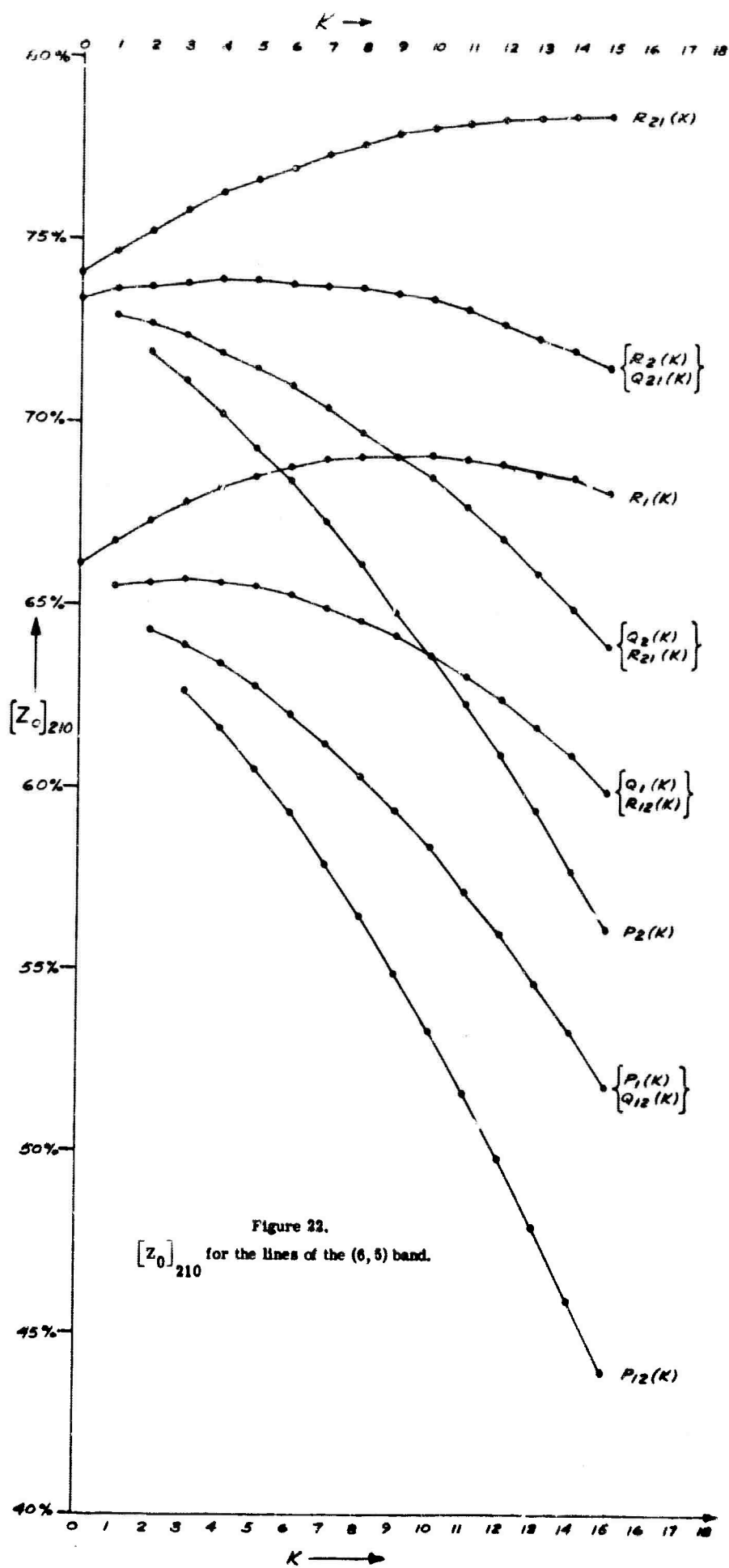


Figure 22.
 $[Z_0]_{210}$ for the lines of the (6,5) band.

Let us suppose that the preparation processes have dissociated a certain quantity of gas at 210° K , to yield some ground-state CN molecules, and have then elevated a certain amount of these to the vibrational state $\text{CN} \cdot \text{X}(v = 5)$. At this time we will assume that no molecules are in the excited electronic state $\text{CN} \cdot \text{A}$. Now if the Nd-glass pump lasers are flashed, and the Nd light contains an appreciable output at $9542.410 \pm 0.01 \text{ cm}^{-1}$, the gas initially will be a strong absorber in the $\text{R}_2(5)$ line. Let us assume that the gas mixture contains enough He, for example, to make the molecular collision frequency high enough to maintain approximate rotational Boltzmann equilibrium in both upper and lower states throughout the flash. Then, more and more $\text{CN} \cdot \text{X}(v = 5)$ molecules will be raised to $\text{CN} \cdot \text{A}(v = 6)$ —taking them out of the upper $J = 4 \frac{1}{2}$ level of the former and putting them into the plus Λ -component of the upper $J = 5 \frac{1}{2}$ level of the latter, with He collisions continually redistributing those excited and those left behind.—until almost 74% of the molecules have been raised up, as a maximum value.

This maximum possible degree of optical excitation by absorption in the $\text{R}_2(5)$ line under Boltzmann equilibrium conditions can only be asymptotically approached. And, a close approach can be made only if the Nd output flux at this wavenumber is quite high. As the percentage excitation is raised from zero toward $[Z]_{210} = 74\%$, the strength of the $\text{R}_2(5)$ absorption line in the gas gradually decreases. The zero-gain point for this $\text{R}_2(5)$ line, 74% excitation, might also be called its "transparency point", as absorption would cease entirely if that

excitation percentage could actually be reached when Boltzmann rotational equilibrium was being maintained at 210° K.

The situation which now gives this arrangement some possibilities for lasing at various other band lines, while it is being thus pumped at $R_2(5)$, is the following. For the line $P_{12}(15)$, zero gain occurs for $[Z_0]_{210} = 44\%$. Then, during the course of pumping molecules from $CN \cdot X(v = 5)$ up to $CN \cdot A(v = 6)$ by absorption in $R_2(5)$, after any more than 44% of the molecules have been excited and after both those raised up and those left behind have been rotationally redistributed by He collisions to maintain Boltzmann equilibria, the $P_{12}(15)$ transition will be in a condition of inversion. Any test beam sent through the gas from any source which included the wavenumber of the $P_{12}(5)$ spectrum line would be enhanced by stimulated emission. That is, pumping sufficiently strongly in the $R_2(5)$ line would cause amplification of a beam at the $P_{12}(15)$ wavenumber at any time after 44% has been passed.

This description has been simplified by the tacit assumptions (a) that none of the molecules originally in $CN \cdot X(v = 5)$ had been transferred away by any processes other than absorption in $R_2(5)$ up to $CN \cdot A(v = 6)$; (b) that no additional molecules had been moved into $CN \cdot X(v = 5)$ by any other process during the flash; and (c) that molecules once moved up to $CN \cdot A(v = 6)$ stayed there. Such extra processes, which will certainly occur in a practical laser transformer, do not alter the real meaning of the zero-gain point $[Z_0]_{210}$ for a line. If at any instant a Boltzmann rotational distribution of molecules at

210° K obtains both in $\text{CN} \cdot \text{X}(v = 5)$ and in $\text{CN} \cdot \text{A}(v = 6)$, and at that instant the ratio of molecules/cm³ in $\text{CN} \cdot \text{A}(v = 6)$ to molecules/cm³ in $[\text{CN} \cdot \text{A}(v = 6) + \text{CN} \cdot \text{X}(v = 5)]$ is greater than the value of $[Z_0]_{210}$ associated with any line of the (6, 5) band, then inversion is present at that instant with respect to that line, regardless of all the processes involved in the maintenance of that condition.

Although this type of calculation displays various Boltzmann equilibrium circumstances under which inversion may become possible, it does not give a clear picture of what total fraction of the molecules in the upper and lower states could be repeatedly transported around a pump-lase-pump-lase cycle under high flux conditions. This subject will be taken up in the next section. It will necessarily involve non-Boltzmann distributions.

10.4 Pumping in R_{21} and Lasing in P_{12} .

There are a great many ways in which the cyanogen bands near 1.06μ could be employed for laser transformer action with Nd-glass laser pumping. Different arrangements could have quite different efficiencies and other properties.

Probably the easiest system for preliminary analysis, although not necessarily the one leading to the best transformer, would consist of pumping in the R_{21} branch and lasing in the P_{12} branch of any one of the bands which will absorb Nd-glass laser light. This arrangement for the (6, 5) band will be discussed here, as a first sample case.

Even the $R_{21} - P_{12}$ cycle will be fairly complex to analyze for the entire volume of the transformer laser medium—clear through from the trigger section down along the length of the amplifying section to the final output window, and in all stages from the initial build-up to the eventual steady state. For a first approach to the problem, let us only look at the steady-state conditions near the output end, in the region of greatest power density.

We will assume that the Nd glass pump lasers are irradiating a typical cubic centimeter in such a position with very great intensity in the spectral range $10,440\text{\AA}$ to $10,470\text{\AA}$, which covers the lines R_{21} (0) to R_{21} (10) of the (6, 5) band. This flux is so intense that each of these transitions is being steadily maintained close to its transparency point, as regards the ratio of population densities for its initial and final states. This statement does not refer

to the $[Z_0]_{210}$ values for the lines, as discussed in the last section, since these imply a Boltzmann distribution. But regardless of what shape of (certainly non-Boltzmann) steady-state distribution may eventually be shown appropriate to these conditions, these curves must necessarily have population density ratios for all pairs of upper and lower levels connected by the R_{21} lines which approximate the "transparency ratios".

That is, for each such pair of upper and lower levels involved in one of the first eleven R_{21} lines, the population density ratio must approximately equal the statistical weight ratio for these levels.

Now, since the analysis of the last section has indicated that inversion in the higher members of the P_{12} branch is probably obtainable under many circumstances with heavy R-branch pumping, we will assume that design of a suitable trigger section will be feasible, which will provide a considerable flux at the frequency of each of the lines from $P_{12}(13)$ to $P_{12}(22)$. These fall in the wavelength range 10,670Å to 10,820Å. By the time this lasing flux has proceeded down the length of the transformer amplifying section, we may assume that very intense radiation in each of the spectrum lines acts on the typical cm^3 near the output end.

In such circumstances, these lines also must be close to their transparency points. That is, for each pair of upper and lower levels involved in one of the lines $P_{12}(13)$ to $P_{12}(22)$, the population density ratios must approximately equal the statistical weight ratios for these levels. Note that none of the transparency

ratios is ever precisely reached, merely asymptotically approached — so that the product of the remaining small coefficients for absorption and stimulated emission times the very large flux levels yields a high power density for pumping and lasing, in the two J-value regions respectively.

As the next step in the analysis, let us at first arbitrarily assume that this pumping and lasing has produced some sort of a steady-state population distribution which amounts to $Z = 67\%$, say. That is, 67% of the molecules of $[CN \cdot X(v = 5) + CN \cdot A(v = 6)]$ are in $CN \cdot A(v = 6)$, although probably neither upper or lower distribution is of Boltzmann type. Now, Figure 23 shows as dotted curves the upper and lower Boltzmann distributions for $Z = 67\%$, being calculated to have their ordinates everywhere equal to this fraction of corresponding ordinates in Figures 20 and 21, as a base from which to try to derive the true steady-state distributions.

We know that: (a) the true curves must be considerably above the dotted Boltzmanns for the low-J $CN \cdot A$ levels involved in the heavy pumping and the high-J $CN \cdot X$ levels involved in the heavy lasing, and (b) the true curves must be considerably below the dotted Boltzmanns for the low-J $CN \cdot X$ levels being drained by pumping and the high-J $CN \cdot A$ levels being drained by lasing, and (c) all appropriate pairs of upper and lower levels as described above must have population ratios equal to their g-value ratios. These conditions will immediately permit empirical sketching on the graph of the general regions

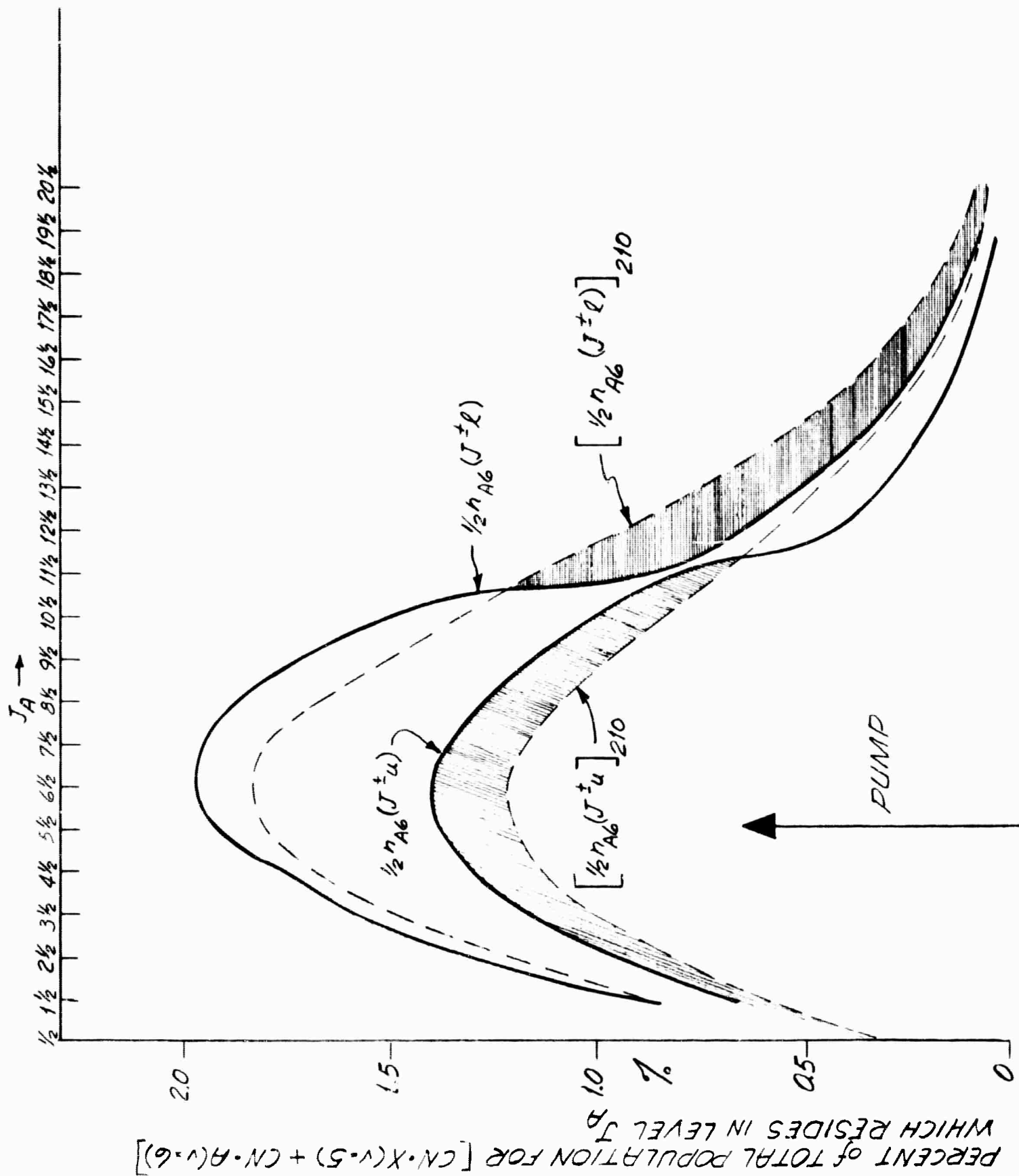
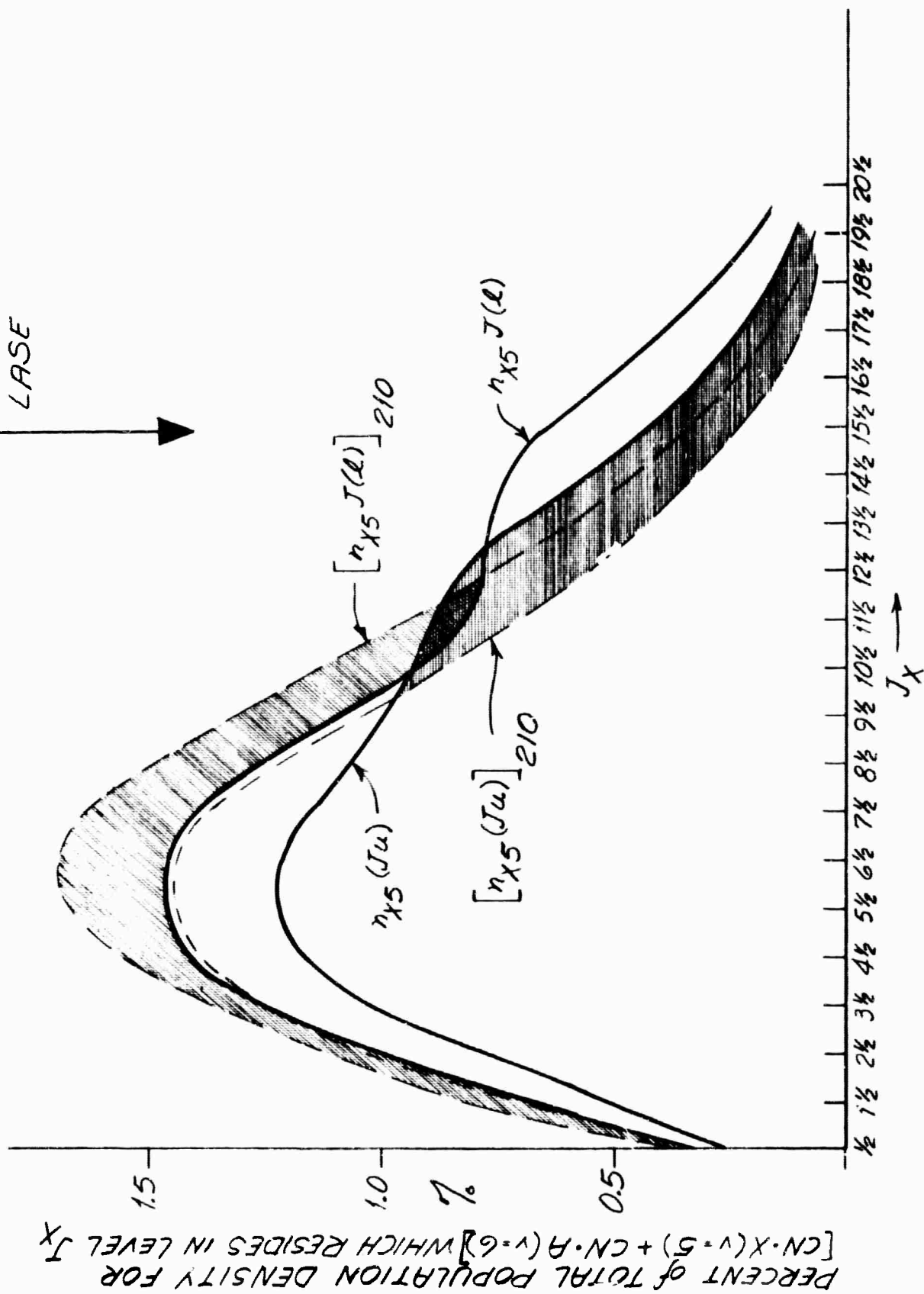


Figure 23.

The steady state distributions for the $R_{21} - {}^{12}$ pump-lase cycle.



where the four constrained segments of the true curves must fall—provided 67% was a reasonable approximation for the steady-state Z. The solid curves shown constitute one choice within such evident regions.

In order to make a choice within the regions described, there is another probable constraint available. It is presumed that a steady-state exists, so that within the chosen cm^3 there must be a continuous pump-lase-pump-lase cycle. Some number of molecules, N , are pumped from $\text{CN}\cdot\text{X}$ to $\text{CN}\cdot\text{A}$ in the low-J region in every microsecond; and the same number N molecules are shifted each microsecond from low-J to high-J in $\text{CN}\cdot\text{A}$ by collisions with He, then lased down to the high-J $\text{CN}\cdot\text{X}$ region and finally shifted back to low-J $\text{CN}\cdot\text{X}$ by He collisions, ready to start around again. This rectangular cycle path is indicated in Figure 23.

The reason that collisions will shift the rotational quantum numbers of the CN molecules to close the cycle in this manner is that the statistical effect of a multitude of collisions is always to try to produce Boltzmann distributions from whatever molecules are available in each vibration state. Figure 23 shows that any agency which continually is trying to convert the true steady-state curves into Boltzmanns will automatically be shifting molecules in the proper direction around the cycle just described.

We now have one more constraint which will serve for approximating the true distribution curves: the four areas shaded in Figure 23, the areas between the true steady-state curves in the constrained regions and the Boltzmanns to which they will immediately relax if the electromagnetic fluxes are suddenly removed, must approximately be equal. This follows from the following argument. The total area under the true steady-state curves for CN·A in the upper part of the diagram, must equal the total area under these relaxation Boltzmanns (actually, the sum of the ordinates instead of the area), because the latter measures the total number of molecules/cm³ in CN·A(v = 6). This number would not have changed appreciably from the steady-state value at a time immediately after the fluxes were stopped and before any large number of molecules had had time to leave this state by vibration-relaxing or electronic quenching collisions, or by fluorescence. This means that the total area lying above the Boltzmanns in the low-J region must equal the area lying below the Boltzmanns in the high-J region. To the approximation that the population densities of levels in the non-constrained sections of the curves are almost equal to those of levels of neighboring energy in the constrained sections, this means that the constrained sections of the steady-state curves will be at such locations as to make the upper left and right hand shaded areas equal. For the same reason, the lower left and right hand shaded areas must be approximately equal.

But the departures of the true curves from the Boltzmanns constitute the driving force which causes the collision processes to move molecules toward the right above and toward the left below, in Figure 23. If the rectangular path in the diagram is to represent a closed-cycle steady-state, then equal numbers of molecules/sec must be transported by the collisions toward high-J in CN·A and toward low-J in CN·X. This will not be so unless the driving forces are equal, top and bottom, and this surely requires approximately equal departures from the Boltzmann, at least whenever Z is fairly close to 50%.

If the relative shapes of the various Boltzmanns will not permit a choice of curve locations which can satisfy the equal-area criterion, then the assumed value of Z should be modified until a Z is found for which such an adjustment can be made. It was by such empirical graphical methods that the value $Z = 67\%$ was chosen, and the approximate steady-state curves drawn in Figure 23.

It is recognized that a correct determination of the steady-state distributions would be a massive computer-scale project in the handling of differential equations—with many of the parameters imperfectly known. The present rough graphical estimate should be useful in giving the order of magnitude of the molecular cycle phenomena.

Having drawn approximate steady-state distribution curves in the four constrained areas of Figure 23, the remaining segments of the curves are drawn so as to cause about equal departures from the Boltzmanns in levels which are energetically near to one another.

It will be noted that this particular cycle pumps into the low-J levels of $^2\Pi_{1/2}$ and lases from medium-J levels of $^2\Pi_{1/2}$. Collisions with He will probably shift most newly-pumped molecules up the $^2\Pi_{1/2}$ ladder and then across to $^2\Pi_{1/2}$ above $J = 10$, rather than crossing directly to the energetically nearby low levels of $^2\Pi_{1/2}$. It is much harder for collisions to shift the electron spins and orbits of a molecule than it is for them to shift total rotational momentum. Thus, in the case of NO-He collisions at 300° K, Broida and Carrington (1963) observed that a spin-doublet shift of only about 0.02 cm^{-1} occurred an order of magnitude less frequently than a rotational quantum shift of about 50 cm^{-1} .

Evenson (1964) has found experimentally that almost every CN-CN collision shifted J, usually by considerably more than one unit. Collisions of CN-He should have a similar effect.

On the question of loss of CN from the lasing cycle through He collisions shifting "prepared" molecules from CN·X ($v = 5$) down to ($v = 4$), for example, there are no direct data. However, Basco, Nicholas, Norrish and Vickers (1963) found that even collisions involving such unsymmetric electric fields as CNBr-CN·X had only about a 1% probability of causing the relaxation ($v = 4$) to ($v = 3$) at room temperature. And Roth (1959) observed that the extremely energetic CN-Xe collisions at about 8000°K required about $10\mu\text{sec}$ to relax a distribution in ($v = 1$) down to predominantly ($v = 0$). In general, the vibrational relaxation behavior of CN should resemble that of CO, which is well known to be highly resistant to change of vibrational quantum number in collisions with He at low temperature.

If one assumes that (a) the pumping and lasing fluxes in the cycle here described are so great at the cm^3 volume in question that the cycle speed is limited only by the molecular rotation-shifting step, (b) that a number of molecules given by one of the shaded areas in Figure 23 is pumped or lased in about the time required for collisions to carry an average molecule across from high to low J, or vice versa, (c) that this rotation-shifting transit time

is about the time needed for four CN-He collisions according to hard sphere classical theory, at the He pressure used and, (d) that a suitable He pressure is about 20 cm Hg, then a very rough estimate can be made of the number of output joules per second of pulse duration which will result from this volume. These assumptions lead to a rather large power density. However, many other factors besides maximum rotation-shifting capacity will set the power density limit for a practical CN transformer laser. As merely one example, the R_{21} and P_{12} lines studied here are very weak transitions, so that the power density limit might well be set by electric field breakdown in the gas before intensities could be reached which would invoke the rotation-shifting limit. Such would probably not be the case if pumping and lasing were done in the strong main branches.

Further investigation of all such matters is planned under the present contract.

11. CONCLUSION

Work during the first six months of this contract has developed some promising candidates for a molecular gas transformer laser medium to be used with Nd glass laser pumps. Cesium vapor cannot yet be ruled out. Metastable nitrogen presents complex collision phenomena, but appears well worth exploring, as does CO. It is planned to concentrate more thoroughly on N_2 during the next period.

The study of CN has only dealt with a few of the possible questions about a transformer design, but no completely unfavorable aspect of the use of this molecule has yet been uncovered, and it appears to date to have promise.

At present the most important feature of the CN transformer laser concept not accessible to analysis is the behavior of the mixture during the preparatory dissociation of $(CN)_2^*$. It is possible that $(CN)_2^* - He$ collisions would always have so high a probability for causing slight vibrational relaxation or quenching, rather than causing dissociation, that it might not be possible to achieve practically complete dissociation of $(CN)_2^*$. Any experimental program on the CN transformer laser concept should probably begin with a test of this matter.

Numerous other possibilities involving rather less stable molecular species remain worthy of some attention for use with Nd glass laser pumps.

12. BIBLIOGRAPHY

- R. M. Badger and J. L. Binder, Phys. Rev. 37, 800 (1931).
- E. A. Ballik and D. A. Ramsay, Jour. Chem. Phys. 29, 1418 (1958).
- R. F. Barrow, pp. 1373-1382 in "Mellor's --- Chemistry, Vol. II, Suppl. II The Alkali Metals, Part I", Wiley, 1961.
- R. F. Barrow, several sections in Vol. II, Suppl. III of the above.
- N. Basco, J. E. Nicholas, R. G. W. Norrish, and W. H. J. Vickers, Proc. Roy. Soc. A272.147 (1963).
- K. D. Bayes, Canad. Jour. Phys. 39, 1074 (1961).
- R. G. Bennett and F. W. Dalby, Jour. Chem. Phys. 36, 399 (1962).
- J. Berkowitz, Jour. Chem. Phys. 36, 2533 (1962).
- L. Brewer, L. K. Templeton, and F. A. Jenkins, Jour. Amer. Chem. Soc. 73, 1432 (1951).
- H. P. Broida and T. Carrington, Jour. Chem. Phys. 38, 136 (1963).
- T. K. Brotherton and J. W. Lynn, Chem. Revs. 59, 841 (1959).
- E. M. Bulewicz and P. J. Padley, p. 647 in "Ninth Symp. on Combustion, 1962", publ. 1963 by Acad. Press.
- J. Callomon and A. B. Davey, Proc. Phys. Soc. Lond. 82, 335 (1963).
- P. K. Carroll, Canad. Jour. Phys. 34, 83 (1956).
- N. P. Carleton and O. Oldenberg, Jour. Chem. Phys. 36, 3460 (1962).
- Centre Nat. d'Etudes des Telecomm., Final Tech. Report 31 Dec 63. ASTIA Doc. AD 431679.
- E. Clementi and A. D. McLean, Jour. Chem. Phys. 36, 563 (1962).
- S. P. Davis and J. G. Phillips, "The Red System ($A^2\Pi - X^2\Sigma$) of the CN Molecule", Univ. Cal. Press, Berkeley, 1963.
- R. N. Dixon and R. W. Nicholls, Canad. Jour. Phys. 36, 127 (1958).

- H. B. Dunford, Jour. Phys. Chem. 67, 258 (1963).
- L. Duoyer, Le Radium 9, 209 (1912).
- F. Duschinsky, Zeits. für Phys. 78, 586 (1932).
- K. M. Evenson, Bull. Amer. Phys. Soc. 10, #2 (1965).
- R. J. Fallon, J. T. Vanderslice, and R. D. Cloney, Jour. Chem. Phys. 37, 1097 (1962).
- W. Finkelburg and O. T. Hahn, Phys. Zeits. 39, 98 (1938).
- W. R. Frederickson and W. W. Watson, Phys. Rev. 30, 429 (1927).
- A. G. Gaydon, "Dissociation Energies", 2nd Edition, London, 1953.
- A. G. Gaydon, "The Spectroscopy of Flames", London, 1957.
- S. N. Ghosh, S. Nand and A. Sharma, Proc. Phys. Soc. Lond. 81, 713 (1963).
- C. Haggart and C. A. Winkler, Canad. Jour. Chem. 38, 329 (1960).
- L. v. Håmos, Zeits. für Phys. 74, 379 (1932).
- A. Henglein, G. Jacobs, and G. A. Muccini, Zeits. für Naturforsch. 18a, 98 (1963).
- J. T. Herron and V. H. Dibeler, Jour. Amer. Chem. Soc. 82, 1555 (1960).
- G. Herzberg, "Molecular Spectra and Molecular Structure. I. Spectra of Diatomic Molecules", 2nd Ed., Van Nostrand, 1950.
- G. Herzberg and J. G. Phillips, Astrophys. Jour. 108, 163 (1948).
- E. L. Hill and J. H. Van Vleck, Phys. Rev. 32, 250 (1923).
- T. R. Hogness and L. S. Tsai, Jour. Amer. Chem. Soc. 54, 123 (1932).
- A. Jablonski, P. Pringsheim and R. Rompe, Zeits. für Phys. 77, 26 (1932).
- A. V. Jakovleva (a), Acta Physicochimica URSS 9, 665 (1938).
- A. V. Jakovleva (b), Acta Physicochimica URSS 10, 433 (1939).

- F. A. Jenkins, Y. K. Roots and R. S. Mulliken, Phys. Rev. 39, 16 (1932).
- M. Jeunehomme and A. B. F. Duncan, Jour. Chem. Phys. 41, 1692 (1964).
- A. Jonescu, Compt. Rend. Acadm. Roumaine 1, 384 (1937).
- C. Kenty, Jour. Chem. Phys. 41, 3996 (1964).
- N. H. Kiess and H. P. Broida, "Seventh Symposium on Combustion, 1958", London, pub. 1959, p. 207.
- N. H. Kiess and H. P. Broida, Jour. Mol. Spect. 7, 194 (1961).
- G. B. Kistiakowsky and H. Gershinowitz, Jour. Chem. Phys. 1, 432 (1933).
- H. T. Knight and J. P. Rink, Jour. Chem. Phys. 35, 199 (1961).
- E. M. Kudryavtsev, E. F. Gippius, S. S. Derbeneva, A. N. Peckenov and N. N. Sobolev, High Temp. 1, 60, 338 (1963).
- F. W. Loomis and P. Kusch, Phys. Rev. 46, 292 (1934).
- T. C. MacAvoy, M. L. Charters and R. D. Maurer, "Proc. 1st Mil. Laser Conf. Nov 63 San Diego", (publ. '64) - Vol. 1, p. 85 (U).
- J. L. Magee, "Radiation Chemistry", in Ann. Revs. Phys. Chem. 12, (1961).
- G. G. Mannella, Chem. Revs. 63, 1-20 (1963).
- L. E. S. Mathias and J. T. Parker, Appl. Phys. Lett. 3, 16 (1963).
- E. Matuyama, Sci. Rep. Tohoku Imp. Univ., Ser. I, 23, No. 1-3, p. 322, (1934).
- R. D. Maurer, "Proceedings of the Symposium on Optical Masers , New York, 1963", publ. by Polytech. Inst. Brooklyn, 1963.
- J. C. McLennan and D. S. Ainslie, Proc. Roy. Soc. A103, 304 (1923).
- J. Mertens and R. L. Potter, Combustion and Flame 3, 525 (1959).

- A. C. G. Mitchell and M. W. Zemansky, "Resonance Radiation and Excited Atoms", Macmillan, 1934.
- C. K. Møller and B. P. Stoicneff, *Canad. Jour. Phys.* 32, 635 (1954).
- R. B. Mconey and H. G. Reid, *Proc. Roy. Soc. Edinburgh* 52, 152 (1932).
- D. F. C. Morris, *Acta Crystall.* 14, 547 (1961).
- R. S. Mulliken, *Rev. Mod. Phys.* 4, 16 (1932).
- R. S. Mulliken, *Jour. Phys. Chem.* 66, 2306 (1962).
- R. Napper and F. M. Page, *Trans. Faraday Soc.* 59, 1086 (1963).
- H. Neujmin and A. Terenin, *Acta Physicochimica URSS* 5, 465 (1936).
- R. W. Nicholls, *Jour. Res. Nat. Bur. Stand.* A68, 75 (1964).
- A. H. Nielsen, "Infrared", chapter 2.2 in "Molecular Physics", ed. by D. Williams; vol. 3 of "Methods of Experimental Physics", Acad. Press, 1962.
- E. R. Nixon and F. D. Verderame, *Jour. Chem. Phys.* 41, 1682 (1964).
- O. Oldenberg, D. G. Bills, and N. P. Carleton, *Jour. Opt. Soc. Amer.* 51, 526 (1961).
- D. E. Paul and F. W. Dalby, *Jour. Chem. Phys.* 37, 592 (1962).
- P. Pringsheim, "Fluorescence and Phosphorescence", Intersci. Publ., 1949.
- J. V. Quagliano, "Cyanides (Survey)", art. in *Ency. Chem. Tech.*, ed. by R. E. Kirk and D. F. Othmer, Intersci. Publ., N. Y., 1949.
- H. E. Radford, *Phys. Rev.* 136, A1571 (1964).
- H. E. Radford and H. P. Broida, *Jour. Chem. Phys.* 38, 644, Errata 3031A (1963).
- D. A. Ramsey, *Jour. Chem. Phys.* 21, 165 (1953).

- M. Rigutti, N. Cim. 26, 597 (1962).
- N.C. Robertson and R.N. Pease, Jour. Chem. Phys. 10, 490 (1942).
- G.W. Robinson, "Electronic Spectra", chapter 2.4 in "Molecular Physics ", ed. by D. Williams; vol. 3 of "Methods of Experimental Physics", Acad. Press, 1962.
- V.S. Rossikhin and I. L. Tsikora, Opt. i Spek. 11, 415 (1961).
- W. Roth, Jour. Chem. Phys. 31, 720 (1959).
- H.G. Smith, Proc. Roy. Soc. A106, 400 (1924).
- F.T. Smith, Disc. Faraday Soc , No. 33, 183 (1962).
- E.W. R. Steacie, "Atomic and Free Radical Reactions", 2nd Ed., Reinhold, 1954.
- A.T. Wager, Phys. Rev. 64, 18 (1943).
- T. Wentink, L. Isaacson and J. Morreal, Jour. Chem. Phys. 41, 278 (1964).
- J.U. White, Jour. Chem. Phys. 8, 79 (1940) (a).
- J.U. White, Jour. Chem. Phys. 8, 459 (1940) (b).
- H.E. Williams, "Cyanogen Compounds - - - ", London, 2nd Ed. 1948.
- J.G. Winans, Zeits. für Phys. 60, 631 (1930).
- S.C. Woo and R. M. Badger, Phys. Rev. 39, 932 (1932).
- S.C. Woo and T.K. Liu, Jour. Chem. Phys. 5, 161, Errata 499, (1937).
- R.W. Wood and E. L. Kinsey, Phys. Rev. 31, 793, (1928).
- A.A. Wyller, Astrophys. Jour. 127, 763 (1958).
- E.C. Zipf, Jr., Bull. Amer. Phys. Soc. 10, 179 (1965).